

# A Computational Study to Assess the Effect of the Coronary Hemodynamics on the Mechanical Stresses of Stenotic Atherosclerotic Plaques

Ramsés Galaz Mendez

Department of Biomedical Engineering McGill University, Montreal

June 2008

A thesis submitted to McGill University in partial fulfillment of the requirements of the degree of Doctor of Philosophy in Biomedical Engineering.

© 2008 Ramsés Galaz Mendez

To my father, Dr. Jesús Galaz Cervantes, who passed away of the same disease studied in this work.

As a physician, he understood the true value of uninterestingly helping people through the advancement of knowledge in medicine.

"Advances in medicine and agriculture have saved vastly more lives than have been lost in all the wars in history"

Carl Sagan

#### Abstract

Atherosclerotic plaque rupture is the common pathological condition of the acute ischemic syndromes of sudden cardiac death and acute myocardial infarction. The rupture of the fibrous cap of a coronary plaque may result in a thrombus formation that would prevent the perfusion of blood downstream of the myocardium. A probable cause of plaque rupture is the mechanical stress induced by the artery wall stretching from the physiological flow of blood and the intraluminal pressure within the coronary arteries.

We used computational fluid-structure interaction methods to analyze the effects of coronary blood flow on stenotic atherosclerotic plaques to determine the mechanical stresses within the plaque's components. We analyzed the effect of the fibrous cap thickness, necrotic core stiffness, and percentage of area stenosis on the mechanical stresses within using comparable models of stenosed arteries. We then analyzed the effect of transient hemodynamic flow using realistic patient-specific geometries under normal coronary flow and pressure. The transient results were used to calculate the amplitude and mean stress for fatigue analyses. Based on this approach, we developed several hypotheses: mechanical fatigue in the fibrous cap is the ultimate characteristic that triggers the rupture; fibrous cap mechanical fatigue (FCMF) can be the result of the combined effects of the cap thickness, relative inclusion stiffness and percentage of stenosis; FCMF can be influenced by the global structure of the obstructive pathology in particular in the context of multiple stenoses, we also show that the anisotropic properties of the collagen fibers within the cap can influence the rupture mechanism.

Our results indicate that the combination of a thin fibrous cap, a soft lipid core and a large percentage of stenosis contribute to high mechanical stress magnitudes. Such stresses in mild stenoses can have similar critical behaviors to those normally associated with higher percentage stenoses. The global structure in multiple plaque scenarios can also play a significant role in influencing the overall mechanical stress and thus affect the fibrous cap mechanical fatigue.

#### Résumé

La rupture de plaques athérosclérotiques est la condition pathologique la plus fréquente impliquée dans le syndrome ischémique aigu pouvant mener à l'infarctus du myocarde et à la mort du à l'arrêt cardiaque. La rupture du cap fibreux de la plaque coronarienne peut résulter dans la formation d'un thrombus qui peut éventuellement empêcher la perfusion sanguine en aval du lit myocardique. Une cause possible de la rupture de la plaque est l'établissement de contraintes mécanique induites par la déformation de la paroi artérielle sous l'écoulement sanguin et la pression intraluminale à l'intérieur des artères coronaires.

Nous avons utilisé des méthodes de simulation par interaction fluide-structure pour analyser les effets de l'écoulement coronarien sur les plaques athérosclérotiques pour déterminer les contraintes mécaniques sur les constituants de la plaque. Nous avons analysé l'effet de l'épaisseur du cap fibreux, la rigidité de l'inclusion nécrotique et le pourcentage en surface de la sténose sur les contraintes mécaniques en utilisant des modèles similaires d'artères sténosées. Nous avons ensuite analysé l'effet de l'écoulement hémodynamique transitoire avec des géométries réalistes spécifiques à certains patients sous des conditions normales de flot sanguin et de pression sanguine. Les résultats transitoires ont été utilisés pour calculer l'amplitude et la valeur moyenne des contraintes pour les analyses de fatigue. En se basant sur cette approche, nous avons développé certaines hypothèses: la fatigue mécanique du cap fibreux (FMCF) est la caractéristique ultime qui initie la rupture; la FMCF peut être le résultat des effets combinés de l'épaisseur du cap, des valeurs relatives des rigidités des inclusions et le pourcentage de sténose; la FMCF peut être influencée par la structure globale de la pathologie obstructive en particulier dans le contexte de sténoses multiples; les propriétés anisotropiques des fibres de collagène à l'intérieur du cap peut influencer le mécanisme de rupture.

Nos résultats indiquent que la combinaison d'un cap fibreux mince, d'une inclusion lipidique molle et un grand pourcentage de sténose contribuent à augmenter les magnitudes des contraintes. De tels contraintes pour des sténoses modérées peut entraîner des comportements critiques en principe associés à des pourcentages de sténoses plus élevés. La structure globale dans le contexte de plaques multiples peut aussi jouer un rôle significatif pour les contraintes mécaniques et ainsi affecter la FMCF. Nos études histologiques ont montré que l'architecture des fibres de collagène dans le cap fibreux est anisotropique. Ceci supporte notre hypothèse que les orientations des fibres se réorientent dans le cap fibreux ce qui peut affaiblir la résistance à la rupture.

# Acknowledgements

This thesis was made possible thanks to the financial support of my supervisors Dr. Rosaire Mongrain of McGill University and Dr. Jean Claude Tardif of the Montreal Heart Institute. I would like to thank my supervisor Rosaire Mongrain for his impeccable supervision, constant support, relevant advice, and for initially convincing me into pursuing my doctoral degree. Thanks also to Jean Claude Tardif for his advice and guidance on performing a study that is relevant to clinicians. Many thanks to the other members of the thesis supervisory committee: Dr. Richard Leask and Dr. Satya Prakash for their constant supervision during the oral examinations.

I appreciate my wife Mabel for her constant support and patience during the course of the doctoral degree and for being the most wonderful partner. I would like to thank my mother, who has always pushed me into reaching higher goals, my brother Jesús, Meche and Mary who have always been there for me.

I would also like to thank the friendship and collaboration from my fellow lab partners, professors and staff whom I met over the course of five long but exciting years at McGill University: Soroush Nobari, Boby Chu, Edgardo Gutiérrez, Akshay Ashok, Ian Campbell, Marika Archambault-Wallenburg, Adrian Ranga, Neil Bullman-Fleming, Jean Brunette, Zineb Idrissi, Juan Mejía, Valerie Pazos, Pablo Rousselin, Youssef Biadillah, Isam Faik, Barbara Roehrnbauer, Bilal Ruzzeh, Tin Nguyen, Dominique Tremblay, Simon Kattoura, Eric Hong, Guy Drapeau, Leonie Rouleau, Irene Cartier, Pina Sorrini, Joyce Nault.

#### **Contribution of authors**

Article 1: Fluid-Structure Interaction Numerical Studies on the Assessment of Mechanical Stress of the Coronary Atherosclerotic Plaque

Authors: Ramses Galaz, Rosaire Mongrain, Richard Leask, Jean Claude Tardif

I conducted all of the numerical analyses and wrote the draft of the manuscript. Rosaire Mongrain supervised the project and proposed some of the ideas on how the project should be done. Richard Leask contributed with ideas on how to refine the analyses done in the research. Jean Claude Tardif supervised the project and suggested ideas from the clinical point of view.

Article 2: Numerical Analyses to Assess the Hemodynamic Effects on the Mechanical Stresses of Patient-Specific Stenotic Coronary Plaques

Authors: Ramses Galaz, Rosaire Mongrain, Valerie Pazos, Richard Leask, Jean Claude Tardif

I conducted all of the numerical analyses and wrote the draft of the manuscript. Rosaire Mongrain supervised the project and proposed some of the ideas on how the project should be done. Valerie Pazos wrote the computational code to process the individual trace files from the intravascular ultrasound segments that were used in the patient-specific model reconstructions. Richard Leask contributed with ideas on how to refine the analyses done in the research. Jean Claude Tardif supervised the project and suggested ideas to make the research relevant to clinicians.

# Article 3: Fibrous Cap Collagen Fiber Remodeling Increases Atherosclerotic Plaque Vulnerability

Authors: Ramses Galaz, Marika Archambault-Wallenburg, Rosaire Mongrain, Richard Leask, Jean Claude Tardif

I conducted the numerical analyses to obtain the principal stress orientations within the fibrous cap that would serve to predict the preferred orientations of collagen fibers of actual human specimens of fibrous caps, I processed the tissue specimens to prepare them for histopathological studies, I wrote the draft of the manuscript. Rosaire Mongrain supervised the project and proposed some of the ideas on how the project should be done. Marika Archambault-Wallenburg wrote the computational code to process the images of collagen fibers taken from the histology studies and she wrote sections of the methodology text. Richard leask contributed with ideas on how to refine the analyses done in the research. Jean Claude Tardif supervised the project and suggested ideas to make the research relevant to clinicians.

# **Statement of originality**

To the best of our knowledge:

- We have presented studies in this thesis suggesting that mild plaques can have stress values similar to severe stenosis. This would help to explain the paradoxical behavior of why plaque ruptures are more frequent in mild stenosis. Also, we have demonstrated through numerical studies that a multiple plaque scenario can have a different degree of vulnerability than single plaques with similar morphologies and material properties. We have also demonstrated through numerical studies that plaques may fail by the progression of cracks at particular spatial locations due to the cyclic stretching nature of pulsatility. This aspect is introduced in this thesis as the concept of fibrous cap mechanical fatigue (FCMF).
- Our studies have been the first to demonstrate through numerical simulations in a
  three-dimensional model that the highest stress concentrations occur in the
  proximal shoulder side of the plaque. The analyses were performed considering
  the interaction between the hemodynamics and the structural domain of the
  components of the plaque.
- We have been the first to demonstrate through the three-dimensional numerical analyses and by using fluid-structure interaction methods that the combination of a thin fibrous cap, a soft atheromatous core and a large percentage of stenosis

contribute to the highest mechanical stresses in the proximal shoulder region of the plaque.

- We are the first to report that the collagen fiber architecture of the fibrous cap is not arranged uniformly. It has preferred orientations depending on its spatial location. Future numerical analyses should be performed considering the true anisotropy of the fibrous cap. Our hypothesis is that the collagen fibers tend to follow the principal stress orientations within the fibrous cap. The numerical studies demonstrated that the principal stresses have a preferred circumferential orientation in the healthy sections of the artery, and they gradually shift to a longitudinal orientation as they approach the peak of the stenosis.
- Our three-dimensional in-vivo reconstructions of ruptured plaques using intravascular ultrasound showed that ruptures tend to occur in the proximal side of the plaque. This supports our hypothesis that ruptures are associated with high mechanical stresses that are commonly located in the proximal region of the plaque according to the numerical analyses.
- We have demonstrated through transient three-dimensional numerical studies of coronary stenosis models that the greatest pressure drop or loss of energy occurs during the highest blood flow rate. The energy lost is dissipated partly as

mechanical deformation of the weakest structural components of the plaque, particularly the fibrous cap. Consequently, the highest mechanical stresses occur also during the highest blood flow rate.

# **Table of contents**

CHAPTER 1 - INTRODUCTION1		
1.1	Introduction to atherosclerosis and atherogenesis	1
1.2	Plaque rupture	5
1.3	2.1 Mechanical factors of plaque rupture	7
	1.2.1.1 Core stiffness	
	1.2.1.2 Fibrous cap thickness	
	1.2.1.3 Plaque size	
	1.2.1.4 Fatigue failure	
	1.2.1.5 Multiple plaque vulnerability	
	1.2.1.6 Myocardium motion	
	1.2.1.7 The role of hemodynamic flow on mechanical stresses	
	1.2.1.8 Anisotropic properties of the tissue	
	1.2.1.9 Viscoelastic properties	
1	2.2 Biological factors of plaque rupture	
	1.2.2.1 Inflammation	
4	2.3 Summary of factors	
	2.4 Summary of hypotheses	
1.3	Imaging methods to assess plaque vulnerability	. 25
1.	3.1 Morphological reconstruction of diseased vessels through intravascular	
ul	trasound	. 27
	Computational methods to assess plaque vulnerability	
	4.1 Finite element method for structural analysis	
1.	4.2 Computational fluid dynamics for solving the fluid domain results	. 32
1.	4.3 Fluid-structure interaction method	. 33
CHA	PTER 2 – ARTICLE: "FLUID STRUCTURE INTERACTION NUMERICAL	
	DIES ON THE ASSESSMENT OF MECHANICAL STRESS OF THE CORONARY	
	IEROSCLEROTIC PLAQUE"	
ЛП	IEROSCEEROTICT EAQUE	33
21	Abstract	27
<b>Z.</b> 1 /	105ti act	. 31
221	ntroduction	38
Z.Z I	ili oddction	. 30
231	Methods	<b>1</b> 1
	3.1 Mathematical models	
	3.2 Mathematical model for the structural domain	
	3.3 Mathematical model for the fluid domain	
2.4 (	Computational models	. 45
2.	4.1 Computational model for the structural domain	. 45
	4.2 Computational model for the fluid domain	

2.5 Results	
2.5.1 Computational fluid dynamic results with analytical validations	49
2.5.2 Numerical results for the structural stress	54
2.6 Discussion	59
	- 4
2.7 Conclusions	61
CHAPTER 3 - DISCUSSION ON ARTICLE: "FLUID STRUCTURE INTERACTION	
NUMERICAL STUDIES ON THE ASSESSMENT OF MECHANICAL STRESS OF TH	Œ
CORONARY ATHEROSCLEROTIC PLAQUE"	
	00
3.1 Discussion on the numerical results	63
3.2 Numerical results plots	68
3.3 Limitations of the analyses	70
3.4 Fibrous cap mechanical fatigue concept (FCMF)	71
CHAPTER 4 – ARTICLE: "NUMERICAL ANALYSES TO ASSESS THE	
HEMODYNAMIC EFFECTS ON THE MECHANICAL STRESSES OF PATIENT-	
SPECIFIC STENOTIC CORONARY PLAQUES"	73
SI LCII IC SI LIVO I IC CONONANT I LAQUES	/ 3
4.1 Abstract	75
7.1 /AOUT 400.	0
4.2 Introduction	76
4.3 Methods	79
4.3.1 Morphological reconstruction of diseased vessels through IVUS (intravascular	
ultrasound)	79
4.3.2 Fluid structure interaction methods	
4.3.3 Fatigue analysis	85
4.4 Results	90
4.4.1 Fluid domain results	
4.4.2 Structural domain results	
4.4.3 Fatigue analysis results	
4.5 Conclusions	. 100
CHAPTER 5 - DISCUSSION ON ARTICLE: "NUMERICAL ANALYSES TO ASSESS	
THE HEMODYNAMIC EFFECTS ON THE MECHANICAL STRESSES OF PATIENT	
SPECIFIC STENOTIC CORONARY PLAQUES"	
SI LCII IC SI LIVO I IC CONONANT I LAQUES	.102
5.1 Transient analyses	. 102
5	
5.2 Transient analyses using unidirectional and fully coupled FSI methods	. 105
, <u> </u>	
5.3 Reconstructions of ruptured plaques using IVUS	. 106

5.4 Linear elastic vs. hyperelastic materials	107
5.5 Fatigue analyses	108
5.6 Multiple plaque vulnerability	109
5.7 Collagen tissue characterization	110
CHAPTER 6 – ARTICLE: "FIBROUS CAP COLLAGEN FIBER REMODELING	
INCREASES ATHEROSCLEROTIC PLAQUE VULNERABILITY"	111
6.1 Abstract	113
6.2 Introduction	114
6.3 Methods	116
6.3.1 Numerical models of flow through stenosed arteries	
6.3.2 Tissue preparation	118
6.3.3 Image processing software development	119
6.4 Results	124
6.4.1 Tissue preparation and staining	
6.4.2 Principal stresses orientations according to the numerical models	
6.4.3 Fiber tracking	129
6.5 Discussion and conclusions	132
CHAPTER 7 – DISCUSSION ON ARTICLE: "FIBROUS CAP COLLAGEN FIBE REMODELING INCREASES ATHEROSCLEROTIC PLAQUE VULNERABILITY	
7.1 Collagen fiber visualization through histopathological studies	134
7.2 Plaque analysis through MicroCT scans	135
7.3 Other methods	137
7.4 Future improvements	137
7.5 Fibrous cap mechanical fatigue relation to collagen fiber orientation	138
FINAL CONCLUSIONS	139
APPENDIX SECTION	142
Ethical approvals from McGill University for tissue research	143
Ethical approval from the hospital involved in the tissue research	145
Translation of the ethical approval letter given by the Mexican Hospital wh	

Author's curriculum vitae	147
REFERENCES	.151

# Table of figures

Figure 1.1: The layered structure of arteries	2
Figure 1.2: Schematic representation of the process of atherogenesis [10]	4
Figure 1.3: The four most common mechanisms of thrombi formation. The rupture of	
fibrous cap represents two thirds to three quarters of all cases [16]	
Figure 1.4: A section of a specimen showing a fibrous cap rupture	
Figure 1.5: Typical exponential behavior of a stress vs. number of cycles curve	
Figure 1.6: Pressure and flow waveforms for a left anterior descending (LAD) coronar	
artery [42]	
Figure 1.7: Failure modes of composite materials [43]	
Figure 1.8: Intravascular ultrasound image trace of a diseased coronary artery	
Figure 1.9: Traces of each IVUS segment and the respective 3D reconstruction	
Figure 1.10: Element-discretized domain or mesh for the artery wall and plaque's	
domains	31
Figure 1.11: Three-dimensional fluid domain results of the lumen of a double plaque	
scenario: a) velocity vector field and b) lumen surface pressure	33
Figure 2.1: A schematic model of a stenosis: a) conical converging section, b) cylindric	ical
throat, c) expansion cone	44
Figure 2.2: Geometric 3D models of stenotic arteries and their respective percentage of	of
stenosed lumen area shown with a fixed fibrous cap thickness.	
Figure 2.3: Central streamline pressure drop across different percentages of stenosis fr	om
the numerical analyses	50
Figure 2.4: Comparison of the mathematical model developed by Back et al [82], clinical	
measurements [85] and numerical results.	
Figure 2.5: Central streamline velocity across different percentages of stenosis	
Figure 2.6: Plaque surface wall shear stress across different percentages of stenosis	
Figure 2.7: Pressure gradient force acting on the normal direction of the stenotic surface	
	53
Figure 2.8: Longitudinal section view of the typical mechanical stress distribution for	
fluid-structure interaction results. All analyses resulted in high stress concentrations in	
proximal side of the plaque.	
Figure 2.9: Local maximum principal stresses at 36% stenosis	
Figure 2.10: Local maximum principal stresses at 51% stenosis	
Figure 2.11: Local maximum principal stresses at 75% stenosis	
Figure 2.12: Local maximum principal stresses at 91% stenosis	57
Figure 2.13: Peak stress values for different percentages of stenosis for a fibrous cap	
thickness of 200 microns and $\gamma$ value of 0.001	59
Figure 3.1: Contribution to total pressure losses of the viscous and geometric terms as	
derived from the Back equations	65
Figure 3.2: Sample numerical results of velocity fields for each case analysed	69

Figure 3.3: Computational Fluid Dynamics (CFD) mesh of the lumen of	
stenosis model	
Figure 4.2: Aortic pressure and phasic coronary flow waveform (LAD) [4	
Figure 4.3: Longitudinal section view of the model mesh and the nodes of	
fatigue analysis	
Figure 4.4: Typical exponential behavior of a stress vs number of cycles	
Figure 4.5: Central streamline pressure drop across the model at various p	<u>.</u>
Figure 4.6: Central streamline velocity increase across the length of the n	
Figure 4.7: Slices of relevant hemodynamic variables from the 3-D nume	rical results
Figure 4.8: Equivalent stress map plot of the structural domain for two di	fferent
arrangements of material properties using the same geometry	
Figure 4.9: Maximum stress patterns and the inlet boundary condition of	the soft-soft
plaque configuration model analyzed under the one-way and fully couple	ed methods
Figure 4.10: Histogram of the number of nodes according to their stress r	ange value
Figure 4.11: Histogram of the number of nodes for the stress range values	
comparison of high (150-110 mmHg) vs. low (120-110 mmHg) pressure	
Figure 5.1: Pressure drop values across the length of the stenosis at differ	
Figure 5.2: IVUS Reconstructed geometries of ruptured plaques	-
Figure 6.1: Vector plot of the principal stress orientations within the fibro	
from a fluid-structure interaction numerical model using idealized and re-	
geometries	
Figure 6.2: Longitudinal cut of the diseased branching point of the left co	ronary artery
specimen	
Figure 6.3: (top) Binarised image of the histopathological specimen. (bot	
orientations as computed by image processing superimposed on a graysca	
collagen fibers. The image corresponds to a lateral view of a longitudinal	
fibrous cap at 10X magnification.	
Figure 6.4: Composition of images of collagen fibers (stained blue) in a l	
section of the peak of the fibrous cap stained with the Masson Trichrome	
magnification factor	
Figure 6.5: Top view of a longitudinal section of the fibrous cap tissue pr	
Masson Trichrome staining protocol	
Figure 6.6: Maximum principal stress vs. percentage of area stenosis at the	
of the peak of the fibrous cap	
Figure 6.7: Deviation angle of the principal stress point atop the peak of the	the plague vs
percentage of area stenosis	
Figure 6.8: Schematic drawing of the orientations of the principal stresses	
of the plaque in different percentages of area stenosis.	
Figure 6.9: Collagen fiber orientation vector plot as a result of computation	
analysis of the lateral-longitudinal section of the peak of the fibrous cap	
Figure 6.10: Rose plot histogram of the image analysis in Figure 6.9	
Figure 6.11. Collegen fiber orientation wester man as a result of accounts	
Figure 6.11: Collagen fiber orientation vector map as a result of computa	
analysis (Top view of fibrous cap)	

Figure 7.2: MicroCT image of a cross-section of the same specimen above. Notice th	e
calcified areas around the edges of the plaque's core.	136

# Chapter 1 – Introduction

# 1.1 Introduction to atherosclerosis and atherogenesis

Atherosclerosis is a pathological condition that is characterized by the formation of plagues that narrow the lumen of arteries. The formation of atherosclerotic plagues within the coronary arteries can stop the perfusion of blood to the lower parts of the myocardium and possibly lead to ischemic syndromes such as sudden cardiac death, acute myocardial infarctions, and unstable angina [1]. This disease is the result of a chronic inflammatory response in the walls of arteries and it involves both lipid and cellular accumulation in the vessel wall. It is now recognized that plaque vulnerability leading to rupture is the major cause of unstable angina, myocardial infarction, and sudden cardiac death [15]. In this study, we discuss the effect of mechanical and pathobiological variables involved in the physical disruption of the coronary plaque. However, it is in the scope of this study to treat biological factors as a pre-requisite for a mechanical event to trigger the disruption. Plaque rupture is a phenomenon that can be approached as either an acute failure of the fibrous cap due to a sudden increase in mechanical stress, or as the culmination of a chronic injury progression due to the cyclic stress or fatigue. We suggest that the ultimate trigger for rupture is the failure of the plaque's fibrous cap due to mechanical fatigue as it is the most critical component in terms of structural stability (Fibrous Cap Mechanical Fatigue or FCMF).

A normal artery wall is composed of three layers: intima, media, and adventitia (Figure 1.1). The intima is normally composed of a monolayer of squamous endothelial

cells surrounded by a thin layer of subendothelial connective tissue called the internal elastic membrane (IEM). The media is the thickest layer and it is mainly composed of circularly arranged connective tissue fibers and it is rich smooth muscle cells in the coronary arteries as these are of the muscular type. The adventitia is the outermost layer and it is mainly composed of collagen fibers.

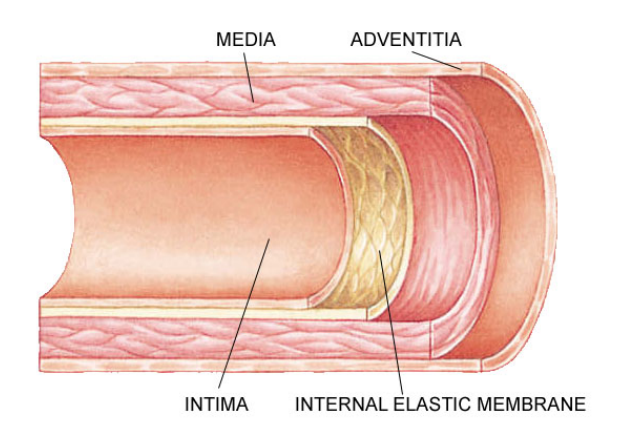


Figure 1.1: The layered structure of arteries

The process of atherosclerosis begins with the infiltration of fatty substances through the endothelium in the intimal layer of the arterial wall [2]. Elevated levels of lipoproteins in the plasma, such as very low density lipoprotein (VLDL) and low density lipoprotein (LDL) have been demonstrated to be associated with an increased incidence of atherosclerosis [3]. A major cause of injury to the endothelium is the infiltration of LDL particles, which can be oxidized and modified within the plaque [4]. Particles of oxidized LDL (oxLDL) promote atherogenesis by altering the normally nonthrombotic and nonadhesive endothelial surface [5]. The oxLDL particles within the plaque, free

radicals, cytokines, and growth factors can damage or activate the endothelium and result in an increased permeability or adhesion of leukocytes to the endothelial surface as well as their migration from the arterial lumen to the intima [6]. They also serve as an active initiator for the recruitment of monocytes and macrophages. Also, the most common factor for the stimulus of intimal hyperplasia is damage to the endothelium and media of the artery, which has been implicated as the initial step in plaque formation [7,8].

The infiltration of monocytes and smooth muscle cells (SMCs) into the developing plaque further enlarge the plaque process by two distinct processes: the migration and proliferation of SMCs into the intima from the media and the accumulation of extracellular matrix deposited by the SMCs such as collagen, elastin and some proteoglycans [9]. The deposition of these matrix components by the SMCs causes an increase in plaque size and the development of a fibrous layer that separates the plaque's contents from direct contact with the bloodstream is known as the fibrous cap. This layer is mostly composed of collagen connective tissue and smooth muscle cells, and to a lesser extent elastin and proteoglycans (Figure 1.2). Fibrous caps can vary widely in thickness, cellular content, and connective tissue content.

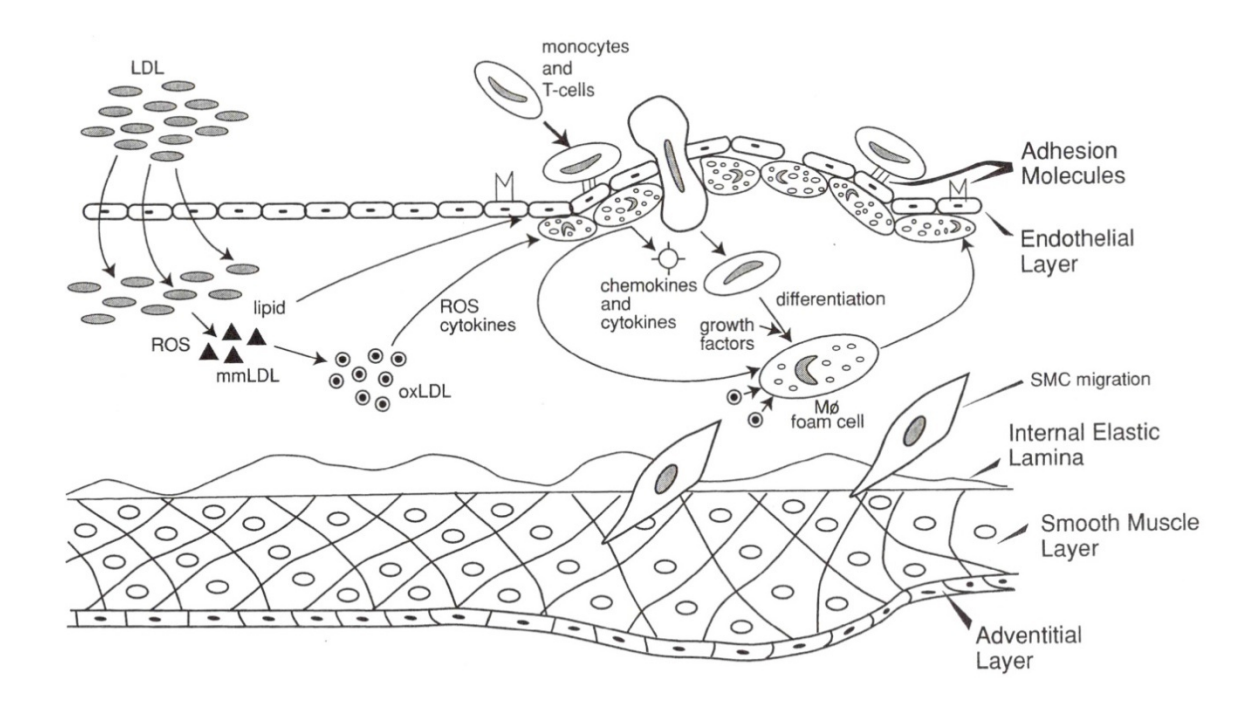


Figure 1.2: Schematic representation of the process of atherogenesis [10]

The fibrous cap's connective tissue content depends on the quantity of growth factors present in the cap's region and their ability to stimulate SMCs to produce extracellular matrix components; some cytokines produced by T lymphocytes and macrophages can inhibit the proliferation of SMCs and their ability to synthesize collagen. Furthermore, proteolytic enzymes secreted by foam cells present as a result of inflammatory activity can degrade the collagenous structure of the plaque.

The plaque's atheromatous core does not contain collagen; it is rich in extracellular lipids, predominantly cholesterol and its esters [11]; it is hypocellular, however, foam cells from macrophage origin are present at the periphery of the core [12]; its material properties can range from a soft consistency to a relatively rigid core in the case of calcified cores. It is believed that macrophage foam cell death by necrosis or apoptosis plays an important role in the accumulation of extracellular lipids [13,14].

In summary, atherosclerosis can be described as an inflammatory disease involving inflammatory cells such as monocytes, macrophages and T cells that play an important role in the initiation and progression of intimal hyperplasia through the production of cytokines and growth factors that can induce SMC migration and proliferation. SMCs in turn deposit extracellular matrix components that further enlarge the plaque.

An adverse possible outcome of atherosclerosis is the formation of a plaque that can lead to a total or partial occlusion of the artery or the rupture of the plaque that can lead to a thrombus formation that could also result in an acute coronary syndrome such as sudden cardiac death, acute myocardial infarction or unstable angina.

# 1.2 Plaque rupture

The rupture of the fibrous cap is clinically significant in cases where the thrombotic response to the rupture occludes the vessel lumen to a high degree, either with a partial or total occlusion. It is now recognized that plaque vulnerability leading to rupture is the major cause of unstable angina, myocardial infarction, and sudden cardiac death [15]. The contact between the plaque's highly thrombogenic contents and the blood flow can lead to a thrombus formation and consequently cause a complete or near-complete occlusion of the vessel which can lead to an acute myocardial infarction. It is estimated that two thirds to three quarters of all arterial thrombi are caused by plaque rupture [16] (Figure 1.3).

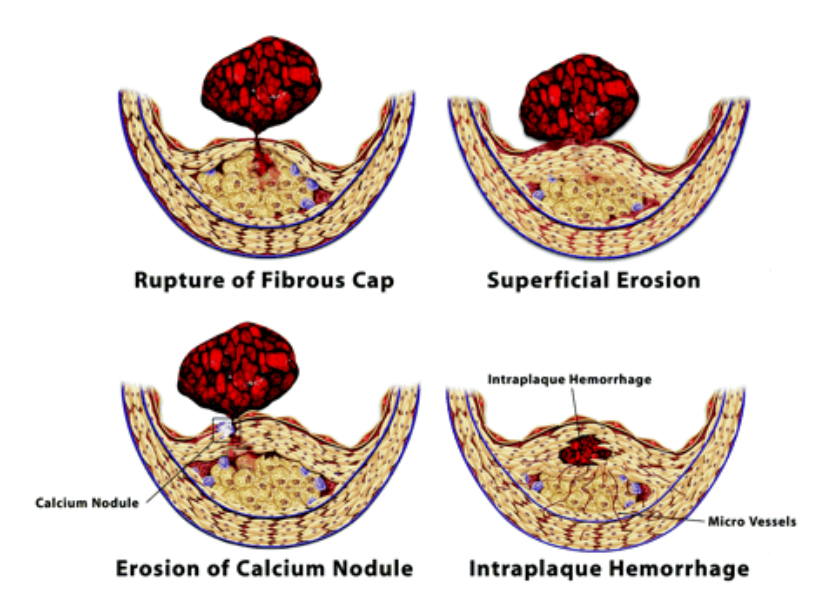


Figure 1.3: The four most common mechanisms of thrombi formation. The rupture of the fibrous cap represents two thirds to three quarters of all cases [16].

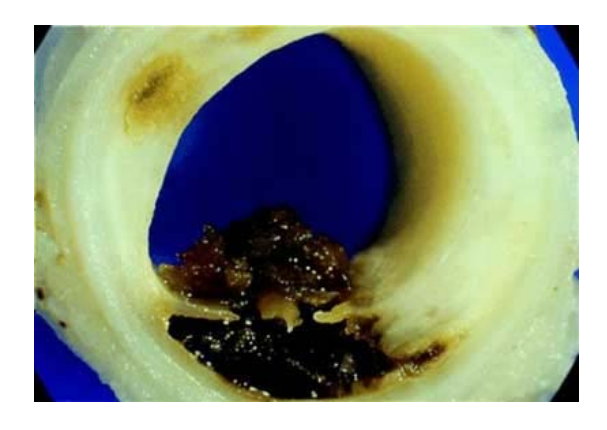


Figure 1.4: A section of a specimen showing a fibrous cap rupture

It is hypothesized that hemodynamic forces and intraluminal pressure play a significant role in the rupture mechanism of the fibrous cap through cyclic fatigue as they induce mechanical stresses to the tissue that could lead to rupture. Recent evidence strongly suggests that mechanical forces and biologically active processes are not

separate factors in the disruption of the plaque, but rather are intricately associated components that can influence the stability of atherosclerotic lesions [17].

Pathologists report from histopathological studies of ruptured plaques that there are common features shared by these ruptured specimens. Typically, ruptured lesions had a large and soft lipid core, many inflammatory cells, and a thin fibrous cap. These types of lesions are also associated with acute coronary syndromes [18,19,20]. While the scientific community agrees that mechanical factors can influence the site and mode of tissue failure, it is not yet fully understood to which extent the different mechanical variables affect the initiation and propagation of such failure. The possible mechanisms could be either by high mechanical stress or by mechanobiological stimulation of the endothelium which would further promote inflammatory activity and thus induce tissue degrading enzymes that would contribute to the weakening of the structural components of plaque [21].

# 1.2.1 Mechanical factors of plaque rupture

#### 1.2.1.1 Core stiffness

Plaques that have larger lipid cores tend to be more vulnerable to rupture than plaques that have smaller lipid cores [22, 23] and lesions with a lipid core occupying greater than 40% of the plaque size have a higher risk of rupture and thrombus formation [24]. Large atheromatous cores contain more material that is softer and more compliant than fibrous tissue. The soft material properties of the plaque can contribute to the instability of the lesion as there is a greater stress imposed on the fibrous caps of these

type of plaques [25]. This effect is further demonstrated in this thesis using three-dimensional numerical models of stenosed arteries. The soft and compliant properties of a large lipid core allow for a greater displacement of the fibrous cap since it takes less deformation energy to strain the core than plaques that have rigid calcified or fibrous cores.

Studies have shown that lipid-lowering agents have been successful in slowing the progression of atherosclerosis and the incidence of acute coronary events [26]. A possible hypothesis of this is that lipid lowering causes the plaque to be stiffer, providing a more rigid structural support to the fibrous cap tissue. A stiffer core would require significantly more mechanical deformation energy to be displaced in the same proportion than a soft core. Therefore, the deformation of the fibrous cap tissue will be lower in a stiff core and thus it will reduce its mechanical strains and consequently its instability.

### 1.2.1.2 Fibrous cap thickness

The fibrous cap thickness and composition is another feature that plays an important role in determining the stability of the plaque. It is mainly composed of collagen fibers and smooth muscle cells [27]. Imbalances in the ability of smooth muscle cells to synthesize extracellular matrix components or the amount of proteolytic enzymes secreted by inflammatory cells that can degrade the matrix components can affect the stability of the plaque. Stable lesions have a significant amount of extracellular matrix in the plaque but more importantly in the fibrous cap; unstable lesions have reduced matrix material present. Therefore, the thickness of a fibrous cap is the result of the balance between the synthesis of extracellular matrix and the degrading effects of proteolytic

enzymes such as matrix metalloproteinases. Mechanically speaking, thin fibrous caps represent a reduced traverse section area of the cap withstanding the same physical forces exerted by the intraluminal pressure and blood flow; this translates directly into a higher mechanical stress.

# 1.2.1.3 Plaque size

Another important feature that influences plaque instability is the plaque size. However, this feature is commonly reported by clinicians as a function of the lipid core size and not the percentage of area stenosis [28,29]. Arterial enlargement in the proximity of stenotic plaques has been reported by Glagov [30], who studied atherosclerotic enlargement in histological cross-sections of human hearts and found that coronary arteries enlarge proportionally to the increase in plaque area. In this thesis, we defined the term of plaque size to be analogous to percentage of area stenosis and assumed that no arterial remodeling or enlargement is involved.

The percentage of area stenosis plays a very important role in the mechanical stress concentrations within the plaque as demonstrated in the following pages in this thesis. The presence of a stenosis in any artery affects the hemodynamic variables of velocity, pressure, and wall shear stress. The result of the overall combination of these variables translates into hemodynamical pressure gradient forces that act directly on the surface of the plaque. The more severe stenoses (75% or more of area occlusion) cause a significant change in the pressure drop or energy loss as a result of viscous and geometrical effect due to the stenosis. This energy loss translates partly into the

mechanical deformation of the entire plaque. However, the weakest and softer structures will suffer the highest deformations and thus high mechanical stresses.

In two-dimensional numerical finite element models used by Loree, Lee, Kumar, and Ohayon [31,32,33,34] of cross-sectional views of diseased arteries, the high stress regions were located at the junction between the plaque and the normal vessel, which corresponds to the regions of rupture. However, these analyses were performed under a two-dimensional environment of cross sections of arteries; they used intraluminal pressure as the only variable of physical force applied to the artery wall and therefore could not account for the kinetic energy loss effect of the axially oriented hemodynamic flow. The work presented in this thesis had the aim of assessing the three-dimensional stress distribution within the plaque in order to obtain the full three-dimensional stress tensor in all spatial locations within the artery and to assess the effect of a three-dimensional hemodynamic and transient flow.

## 1.2.1.4 Fatique failure

Plaque rupture is a phenomenon that can be approached as either an acute failure of the fibrous cap due to a sudden increase in mechanical stress, or as the culmination of a chronic injury progression due to the cyclic stress or fatigue [35]. Analyses that consider the realistic and time-dependent conditions of the coronary flow and pressure waveforms acting on the plaque can provide more accurate information on the spatial and time distribution of the stresses. Given the appropriate fatigue life curves for the soft tissue, fatigue life could be estimated for each node in the numerical model parting from the calculated mean stress, frequency and the amplitude of the cyclic stresses.

We assumed an exponential pattern for the fatigue curve behavior of the fibrous cap tissue based on the work of Gilpin [36] that demonstrated and extrapolated such behavior based on experimental results as a function of cycles count (Figure 1.5).

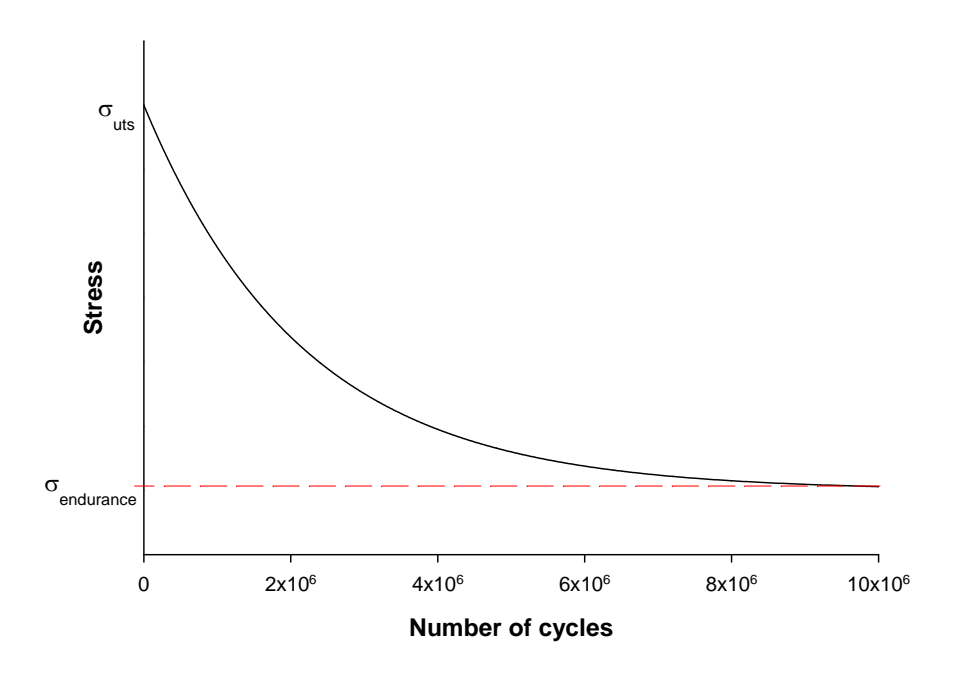


Figure 1.5: Typical exponential behavior of a stress vs. number of cycles curve

The failure criterion used to predict fatigue failure was derived from the Goodman criterion [37] which states that the sum of the mean stress divided by the endurance limit plus the ratio of the and stress amplitude divided by the ultimate tensile strength shall be equal to one in order to achieve a life infinite number of cycles (equation 1.1).

$$\frac{\sigma_{\text{mean}}}{\sigma_{\text{endurance}}} + \frac{\sigma_{\text{amp}}}{\sigma_{\text{uts}}} = 1 \tag{1.1}$$

Our modifications to the Goodman criterion did not establish a value at which no failure would occur. We rather defined a ratio of the exponential shape of the curve and the endurance limit (equation 1.2). With this, we were able to estimate the number of cycles before failure based on the calculated values of mean stress and stress amplitude for each particular node in the transient numerical analyses and based on a hypothetical S-N curve for fibrous cap tissue.

$$\frac{\sigma_{\text{mean}}}{\sigma_{\text{endurance}}} + \frac{\sigma_{\text{amp}}}{\sigma_{\text{uts}}} = \frac{\left(\sigma_{\text{uts}} - \sigma_{\text{endurance}}\right)e^{-\alpha n} + \sigma_{\text{endurance}}}{\sigma_{\text{endurance}}}$$
(1.2)

We focused in the assessment of the mechanically induced and transient stresses in the fibrous cap tissue due to the hemodynamic changes across the stenosis in a three-dimensional field over one cardiac cycle. This three-dimensional and transient perspective provided information on the spatial and temporal distribution of the principal stresses to assess the possible initiation and paths of fissure propagation. Computational finite element methods and fluid-structure interaction analysis were used to develop a predictive model of the physical interaction between the blood fluid domain and the diseased arterial wall structural domain. The analyses were done using realistic models reconstructed from intravascular ultrasound (IVUS) imaging of in-vivo cases of human diseased coronary arteries. The main physical variables of localized pressure, shear stress, velocity and pressure gradient forces were calculated to assess their effect on the arterial wall stresses. The transient numerical analyses provided the necessary data to compute the individual node values of the mean stress and stress amplitude and thus the number of cycles to failure. Using this information, we were able to introduce the concept of fibrous

cap mechanical fatigue (FCMF). Such concept establishes that the plaque's fibrous cap ultimately fails by the cyclic stretching caused by the pulsatility of the artery rather than a nominal stress threshold value.

# 1.2.1.5 Multiple plague vulnerability

Another factor that we considered relevant in this thesis was to analyze the effect of the hemodynamic patterns in the presence of multiple plaques and their outcome on the mechanical stress distribution on the plaques. To the best of our knowledge, there is no literature mentioning the vulnerability of a multiple plaque configuration. In this research work, we demonstrated that the mechanical stresses can vary greatly in magnitude and location depending on the position of the plaques relative to each other, their material properties, and their morphological features such as the percentage of area stenosis, fibrous cap thickness, and lipid core size.

#### 1.2.1.6 Myocardium motion

The myocardium's extensive movement and stretching may have some impact on the mechanical stresses within the plaque. However, we only considered an Eulerian frame of reference to analyze the diseased section of the coronary arteries in order to reduce the complexity of the numerical simulations and thus avoid non-convergence. Furthermore, the element count would have had to be significantly larger to analyze the entire coronary branch and at the same time maintain a reasonable element resolution to assess the mechanical stresses at the fibrous cap scale level. Zeng [38] reported that the

hemodynamic effects of the right coronary artery (RCA) motion based on cineangiograms can be neglected in computational studies as only modest differences were found between fixed and moving RCA models. Other studies by Ramaswamy [39] and Kolandavel [40] have suggested that the myocardium motion does have an effect on the overall hemodynamics, more specifically when dealing with high degrees of curvature of the artery. For the purposes of our analyses, we only considered a straight section of the artery under no motion as we did not have information available on the subject's myocardium motion from the intravascular ultrasound studies.

#### 1.2.1.7 The role of hemodynamic flow on mechanical stresses

While many researchers have investigated the role of intraluminal pressure to analyze the tissue mechanics and predict rupture-prone areas, few publications have addressed the issue of the effect of blood flow, not pressure, on the mechanical stresses. Doriot [41] performed steady-state analyses on a two-dimensional longitudinal stenosed artery model and concluded that the flow influences the mechanical stresses of the fibrous cap.

A common method used by clinicians to determine the mechanical tension within the artery wall is Laplace's law (equation 1.3), which states that tension in the vessel wall is proportionally higher with increasing blood pressure and intraluminal diameter.

$$T = \frac{P \cdot R}{M} \tag{1.3}$$

In equation 1.3, P represents the intraluminal pressure, R is the radius of the external surface of the vessel, and M is the thickness of the vessel wall. Laplace's equation may does not account for all the structural components of the plaque. Moreover, it only considers intraluminal pressure as the only variable that can affect the tension in the artery wall, therefore, it cannot account for the hemodynamic effect of blood flow. Pressure in a fluid may be considered to be a measure of energy per unit volume or energy density. Pressure alone just represents the potential energy in the system, and it does not account for the kinetic energy provided by the blood flow entering the system. Moreover, the pressure term used in Laplace's law can only be used as a single hydrostatic value without considering the pulsatile flow changes or pressure patterns across the stenosis. In this context, it becomes necessary to analyze the three-dimensional and transient perspective of the fluid domain to evaluate the blood flow or kinetic energy effects on the mechanical stresses. Realistic patterns of blood flow and pressure waveforms of a left anterior descending (LAD) coronary artery were used to simulate the inlet conditions of our numerical models [42] (Figure 1.6).

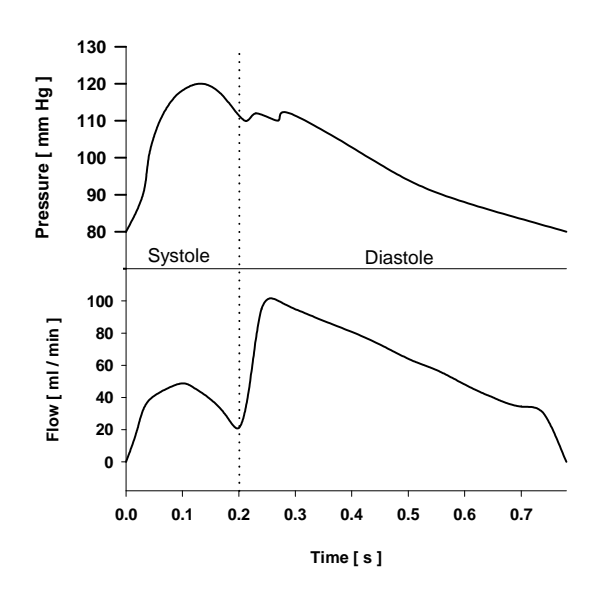


Figure 1.6: Pressure and flow waveforms for a left anterior descending (LAD) coronary artery [42]

# 1.2.1.8 Anisotropic properties of the tissue

Anisotropy is the property of being directionally dependent for a particular physical property. In the context of this research, we were interested in measuring the elastic anisotropic properties of the collagenous tissue of the plaque as it becomes relevant when analyzing the mode of failure and crack propagation in the tissue. The fibrous cap is a collagen fiber reinforced biological material inside a smooth muscle cell matrix; our hypothesis is that it will behave similarly to composite materials. The stiffness properties of any composite material will depend on the orientation of the fibers; it will show strong properties in the direction of the fibers, and relatively weaker properties at a perpendicular angle to them, suggesting that failure can occur in the matrix material and propagation of such failure could follow a pattern parallel to the fibers (Figure 1.7).

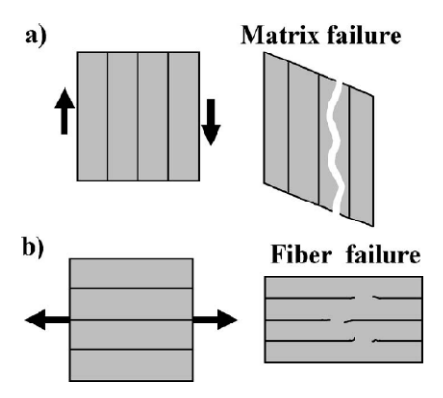


Figure 1.7: Failure modes of composite materials [43]

a) A matrix failure can occur if the forces are perpendicular to the fibers or they induce shear stress. b) Fiber failure occurs when the applied forces are parallel to the fibers.

The orientation of the collagen fibers inside most biological tissues tend to be parallel to the principal tensile stresses [44,45,46]; we hypothesized that the fibers within the fibrous cap follow the principal stresses as predicted by computer models of stenosed arteries under the effect of blood flow. However, our numerical models did not consider anisotropic properties of the plaque's components based on collagen fiber orientation as we did not have any information regarding the true anisotropy of the tissue. Therefore, the numerical models used in this work were considered as solid homogenous bodies. Our main goal in the third article of this thesis was to provide a first insight into the diseased vessel anisotropy by measuring the angle orientations of the fibers with respect to the longitudinal axis of the vessel. We performed histopathological studies of human fibrous caps cut in longitudinal sections in different perspectives in order to visualize the orientation of the connective tissue by computational image processing techniques. The

results provided by these image processing methods can help in future numerical analyses when coupled with realistic anisotropic models and thus obtain very accurate information on the distribution of stresses and the modes of tissue failure and crack propagation.

# 1.2.1.9 Viscoelastic properties

The rate at which blood travels through the diseased artery will most likely have a significant effect in the mechanical stresses in the plaque. The simplest form of the constitutive model for linear elastic materials can be modeled using Hooke's law  $\sigma$ =E $\epsilon$ , where  $\sigma$  is the stress, E is the elastic modulus of the material and  $\epsilon$  is the strain occurring under a given stress. Similarly, the viscoelastic behavior can be modeled with the Maxwell equation:

$$\frac{d\varepsilon}{dt} = \frac{\sigma}{\eta} + \frac{1}{E} \frac{d\sigma}{dt} \tag{1.4}$$

Where  $\eta$  is the viscosity of the material,  $\sigma$  is the mechanical stress, d $\varepsilon$ /dt is the time derivative of the stress, and E is the Young's modulus of the material. Under a viscoelastic scenario, the material stresses in the plaque would be suffering higher or lower stress values depending on the rate of strain. In normal coronary flow waveforms there is a steep rise in flow at the beginning of diastole. Based on our numerical results further explained in the second article number of this thesis, this rapid rise in blood flow has a great impact on the mechanical stresses and

it may initiate plaque fissuring. Our analyses did not consider the viscoelastic properties of the tissue as they are still unknown for the fibrous cap tissue.

### 1.2.2 Biological factors of plaque rupture

#### 1.2.2.1 Inflammation

Inflammation is the biological response of the body to injury, pathogens or irritants. It is a protective attempt of the organism to remove the injurious stimuli and initiate the healing process of the tissue. In the initial stages of its process, inflammatory cells have a protective function. However, when the inflammation reaches a chronic stage, secretory products from the same cells may damage tissue components and thus induce even more inflammatory activity to repair the newly damaged tissue [47].

A number of studies have shown that atherosclerosis is an inflammatory process as a number of inflammatory mediators have been detected in plaques [48, 49]. The inflammatory processes can stimulate the synthesis of extracellular matrix components and reinforce the structural integrity of the plaque. On the other hand, the same inflammatory process can stimulate the degradation of the connective tissue through the secretory products of inflammatory cells or by inhibiting the collagen production in the fibrous cap and thus induce plaque instability. Intraplaque inflammation is closely related to plaque ruptures [50, 51].

Another mechanism for the weakening of the plaque caused by inflammatory activity is the inhibition of collagen production in the fibrous cap. Smooth muscles cells (SMCs) produce all the matrix components of the plaque: collagen, elastin and some

types of proteoglycans. The T-cell cytokine, IFN- $\gamma$ , produced by activated T lymphocytes and macrophages in plaques, inhibits the proliferation of SMCs and thus can decrease their collagen synthesis capabilities [52].

# 1.2.2.2 Extracellular matrix degradation

A mechanism that may assist and result in plaque rupture is the weakening of the fibrous cap through the degradation of the extracellular matrix, the component of the plaque that provides its structural integrity. The matrix is degraded by proteolytic enzymes called proteases, of which the main type that are associated with unstable plaques are the matrix metalloproteinases (MMPs) [53]. More than 20 types of the MMP family of enzymes have been identified so far and each can degrade at least one and sometimes several components of the extracellular matrix [54]. In human atherosclerotic plaques there is increased expression of MMPs in the regions where ruptures commonly occur. Studies have demonstrated the presence of active enzymes such as MMP-1, MMP-2, MMP-9, and MMP-12 as an expression of macrophages present in the plaque [55,56]. The activity of these enzymes can result in an accelerated weakening of the matrix proteins of the plaque, in particular collagen type I, the main protein type of connective tissue in the fibrous cap.

# 1.2.3 Summary of the biomechanical factors involved in plaque rupture

In the following table we present a summary of the factors that are known to be associated with the disruption of the coronary plaque and that were discussed in this chapter:

#### Physical, Mechanical, Morphological

- Area stenosis
- Fibrous cap thickness
- Core stiffness
- Intraluminal pressure magnitude
- Blood flow magnitude
- Anisotropic properties of the tissue
- Fatigue failure
- Multiple or single plaque configuration
- Viscoelastic properties of the tissue
- Stretching and flexing of the myocardium

# **Biological**

- Active intraplaque inflammatory processes
- Increase in macrophage activity
- Extracellular matrix degradation through MMPs
- Decreased or inhibited collagen synthesis by SMCs

Table 1. Summary of the factors that may affect plaque instability

The respective role of biological and mechanical variables in the rupture of vulnerable plaques (VP) is not completely elucidated. Although it was shown that ultimately the rupture process is biologically rooted, mechanical variables play an important role both for the initiation and progression of the disease. Mechanical variables are always present before and during the pathology and are directly involved in its evolution. In fact, given that the mechanical disturbances get more important with plaque morphological changes the mechanical variables contribute to accelerate the progression of the pathology.

However, the detailed mechanisms responsible for the plaque rupture are not completely known. In fact, vulnerable plaques exhibit some paradoxical features. Indeed, they generally have small percentage stenoses (< 50 %). Given that the associated hemodynamic perturbations are less than with larger plaques, this raises questions in terms of the reasons why they are the ones more prone to rupture.

As previously discussed, certain biological characteristics have been correlated with vulnerable plaques (MMPs, thin fibrous cap, large lipid inclusion in the vicinity of a hard inclusion). However, we think that certain anatomico-structural aspects that were unexplored before could play a significant role in the rupture of VP. We hypothesize that these aspects would also contribute in answering the paradoxical behaviours of VP. We consider three such mechanical variables that could play an important role in the rupture of VP.

# 1.2.4 Summary of hypotheses

In this section we present a summary of the most relevant hypotheses and results of plaque rupture analyses that were based from the explanations addressed in this thesis. We hypothesize that mechanical fatigue in the fibrous cap (FC) is the ultimate characteristic that triggers the rupture. For this, we have elaborated three main hypotheses and have demonstrated them through the results obtained in this thesis:

Hypothesis: Fibrous cap mechanical fatigue (FCMF) is the result of the combined effects of the cap thickness, relative inclusion stiffness and percentage of stenosis. This possibility was recently suggested by Finet [57] but still remains unexplored.

Results: In chapters 2 and 4 of this thesis, we confirm the hypothesis of the combined effects and we show that FCMF of VP exhibit similar critical behaviours normally associated with higher percentage stenoses.

Another underexplored observed phenomenon in the fact that for similar cap thickness, similar relative inclusion stiffness and similar percentage stenosis, certain plaques appear to be more stable.

Hypothesis: FCMF can be influenced by the global structure of the obstructive pathology in particular in the context of multiple stenoses [58, 59]. This specific hypothesis is supported by a recent case report [60].

Results: In chapter 4 of this thesis, we show that in the case of multiple stenoses (modeled as two adjacent stenoses) that FCMF is higher when the VP is

downstream of a stable plaque (SP) as compared to a VP upstream of a SP. The effect can be maximum with a specific stenosis to stenosis distance (depending on plaque morphologies, material properties and hemodynamic conditions) and a relative angular eccentric position of 180 degrees from each plaque.

VP are also known to be more prone to rupture under physical exercise [61, 62]. In addition, to the previous mechanical conditions that become more severe under exercise and the recent involvement of C-reactin [63].

Hypothesis: We also hypothesize on the possible role of the ultrastructure of the FC for the FCMF. Specifically, we considered the anisotropic effects of the collagen fibers architecture in the caps.

fibers is strongly dependent on the stress in the FC. In fact, the collagen fibers align with the principle stresses orientations to sustain the new loading conditions. As a result, for certain plaque morphologies the collagen will establish a certain anisotropy (characterized with a transversely anisotropic model with certain values angular orientations of

Results:

of blood pressure and flow rate which create new loading conditions for

the fibers). This new arrangement is mainly established under rest

conditions. However, at exercise the plaque is deformed due to an increase

In chapter 6 of this thesis, we show that the anisotropy of the collagen

which the deformed fibers arrangement with respect to rest condition render the composite fibrous cap fragile.

The rupture of the fibrous cap is a complex phenomenon that is not yet fully understood. The analysis of the interaction between all the possible mechanical and biological variables involved in a heuristic approach makes the analysis a very challenging task. Furthermore, the exact biological responses of cells from mechanical stimulation are still an unknown issue. Instead, and in order to simplify the work in this thesis, we only considered the mechanical variables to be the triggers of plaque disruption; the biological onset of a vulnerable plaque was considered to be a prerequisite for a mechanical event to trigger the disruption of the fibrous cap.

# 1.3 Imaging methods to assess plaque vulnerability

The current methods and technologies employed by clinicians to assess plaque vulnerability can only assess the severity of the lesion in terms of measuring the percentage of area stenosis or measuring the morphological features of the fibrous cap. For example, coronary angiography is a luminographic method that only visualizes the silhouette of the lumen by injecting contrast media that is visible in X-rays; however, angiography may fail to demonstrate the severity of the disease in complex lesions with highly eccentric luminal shapes. Intravascular ultrasound (Figure 1.8), and optical coherence tomography (OCT) can image with good detail the morphological or material features of the plaque.

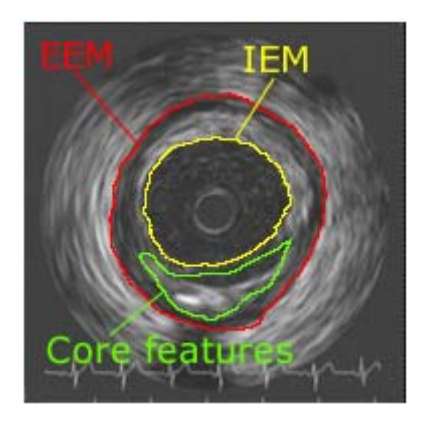


Figure 1.8: Intravascular ultrasound image trace of a diseased coronary artery.

Laser spectroscopy can identify the material properties of the plaque by studying the spectral content of white light diffusely reflected from biological tissue; or by studying the fluorescence emissions of the tissue when excitation light is present. These technologies allow to characterize the lesion's properties by identifying calcified inclusions, fibrous tissue and fibro-fatty components within the plaque as well as their material compositions and properties. The clinician can then assess the degree of the lesion vulnerability by personal experience or by statistical references of the features of the plaque. However, these methods for plaque vulnerability assessment are semiempirical as they still make use of statistical references on the plaque's features as a guide to determine whether it will fail or not. Intravascular elastography is the only technology that was developed to indirectly assess the mechanical stresses by measuring the localized plaque compression values per angle from IVUS images. Circumferential stresses can then be calculated from the radial strains measured from these images. IVUS, OCT, and elastography can only analyze the plaque's morphology in a two-dimensional crosssectional view and thus their analyses do not account for the three-dimensional physics that occur in the diseased artery.

As mentioned before, plaque vulnerability is not only a mechanical process, but a combination of both mechanical and biological factors that may trigger plaque instability. A technique that could deterministically assess the mechanical stresses in three-dimensions coupled with a technology that could identify inflammatory activity in-vivo would be desirable in order to further refine plaque vulnerability prediction.

The work done in this thesis uses a deterministic approach by numerically calculating the mechanical stresses of the fibrous cap in a three-dimensional field as a measurable variable that can be correlated with tissue failure experiments. Transient blood flow effects are considered in the analyses in order to better understand the hemodynamic effect on the mechanical stresses of the fibrous cap.

# 1.3.1 Morphological reconstruction of diseased vessels through intravascular ultrasound

The reconstruction of the three-dimensional geometry models of the diseased vessels was done using a series of multiple IVUS segment images. The reconstructed models were used for the fluid-structure interaction computational analysis to obtain the mechanical stresses. Patient-specific cases of diseased coronary arteries were reconstructed using IVUS images of cross-sectional views in the longitudinal direction. All IVUS segment images were created using motorized pullbacks of the ultrasound transducer commencing from the distal side of the stenosis. Only those segments distanced 1 mm apart were kept in order to simplify the 3D geometry reconstruction process even though the IVUS pullback was able to interrogate images at higher resolution intervals. The distance between segments of 1 mm was chosen as it provided

results with sufficient details when connecting each of the segments using a loose fit spline-based swept surface. Our goal was to reconstruct a surface that avoided jagged edges or discontinuities in the numerical model that would later influence the mechanical stress results. At distances of less than 1 mm (say 0.5 mm), the swept surface produced an unrealistic bumpy surface produced by the small inaccuracies of the traces of each segment at different points in time during the cardiac cycle.

For each IVUS segment, the lumen boundaries were traced at the innermost echogenic layer: the internal elastic membrane (IEM), which is located in the intimal layer. Since there is no acoustic interface between the true adventitia and the perivascular tissue [64], it becomes difficult to assess the true size of the adventitia. Therefore, it was assumed that its outermost layer was located at a mean offset distance of 100  $\mu$ m [65] from the external elastic membrane (EEM) which is located at the medial-adventitial interface.

The coronary arteries are of the muscular type and are normally composed of three layers: intima, media and adventitia. Since intravascular ultrasound (IVUS) cannot clearly distinguish the boundary between the intima and the media or the outermost surface of the adventitia, the artery walls were reconstructed in 3D as a single homogeneous body comprising all three layers from the innermost surface of the lumen up to the outermost layer of the adventitia. In the presence of an atheromatous core, the fibrous cap tissue would be part of the same single body as the artery wall and thus share the same mechanical properties in the numerical models of the stress analyses.

The contour lines were hand traced and smoothed with spline curves using commercial software (Rhinoceros v3.0, Palo Alto, CA) in order to avoid jagged edges or

singularities in the geometry that would result in artifactual stress concentrations when performing the fluid-structure interaction computational analyses as a result of unrealistic sharp corners. None of the reconstructions considered the three-dimensional spatial path of the catheter and therefore the geometries were reconstructed only in a straight formation as there was no curvature data available from the IVUS records (Figure 1.9). A high level of curvature of the vessel segment could potentially affect the numerical results as it can influence the hemodynamic variables such as velocity or wall shear stress to be of greater magnitude in one side of the vessel or plaque. The patient-specific configuration of the vessel would ultimately determine the level of stress of a plaque when comparing a straight formation vs. a curved vessel.

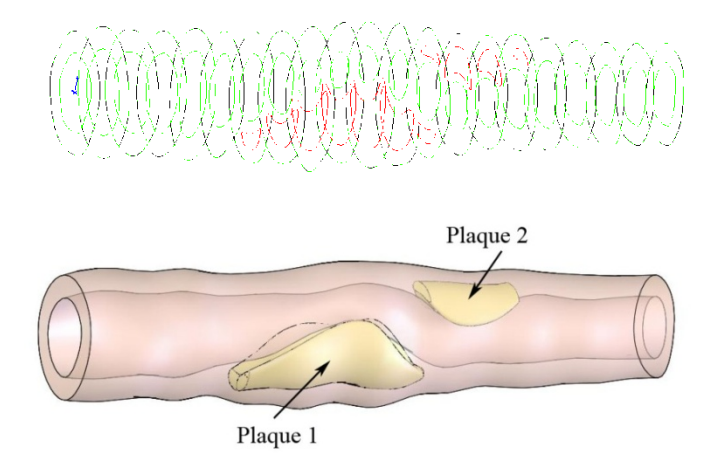


Figure 1.9: Traces of each IVUS segment and the respective 3D reconstruction

Using the same methodology of IVUS segmentation, we also reconstructed seven cases of in-vivo ruptured plaques as they would prove helpful in a reverse engineering approach to determine the true morphology and accurate location of the rupture of the plaques and to better understand how plaque fissuring occurs in real life scenarios.

# 1.4 Computational methods to assess plaque vulnerability

The complexity of the geometry of the plaque, fibrous cap, and necrotic core make it difficult to derive an analytical solution to calculate the mechanical stresses within the plaque's components. Moreover, an analytical solution of patient-specific geometries would prove to be an even more difficult task. Instead, we opted for the analysis of mechanical stress through well known the computational method of finite element analysis (FEA), and fluid-structure interaction (FSI); both methods use the finite element method (FEM) as the basis for numerical calculations.

#### 1.4.1 Finite element method for structural analysis

The Finite Element Method (FEM) is a commonly used tool to find approximate solutions of partial differential equations and integral equations over complex domains. The solution approach is based by approximating the equation to be studied by creating another equation that is numerically stable and does not amplify errors when solving iteratively. A mesh discretization of a continuous domain is performed by dividing such domain into finite triangle subregions or piecewise linear or higher degree basis functions for solution of second order partial differential equations.

The analyses used computational geometric models of stenosed coronary arteries of typical dimensions. The stenosis models were treated as separate compliant bodies of various degrees of stiffness. Figure 1.10 shows an example of the element discretization for the continuous domain of the artery and including two separate bodies representing the atheromatous cores of the plaques. The grid of arranged elements is called a mesh.

Each element is connected to each by discrete points called "nodes", and the number of these depends on the complexity of the element type that would best serve as a solution for a specific analysis. Nodes represent points at which features such as displacements or strains are calculated and they serve as an identification tool when viewing the solutions in structures. Since the scope of this research was to determine the mechanical stresses only at the regions where a plaque and a fibrous cap were present, we only looked at the post-processed results of nodes in the nearby regions adjacent or on top of the plaques in order to have a more accurate statistical measurement of the stress concentrations; but the analyses were performed considering the full set of nodes. The type of element used in our models was SOLID187 and it is a 10-node high order, quadratic displacement behavior element that is well suited to model highly irregular meshes such as the one from figure 1.10.

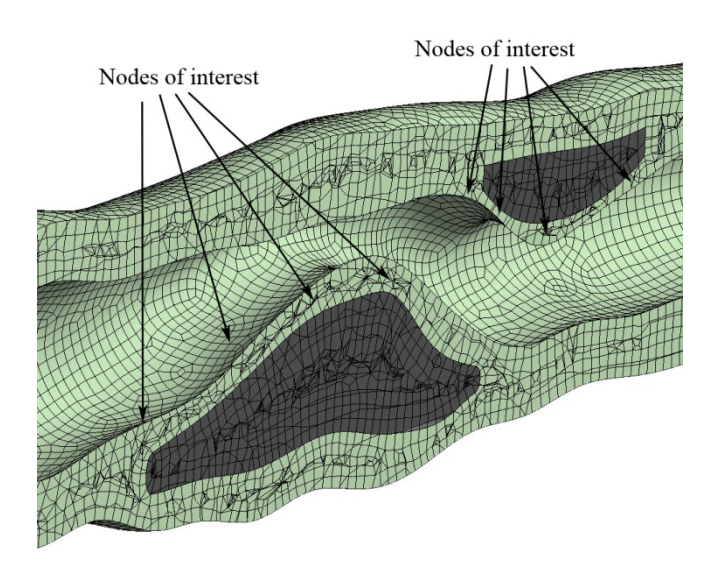


Figure 1.10: Element-discretized domain or mesh for the artery wall and plaque's domains

.

# 1.4.2 Computational fluid dynamics for solving the fluid domain results

The same principle of discretization of the fluid domain into elements is used for computational fluid analysis. The basic principle of solving models in fluid domains is to numerically approach a solution of the Navier-Stokes and continuity equations (equations 1.5, 1.6). These equations establish that any changes in the momentum in infinitesimal volumes of fluid are the sum of the viscous forces, changes in pressure, gravity, and other forces acting inside the fluid; and they dictate a velocity result rather than a strained position as in solid mechanics theory.

$$\rho \left( \frac{\partial \mathbf{v}}{\partial t} + \mathbf{v} \cdot \nabla \mathbf{v} \right) = -\nabla p + \mu \nabla^2 \mathbf{v} + \mathbf{f}$$
 (1.5)

$$\nabla \cdot \mathbf{v} = 0 \tag{1.6}$$

The inlet conditions were established using normal transient coronary blood flow and pressure values (Figure 1.6). Once the fluid domain results were available for a particular timestep (Figure 1.11), they were coupled with the structural domain to obtain the mechanical stresses of that particular timestep. Blood properties were assumed to be constant in all analyses: incompressible as the water content in the plasma is very high and the viscosity was kept at 3.6 centipoises. No turbulence models were used in the CFD analyses as the typical Reynolds number of blood flow in the coronaries is relatively low (around 200). Moreover, turbulence models such as k-Epsilon, k-Omega, eddy viscosity

transport equation, Omega Reynolds stress, etc. usually required several unknown parameters from blood viscous properties that would have to be assumed also. For simplicity of the model, we used a non-turbulent fluid domain model. However, such CFD model still allowed for flow separation and recirculation.

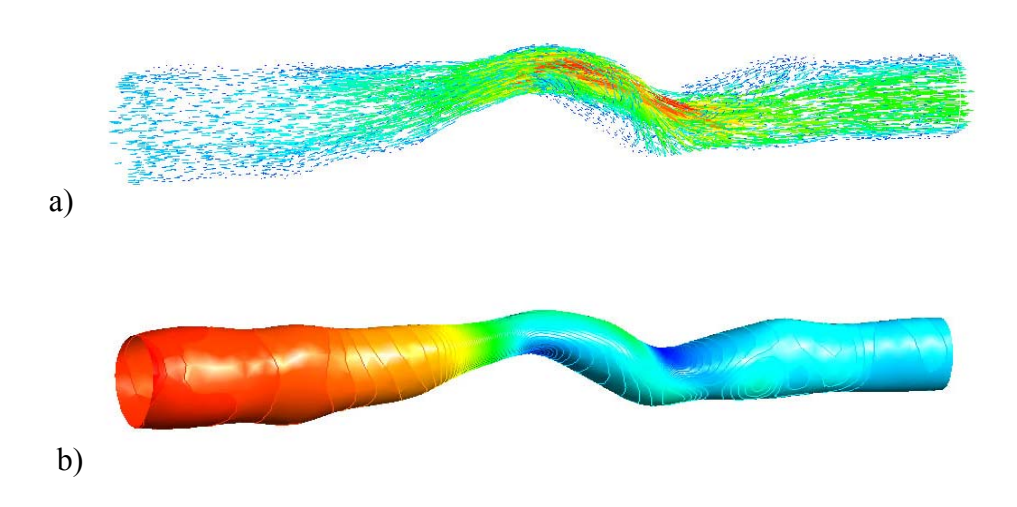


Figure 1.11: Three-dimensional fluid domain results of the lumen of a double plaque scenario: a) velocity vector field and b) lumen surface pressure

#### **1.4.3** Fluid-structure interaction method

Fluid-structure interaction (FSI) occurs when a fluid interacts with a solid structure, exerting pressure that may cause deformation in the structure and alter the flow of the fluid itself. The only physical variable of communication between the fluid and structural domains of the model is pressure, which is derived from the numerical results.

Two approaches are used when solving fluid-structure interaction models: one-way coupled and fully coupled methods. The one-way coupled method only applies the undeformable fluid domain results onto the structural domain at each time step; this method has the advantage that it consumes significantly less computational time than the fully coupled method and was used when we performed in the first article of this thesis the numerous sensitivity analyses of the different variables that might affect plaque stability. The fully coupled method solves by applying the results of the fluid domain onto the structural domain; this causes a deformation of the latter and subsequently affects the fluid domain (e.g. the expansion of the fluid domain volume as a result of artery diameter enlargement due to intraluminal pressure). The following time steps will have different fluid and structural domain shapes as they progress forward in time. This type of analysis was used when a transient inlet condition was imposed in the model to obtain accurate information on how transient waveforms of blood flow and intraluminal pressure affect the mechanical stresses within the plaque's constituents.

# Chapter 2 – Article: "Fluid structure interaction numerical studies on the assessment of mechanical stress of the coronary atherosclerotic plaque"

#### **Authors:**

Ramses Galaz, Rosaire Mongrain, Richard Leask, Jean Claude Tardif.

# **Objectives:**

- To analyze multiple scenarios of plaque configurations under a constant static flow.
- To construct a sensitivity analyses based on the different morphological variables that are reported by pathologists to influence plaque rupture: plaque size (as a percentage of stenosis), fibrous cap thickness and the material properties of the core ranging from very soft (lipid pool) to very hard (calcified plaque).
- To introduce the concept of fibrous cap mechanical fatigue (FCMF) as the result
  of the combined effects of fibrous cap thickness, relative inclusion stiffness and
  percentage of stenosis.

# **Hypotheses:**

- Thin fibrous cap thickness can increase the mechanical stress within the plaque.
- Large percentage of stenosis can increase the mechanical stress.
- Soft atheromatous core can increase the mechanical stress within the plaque as it may act as a weak structural foundation and thus allows greater mechanical deformation.

- Pressure drop is related to energy losses and high mechanical stresses.
- The analyses presented in this chapter are aimed at demonstrating the effects of the combination of certain mechanical and morphological variables such as fibrous cap thickness, inclusion stiffness and percentage of stenosis under a constant stable flow (i.e. no transient analyses). These results will serve as a basis in the next chapters for doing analyses with time-dependant flow in order to properly determine the cyclic stress amplitude and mean stresses to calculate a fatigue life for each node in the numerical analyses. Our hypothesis establishes that fibrous cap mechanical fatigue (FCMF) is the ultimate trigger for plaque disruption and it is the end result of the combination of certain mechanical and morphological variables coupled with time-dependant flow conditions.

#### 2.1 Abstract

Cardiovascular diseases are the leading cause of death in developed countries. Atherosclerosis is a chronic inflammatory response that narrows the lumen of arteries by a gradual deposition in the vascular wall of fatty substances, cholesterol crystals, cellular waste products, calcium minerals, and the growth of connective tissue [66, 67]. These localized pathological lesions are known as atheromatous plaques. Covering the plaque's core is a protective layer of connective tissue called the fibrous cap. The rupture of this layer has been extensively associated as one of the causes of acute myocardial infarctions [1].

In this study, we analyzed the role of material properties and morphological features of the plaque that are commonly associated with those characteristic of vulnerable plaques. The thickness of the fibrous cap, the percentage of stenosed area, and the stiffness of the core were studied to quantify their effects on the plaque's mechanical stress state by performing analyses using computational fluid-structure interaction methods.

The numerical results yielded a pressure drop in the fluid domain across the stenosis attributable to energy losses due to viscous and geometric effects. When these pressure gradient results were applied onto the interface surface, the mechanical stress levels significantly increased within the fibrous cap structure at the upstream side of the plaque. The highest stresses were calculated when a severe stenosis and a thin fibrous cap were present. Moreover, a weak structural support such as a soft lipid pool beneath the fibrous cap allowed for the hemodynamic pressure gradient forces to displace the fibrous

cap in the direction of the flow, resulting in higher strains and thus higher mechanical stresses, potentially increasing the risk of cap rupture.

When we analyzed the peak stress behavior of the most critical cases of thin fibrous cap and soft core at various degrees of stenosis, we found that there is a "plateau" region between the percentages of stenosis of 43% and 75% with a relatively small slope in the plot. These similar stress values could help explain the paradoxical behavior that mildly stenotic plaques can rupture as they are subjected to mechanical stresses similar to those of severe stenoses.

In conclusion, the particular combination of a mild to severe stenosis, a thin fibrous cap and a soft lipid core resulted in the highest mechanical stresses calculated at the proximal side of the plaque. These results help to explain the clinical observations of characteristic features of ruptured plaques [18,19,20].

#### 2.2 Introduction

Atherosclerosis, a very common cardiovascular disease, is a chronic inflammatory response in the arterial walls that narrows the lumen of vessels by a gradual deposition of fatty substances, cholesterol crystals, cellular waste products, calcium minerals, and the growth of connective tissue [66, 67]. These localized pathological lesions are known as atheromatous plaques. Covering the plaque's core is the fibrous cap, which is a layer of fibrous connective tissue and smooth muscle cells that prevent the core's highly thrombogenic contents from being in contact with blood. The rupture of the fibrous cap either by mechanical or biological factors may trigger a biological response of platelet activation and subsequently thrombus formation. It is estimated that two thirds to three

quarters of all arterial thrombi are caused by plaque rupture [16]. This event could potentially occlude the vessel and stop the blood perfusion downstream, resulting in an acute myocardial infarction. Clinicians have established from histopathological studies that ruptured plaques share certain morphological and biological features that would make them more vulnerable to rupture. Unstable lesions with a large and soft lipid core, many inflammatory cells, and a thin fibrous cap are typically associated with acute coronary syndromes [18,19,20]. It is now recognized that plaque vulnerability leading to rupture is the major cause of unstable angina, myocardial infarction, and sudden cardiac death.

Many authors have proposed that physical factors such as hemodynamics, material properties and morphology play an important role in plaque rupture as they influence the mechanical stress distribution in the fibrous cap tissue [32, 68, 69, 70, 71]. Moreover, some have shown through 2D finite element models of cross sectional views of stenosed arteries that the high stress zones correspond to the culprit zones in histopathological studies.

While there is agreement in the scientific community that mechanical factors influence the site and mode of tissue failure, it is not yet fully understood to which extent the different mechanical variables, such as shear or tensile stress, affect the initiation and propagation of such failure. The possible mechanisms could be either by high mechanical stress or by mechanobiological stimulation of the endothelium which would indirectly promote inflammatory activity and thus induce tissue degrading enzymes that would weaken the structure of the fibrous cap [16].

Studies have shown through 2D finite element models of cross-sectional views of stenosed arteries that the high stress regions correspond to the culprit zones in

histopathological studies. However, 2D models do not fully represent the true state of the stress tensor in both the structural and fluid domains. Therefore, in order to have a better understanding of the true physical events taking place in the diseased vessel, it becomes necessary to use 3D models as they would provide more accurate numerical evidence on the spatial stress distribution and the longitudinal component of the shear stress caused by blood flow. Moreover, when combined with localized anisotropic material properties and a mechanical failure criterion, the analyses would define the proper orientation and the extent of fissure propagation. The 3D numerical results would serve as a basis to compare the spatial location of the fissures with clinical evidence that often reports plaque rupture locations such as the upstream regions of the stenosis [72, 73].

A histopathological study of patients who had died during physical exertion showed that ruptures were commonly located in the midcap regions of the plaques, while those who died at rest showed shoulder rupture predominance [74, 75]. This suggests that different mechanisms act on different cases and that mechanical stress does play a role as physical activity increases the cardiac output. It has been proposed that lateral plaque shoulder ruptures are the result of cyclic tensile stress of the pressure wave [75] and that the high shear stress upstream of the plaque induces fibrous cap thinning [76].

In this study, we evaluate the role of 3D mechanical stress as a factor that may contribute to the vulnerability of plaques, emphasizing the morphological and material property features. The physical interaction between blood flow and the tissue are examined using fluid-structure interaction computational models of well defined and unbiased geometries of coronary arteries with varying degrees of stenosis. The thickness of the fibrous cap, the size of the lipid pool and the stiffness of the core were studied to quantify their effects on the plaque's mechanical stress. These three variables have been

described by pathologists and clinicians as those that might increase plaque vulnerability [18, 19, 20].

#### 2.3 Methods

#### 2.3.1 Mathematical models

The plaque is a complex structure and its analysis is facilitated by breaking down the structure into simpler components. The particular geometry of the stenosis makes the problem mathematically difficult to solve for the structural and fluid domains by using elasticity theory and the Navier-Stokes equations. Furthermore, the problem becomes even more challenging when the structural and fluid equations are coupled, resulting in the deformation of both domains. Simplified approximations of the problem's physics were done using ideal models to analyze the hemodynamic disturbances due to the presence of a stenosis.

#### **2.3.2** Mathematical model for the structural domain

The coronary arteries are of the muscular type; containing mainly smooth muscle cells in the media and to a smaller extent collagen and elastin fibers that have different mechanical properties and that are not well organized into layers as with elastic arteries. For simplification in our analyses, it was assumed that no anisotropic changes existed within the material properties of the structural domain. Therefore, the entire structure of the arterial wall and fibrous cap were modeled with the same mechanical characteristic.

In order to obtain the proper theoretical values of material properties and the respective magnitudes of stress, ideal coronary artery models were treated as perfect cylindrical geometries since for that case the exact solution for a thick wall cylinder under internal pressure is known; this solution was derived from elasticity theory and it is known as the Lamé equations [77] (Equations 2.1-2.3).

$$\sigma_r = \frac{a^2 p_i - b^2 p_0}{b^2 - a^2} - \frac{(p_i - p_0) a^2 b^2}{(b^2 - a^2) r^2}$$
(2.1)

$$\sigma_{\theta} = \frac{a^2 p_i - b^2 p_0}{b^2 - a^2} + \frac{(p_i - p_0) a^2 b^2}{(b^2 - a^2) r^2}$$
 (2.2)

$$u_{r} = \frac{1 - \nu \left(a^{2} p_{i} - b^{2} p_{0}\right) r}{b^{2} - a^{2}} + \frac{1 + \nu \left(p_{i} - p_{0}\right) a^{2} b^{2}}{\left(b^{2} - a^{2}\right) r}$$
(2.3)

We defined the values of the lumen radius a = 1.5 mm and external vessel radius b = 2 mm based on typical dimensions of coronary arteries in the proximal side of the coronary branch where most plaque ruptures occur [78]. The internal pressure  $p_i$  was defined as the normal average intraluminal pressure of 100 mmHg (13.3 KPa), while the external pressure  $p_o$  was set to 0 mmHg relative to the normal pressure of 1 atmosphere. The material was assumed to be incompressible due to the high water percentage content in the tissue, therefore a Poisson's ratio of v=0.49 was defined. Equation 2.3 yields the radial displacement  $u_r$  and it was solved for the elastic modulus E that corresponded to the typical maximum luminal diameter expansion of around 5% under normal hemodynamic conditions for healthy coronary arteries [79]; the approximate value of E was calculated

at around 800 KPa and agrees in the order of magnitude with other reports of linear elastic modulus values [32, 68].

A well known fact is that the stress-strain curve of cardiovascular tissue behaves as a hyperelastic material model [80], thus a non-linear material would be more representative of the global mechanical deformation. However, the values of the strains which the coronary arteries are subjected to under normal physiological conditions are well within the linear elastic region of the stress-strain curve before the hardening region. Using equation 2.2 with these parameters, a maximum stress value of 47.6 KPa was calculated for the inner surface of the cylinder that yields a strain value of 0.059; this strain level is well below the hardening value of about 0.20 seen in the stress-strain curves of human coronary arteries [81].

#### **2.3.3** Mathematical model for the fluid domain

The presence of a stenosis acts as a resistance in the arterial hemodynamics and this constriction causes a pressure drop in the flow. For purposes of the validation of the fluid numerical results, we used a mathematical model developed by Back et al [82] (equations 2.4 - 2.8); this model considers that the overall pressure drop can be approximated by summing up the geometric and viscous losses along the stenosis. Figure 2.1 depicts the sections used by Back, which include a conical section at the entrance, a cylindrical passage in the throat of the stenosis and an expansion cone.

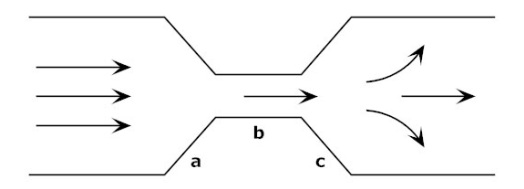


Figure 2.1: A schematic model of a stenosis: a) conical converging section, b) cylindrical throat, c) expansion cone

The corresponding pressure losses from the Back model [82] are:

$$\Delta p_{\text{total}} = \Delta p_{\text{fc}} + \Delta p_{\text{fs}} + \Delta p_{\text{con}} - \Delta p_{\text{exp}}$$
 (2.4)

$$\Delta p_{\rm fc} = \frac{128\eta L_c I_s Q}{\pi d_i^4} \tag{2.5}$$

$$\Delta p_{\rm fs} = \frac{128\eta L_{\rm s}Q}{\pi d_{\rm s}^4} \tag{2.6}$$

$$\Delta p_{\rm con} = 0.5 \rho \left[ \left( \frac{1}{A_s} \right)^2 - \left( \frac{1}{A_i} \right)^2 \right] Q^2$$
 (2.7)

$$\Delta p_{\rm exp} = 0.85 \rho \left( \frac{A_s}{A_i} \right) \left( 1 - \frac{A_s}{A_i} \right) \left( \frac{Q^2}{A_s^2} \right)$$
 (2.8)

Equation 2.4 describes the sum of all the pressure drop or gain terms,  $\Delta p_{fc}$  represents the viscous factors in the conical entrance,  $\Delta p_{fs}$  is the loss in the straight section of the stenosis and is derived from Poiseuille's law,  $\Delta p_{con}$  accounts for the loss due to the geometrical constriction and is also derived from Bernoulli's equation and  $\Delta p_{exp}$  is the pressure gain due to the sudden conical expansion and the resulting velocity decrease. Other models have taken a similar approach, Young and Tsai [83] proposed a semi-

empirical method that provides good results but requires more intricate experimentation to obtain the semi-empirical coefficients.

# 2.4 Computational models

### 2.4.1 Computational model for the structural domain

To assess the magnitude of mechanical stress within the fibrous cap, a sensitivity analysis was performed by creating an ideal geometry of the diseased artery wall and by varying the values for the three features mentioned. The analyses were done with finite element software capable of performing fluid-structure interaction. In order to be consistent with the analytical models, a set of computational models were created as simple cylindrical shapes with the typical dimensions of the proximal third of coronary arteries, where most plaque ruptures occur and where they represent the most danger of obstructing blood flow to large regions downstream of the myocardium [78]. These dimensions were set to be 3 mm for the lumen diameter of the artery, 0.5 mm for the artery wall thickness, 20 mm for the length of the cylinder and 15 mm length for the stenosis, which corresponds to a slightly diffuse thickening; the center of the stenosis was located at x = 10 mm. The stenosis geometry was modeled as an eccentric blister type protrusion using symmetrical Gaussian curves along the longitudinal axis and different heights to account for the different degrees of stenosis.

The size of the plaque was controlled by varying the height of the longitudinal Gaussian curve that defined the typical stenosis shape and the values ranged from 19% to

91% stenosed lumen area. The thickness of the fibrous cap ranged from 200 to 500 microns (Figure 2.2).

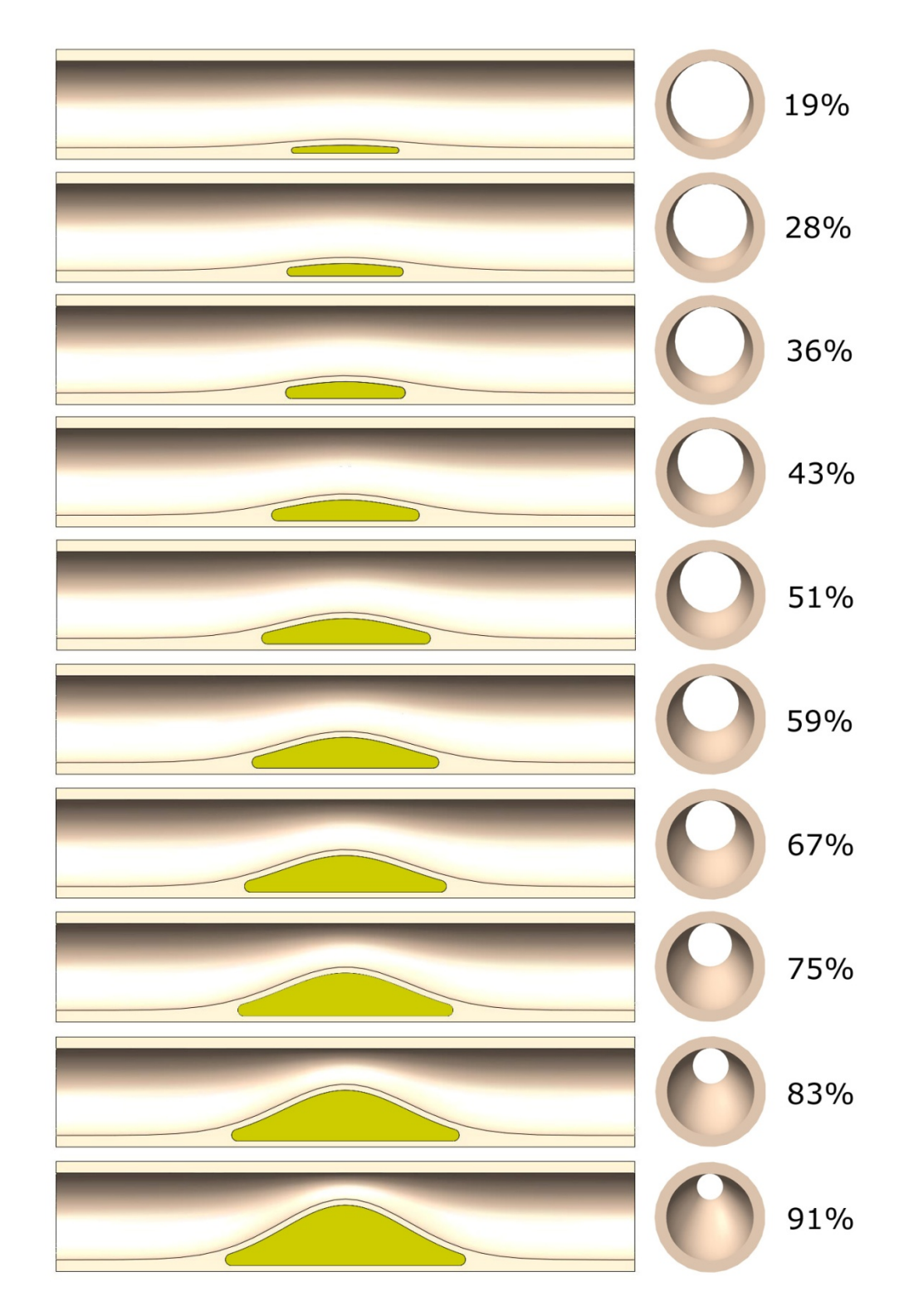


Figure 2.2: Geometric 3D models of stenotic arteries and their respective percentage of stenosed lumen area shown with a fixed fibrous cap thickness.

The stiffness of the necrotic core values ranged from a very low Young's modulus  $E_c \approx 0 \text{ Pa representing a soft lipid core to a very high number } E_c >> E_{wall} \text{ representing a}$  very stiff object such as calcifications. A value  $\gamma$  was defined to be the stiffness ratio between the core and the artery wall.

$$\gamma = \frac{E_c}{E_a} \tag{2.9}$$

Since no large deformation mechanics are present in the system, plain elastic and isotropic material properties were defined for the arterial wall and the fibrous cap with the previously calculated value of  $E_a$ =800 KPa obtained from the Lamé equations. A total of 80 individual fluid structural interaction analyses were performed by combining the three main variables of study (4 levels of stenosis, 5 stiffness ratio values, 4 levels of fibrous cap thickness). The percentages of area of stenosis were set at four different values (36%, 51%, 75%, and 91%) that were the most representative for each stage of the stenosis instead of the total 10 cases (from 19% to 91%) to avoid the time consuming task of doing a much larger number individual analyses. The fibrous cap thicknesses were defined using 4 values ranging from 200 to 500 microns, and the stiffness ratios  $\gamma$  were defined using 5 different values ranging from 0.001 to 1. The results of these individual analyses were used to construct a surface plot of the peak stress values within the plaque.

### 2.4.2 Computational model for the fluid domain

The fluid domain was analyzed using a standard commercial computational fluid dynamics package (ANSYS CFX, Canonsburg, PA). The fluid was assumed to be Newtonian as it has been reported to be a reasonably good approximation due to the large content of water based plasma in the blood and the size of the coronary arteries [84]. Normal hemodynamic parameters were defined as follows: maximum average phasic coronary flow of 100 ml/min [42], blood viscosity of 3.6 centipoises and a base inlet pressure of 100 mmHg were used. The values for the flow rate were fixed to be able to study only the morphological and material properties features. The fluid was analyzed as steady and fully developed flow with the averaged conditions over one cycle.

#### 2.5 Results

# 2.5.1 Computational fluid dynamic results with analytical validations

The presence of any stenosis in the vessel resulted in a pressure drop effect (Figure 2.3). The magnitude of the pressure drop between the proximal and distal sides of the plaque increased as the percentage of stenosis was higher; these values were consistent with catheter-based clinical measurements of pressure differences at several percentages of stenosis [85]. The same behavior of the pressure drops has also been reported by Mates [86] for an eccentric coronary stenosis.

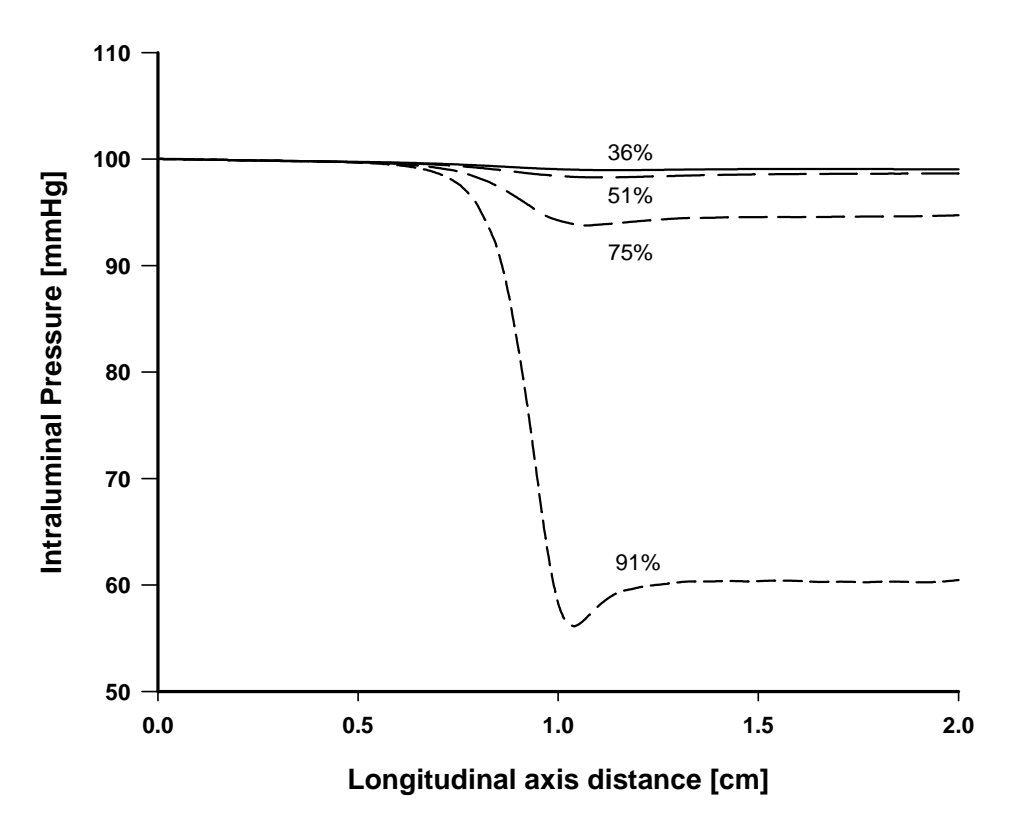


Figure 2.3: Central streamline pressure drop across different percentages of stenosis from the numerical analyses

In particular, it is observed that there was an important increase in pressure loss for lesions causing more than 75% area stenosis; this is also coherent with the clinical observations [85]. It is also interesting to note that for stenoses below 50% in area the pressure loss is relatively negligible. This suggests that pressure loss is not the predominant mechanical variable involved in plaque rupture of mild stenoses.

As a validation procedure for our model we compared the mathematical model by Back et al [82] and clinical observations by Baumgart [85] with the computational results (Figure 2.4). The clinical values were provided with percentage stenosis data, but lacked information on the overall length of the stenosis; this could

explain the poorer agreement between the clinical data and the models after 60% stenosis as the length of the lesion can further contribute to total pressure losses. Nevertheless, these results support the validity of our models.

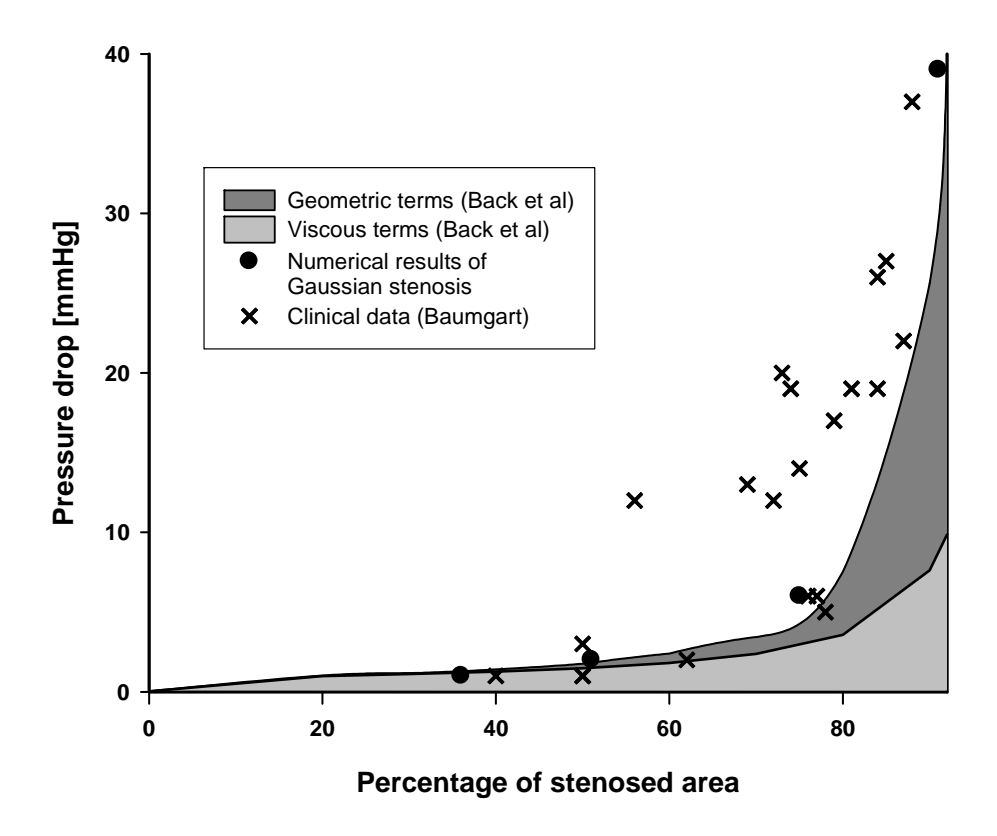


Figure 2.4: Comparison of the mathematical model developed by Back et al [82], clinical measurements [85] and numerical results.

Blood velocity and wall shear stress were also extracted from the analyses (Figures 2.5, 2.6) and used for validation of the numerical results against the mathematical formulas and known clinical data. The entrance velocities at the non-stenosed sections of the artery were calculated at 24 cm/s (Re = 200) and the peak intrastenotic velocity for the 91% stenosis was 3.3 m/s; these values are consistent to those reported by Krzanowski using Doppler ultrasound velocity measurements of

diseased coronaries [87]. Wall shear stress was computed at 3.5 Pa at the non stenosed sections and reached a value of 190 Pa at the peak of the 91% stenosis. The pressure gradient force is a measure of the change of pressure along a distance. It results in the net force created from high pressure zones to low pressure zones. Figure 2.7 shows the values of the pressure gradient forces acting on the surface of the stenosis, with their highest magnitudes occurring on the upstream side of the plaque.

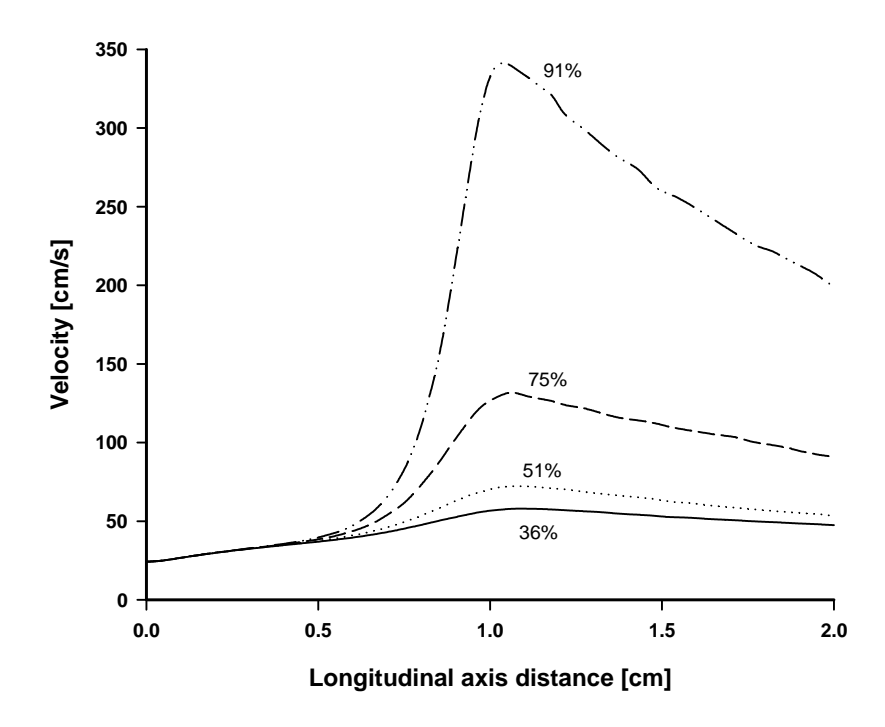


Figure 2.5: Central streamline velocity across different percentages of stenosis

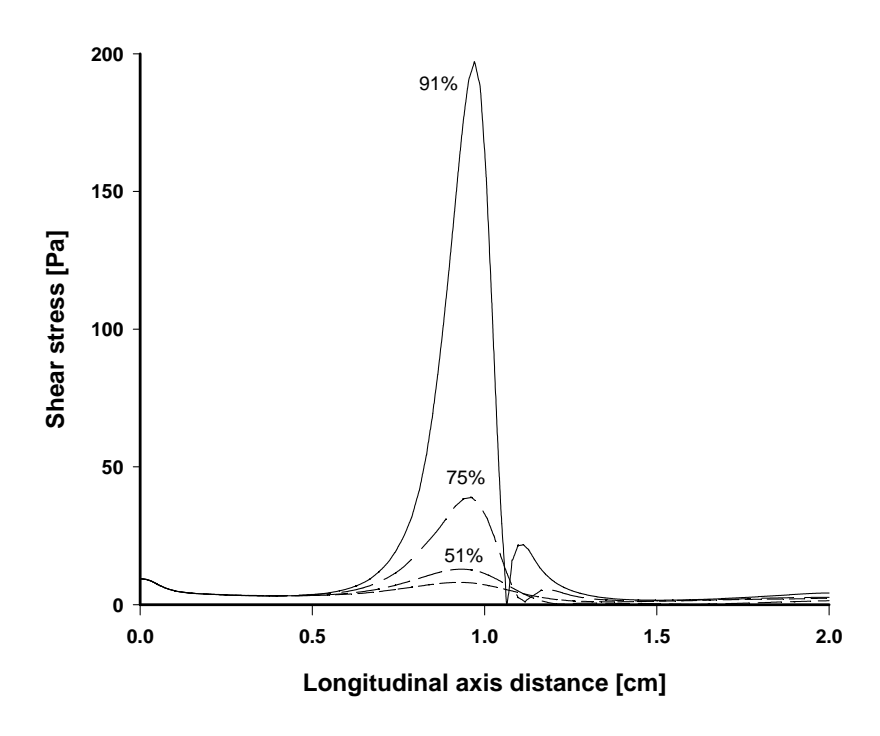


Figure 2.6: Plaque surface wall shear stress across different percentages of stenosis

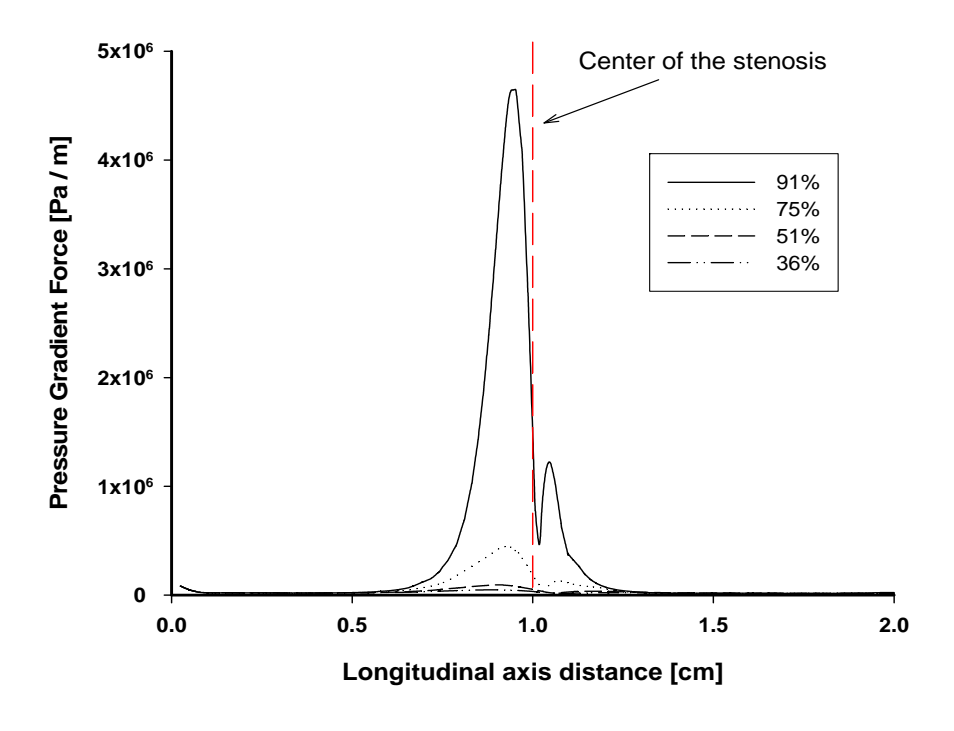


Figure 2.7: Pressure gradient force acting on the normal direction of the stenotic surface.

It can be observed that for stenoses below 50% in area the resulting velocity changes, shear stress and pressure gradient forces do not reach extreme values. This suggests that these variables would have a secondary role in rupture of most vulnerable plaques. However, because the shear stress and pressure gradients have skewed distribution (Figures 2.5, 2.6) with higher values in the proximal part of the stenosis, these variables could be involved in the fatigue process contributing to the observed ruptures in the region.

#### 2.5.2 Numerical results for the structural stress

In this section, we investigate the role of the resulting solid stresses in the vascular wall as potential contributors to the rupture of plaques causing mild stenoses. After performing the fluid-structure interaction evaluation, all analyses resulted in a stress concentration at the upstream side of the plaque (Figure 2.8).

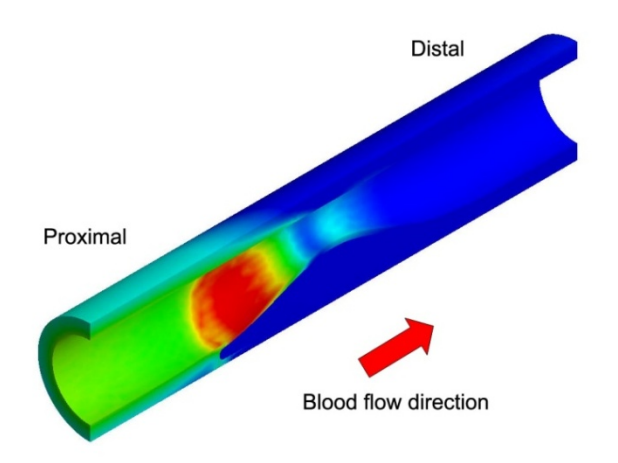


Figure 2.8: Longitudinal section view of the typical mechanical stress distribution for the fluid-structure interaction results. All analyses resulted in high stress concentrations in the proximal side of the plaque.

Since the goal of our study was the assessment of stresses within the plaque, we only considered the local maximum stresses within the fibrous cap area as proposed by Tang [88]. Figures 2.9-2.12 summarize the findings of the maximum equivalent stresses within the fibrous cap of all the individual fluid-structure interaction analyses. The overall results show that the combination of a thin fibrous cap with a soft lipid core increased the magnitude of the stresses. Moreover, the magnitude of the stresses also became higher as the stenosis became more severe. The circumferential stress of 47.5 KPa at the inner surface of the non-stenosed sections of the lumen was consistent with the values provided by the Lamé equations. The structural domain changed by 4% in the intraluminal diameter. Consequently, the fluid domain would change in the same proportion. We neglected this effect and assumed that the problem could be treated by using unidirectional coupled fluid-structure interaction, in which the pressure gradient results are directly applied onto the structural domain neglecting the hemodynamic changes in the flow field due to such deformation.

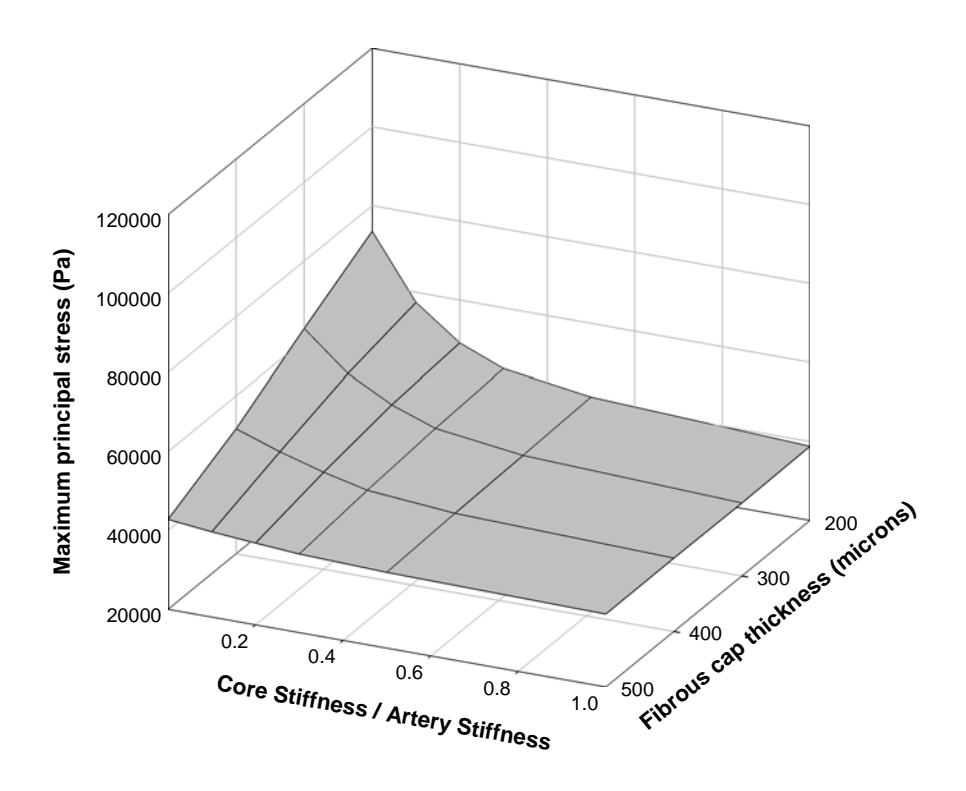


Figure 2.9: Local maximum principal stresses at 36% stenosis

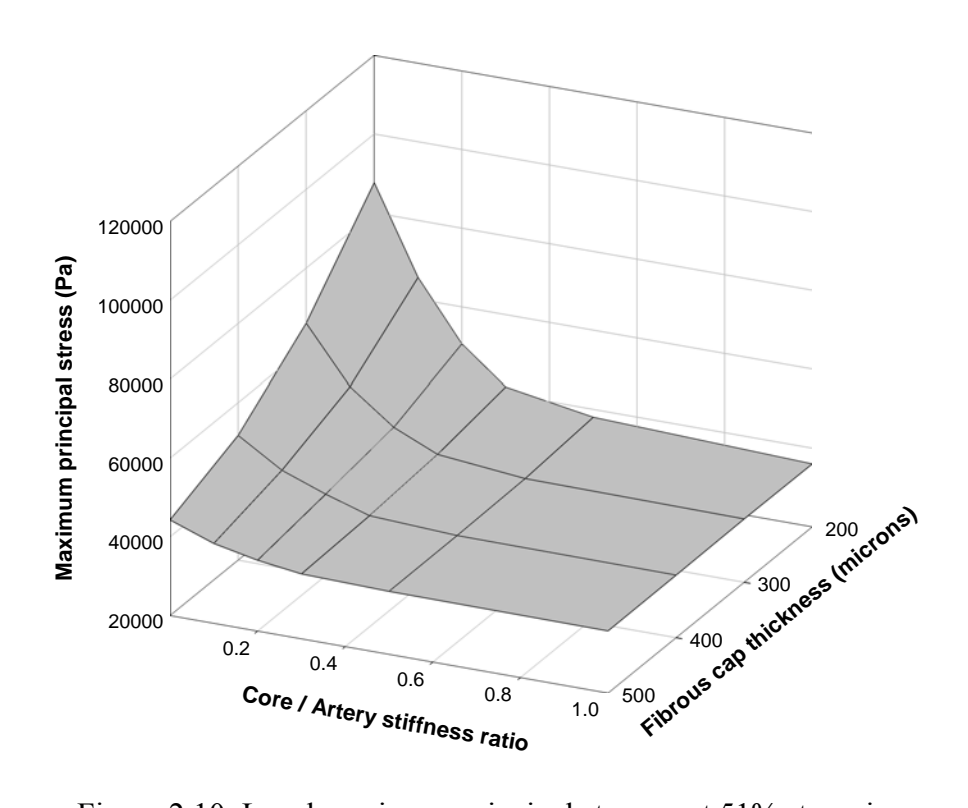


Figure 2.10: Local maximum principal stresses at 51% stenosis

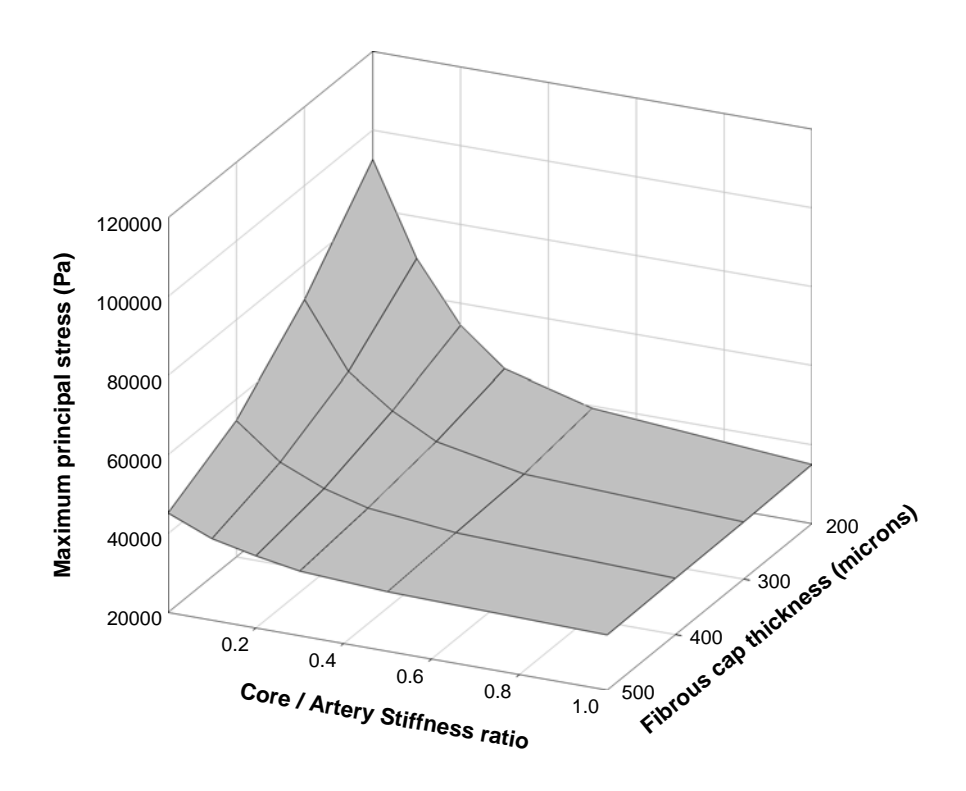


Figure 2.11: Local maximum principal stresses at 75% stenosis

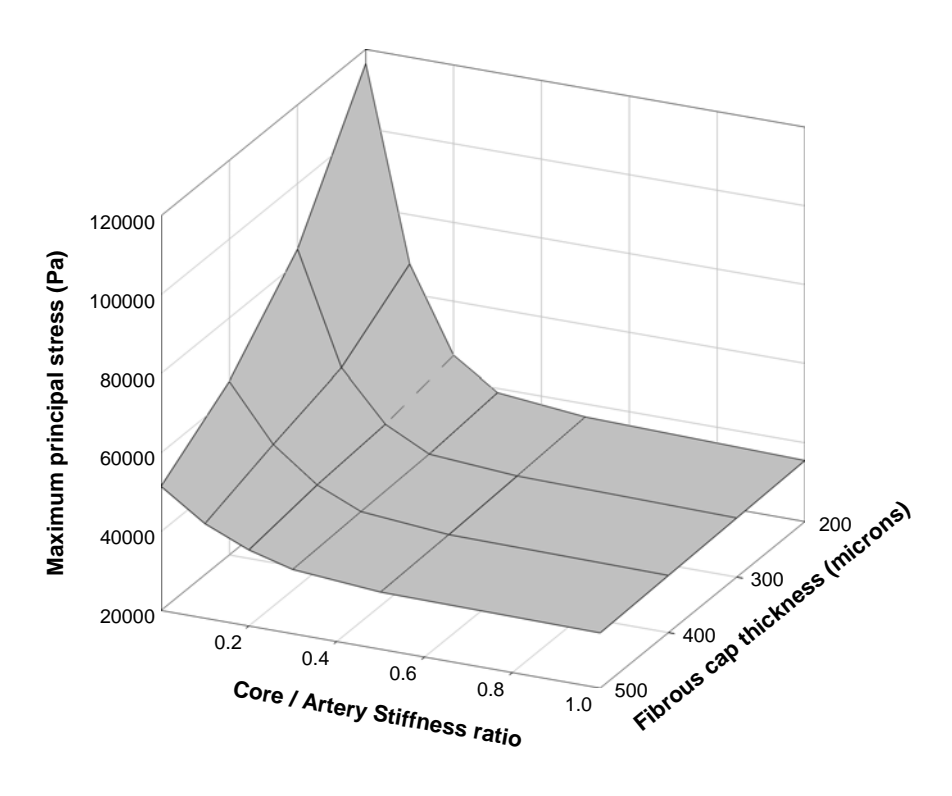


Figure 2.12: Local maximum principal stresses at 91% stenosis

Once we had identified the pattern that the peak stresses occurred at the combination of a thin fibrous cap and with a soft core, we performed the analyses of all the geometric cases (Figure 2.2) of the different percentages of area stenosis (19%, 28%, 36%, 43%, 51%, 59%, 67%, 75%, 83% and 91%). The peak results of the scenarios of thin fibrous caps of 200 microns and lowest  $\gamma$  values as a function of the percentage of stenosis produced an interesting plot with a plateau region (Figure 2.13). This plot suggests that for low percentages of stenosis from 19% to 43% the peak stress climbs as the percentage of area stenosis rises. For mid-range stenosis from 46% to 75%, there is a plateau region with a relatively small increase of the peak stresses. This plateau also suggests that the level of plaque vulnerability to mechanical rupture might have similar values between 43% and 75% in these particular cases. For area stenoses higher than 75%, the peak stresses drastically increased with a relatively steep slope. This could mean that for very high percentages of stenoses (above 75%), plaque vulnerability to mechanical failure is very sensitive to minor changes in size.

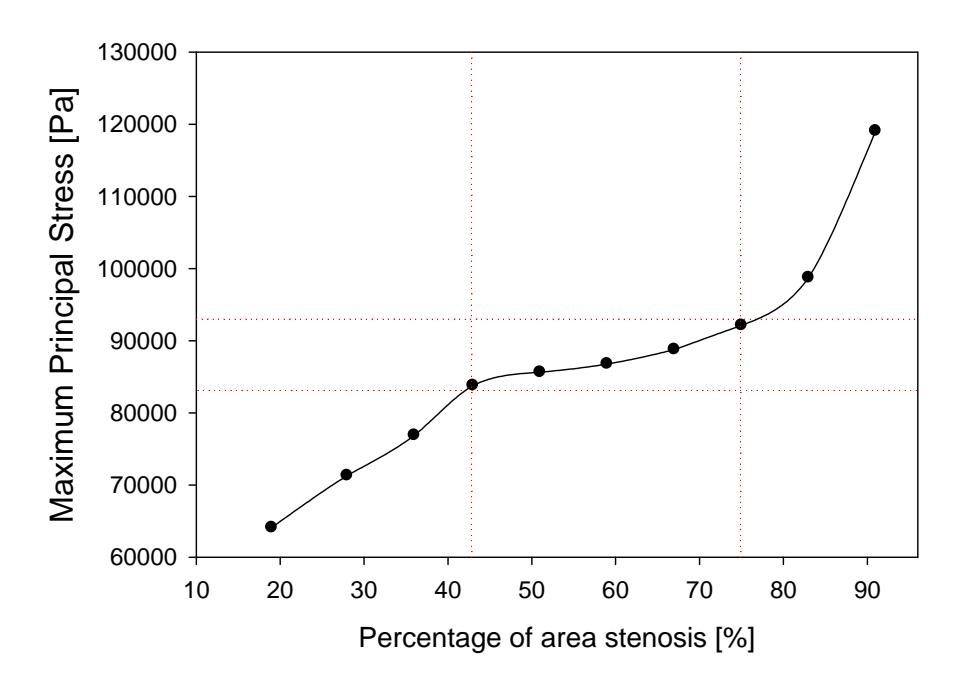


Figure 2.13: Peak stress values for different percentages of stenosis for a fibrous cap thickness of 200 microns and  $\gamma$  value of 0.001

#### 2.6 Discussion

The results from our models reveal that for all stenoses, the most important factor that has a direct impact for plaque rupture is the solid stresses. Physically speaking, the impedance to blood flow across a stenosis results in an energy loss due to geometrical changes and viscous effects. This energy loss is dissipated from the system partly as generated heat that is carried away by flow advection and partly as mechanical deformation of the plaque constituents and the surrounding tissue; the consequences of this are reflected in a pressure drop across the stenosis. The numerical results of the

pressure drops that we obtained are consistent with reports of in-vivo catheter-based pressure measurements of stenosed coronary arteries [85].

When the fibrous cap of the plaque is thin and has a weak structural support underneath it, as in the case of a soft lipid core acting as a weak elastic foundation, the hemodynamic pressure gradient is allowed to push against it in the direction of the flow and strain it to a greater extent at the upstream side location. Consequently, the structural deformation increases the fibrous cap internal stresses at the upstream side. This effect has also been proposed by Doriot [41] using theoretical and numerical calculations with only two-dimensional longitudinal models of stenosed arteries. Our numerical results are consistent with clinical observations of the sites of plaque rupture. Fujii et al [72] reported that most of the ulcerated ruptured plaques in culprit lesions of acute coronary syndrome patients were proximal to site of minimal lumen dimension based on intravascular ultrasound imaging studies. Hiro et al [73] have also reported ultrasonographic longitudinal views of ruptured coronary plaques, and most of them were also located in the proximal region of the plaque.

In order to obtain a more accurate model in terms of anatomical structure and physiological conditions, it becomes necessary to analyze realistic geometries of the coronary arteries and include more realistic material properties such as viscoelasticity and anisotropy of the connective tissue. Furthermore, transient fluid-structure interaction numerical models using phasic coronary flow waveforms as the inlet values need to be performed and then combine the results with a failure criterion that accounts for the fracture mechanics in order to assess fatigue life before failure due to the heart pulsatility. These transient analyses will serve as a basis in order to determine a fatigue life for each node in the numerical analyses and thus demonstrate that the ultimate trigger for plaque

disruption is the fibrous cap mechanical fatigue (FCMF). Plaque rupture is not only a mechanical failure process, but rather one that is intricately associated with biological factors such as inflammatory activity and the presence of tissue degrading enzymes that could weaken the structural stability of the plaque. It should be attempted to take the latter factors into account in future models.

#### 2.7 Conclusions

The presence of a stenosis in the artery resulted in an energy loss or pressure drop due to viscous and geometry factors. This energy loss translates partly into a mechanical deformation of the fibrous cap as it is the weakest structural component of the plaque. Furthermore, the stress magnitude is accentuated when the fibrous cap is thin and it does not have a good structural support underneath it such as a soft lipid core acting as a weak elastic and incompressible foundation. This allows for the hemodynamic pressure gradient forces to push against it in the direction of the flow and strain it more at the upstream side.

A pressure drop across the stenosed vessel was observed in all the numerical analyses; the magnitude of the wall shear stress, fluid mean velocity and pressure difference between the proximal and distal side increased exponentially at high percentages of lumen narrowing, more specifically at more than 75% of area stenosis.

The combination of a mild to severe stenosis, a thin fibrous cap and a soft lipid core resulted in the highest mechanical stresses calculated at the proximal side of the plaque for all numerical analyses. These results help to explain the clinical observations of characteristic features of ruptured plaques. Lastly, the plateau region of the peak

stresses observed at percentages of stenoses from 43% to 75% could indicate that these plaques could have the same degree of vulnerability to mechanical failure. Lastly, the concept of fibrous cap mechanical fatigue (FCMF) can be introduced using these same numerical models but under time-dependent flow conditions in order to calculate the stress amplitude and mean stress of each node over one cardiac cycle and thus determine the fatigue life of each node within the structural domain of the plaque.

# Chapter 3 – Discussion on article: "Fluid structure interaction numerical studies on the assessment of mechanical stress of the coronary atherosclerotic plaque"

#### 3.1 Discussion on the numerical results

The results in the article described in this chapter demonstrate that certain morphological features can influence the propensity to induce high mechanical stresses in the plaque, particularly at the shoulder regions of the fibrous cap where plaque ruptures tend to occur. Therefore, if clinicians want to deterministically assess a plaque's vulnerability to rupture using computational methods, they must first recreate the exact physical and biological conditions to which the plaque is subjected, these may include:

- Pulsatile and transient flow
- Accurate 3D modeling of the components of the plaque
- Accurate characterization of the hyperelastic tissue properties
- Accurate anisotropic properties of the tissue
- Inflammatory cell activity location

From the analyses, we can hypothesize that the mechanical properties of the healthy sections of artery wall have little influence on the outcome of the distribution of the mechanical stresses, this is due to the fact that the hemodynamic forces act primarily on the surface of the weakest structural component of the plaque: the fibrous cap. Therefore, it becomes more important to fully characterize the cap's collagenous material

properties rather than the artery wall's layered composition of collagen, elastin and smooth muscle cells. We performed a few studies defining stiffer or weaker mechanical properties on the same structural domain only to find that the magnitude of the stresses changes, but not the overall spatial distribution. This suggests that the geometry of the plaque is a more important factor rather than its mechanical properties as evidenced by the results on the highly stenotic cases. Figure 3.1 describes the relevance of both viscous and geometric effects as the percentage of area stenosis increases as derived from the Back [82] equations. It can clearly be seen that as the area stenosis increases, the geometric constraints induce proportionally greater pressure losses than the viscous counterparts. Some of that energy loss is translated into the mechanical deformation of the weakest structural component of the plaque: the fibrous cap. When analyzing Figure 3.1, we must remember that even though viscous losses contribute to the vast majority of total losses when the percentage of area stenosis is low, the magnitude of those total losses is negligible.

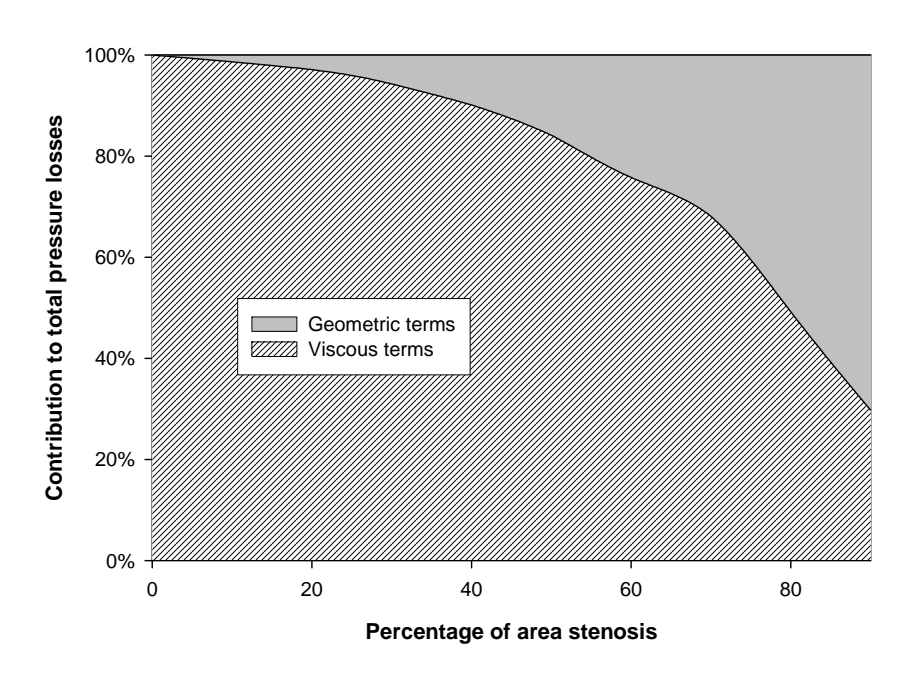


Figure 3.1: Contribution to total pressure losses of the viscous and geometric terms as derived from the Back equations

This set of equations to mathematically derive the total pressure losses is the best approximation we have in terms of analytical models. Even though the Back [82] equations are limited to a concentric "necking" of the cylinder and do not accurately represent the physics of an eccentric lesion, they still give a good approximation to the values calculated to the eccentric numerical model (Figure 2.4). It would be difficult to develop an analytical model that would accurately predict the pressure losses in an eccentric "Gaussian curve" type of stenosis. Even then, such models of stenosis could not realistically represent the true nature of the plaque's different shapes.

An important aspect to discuss about the results presented in this chapter is the controversy about why mild stenoses present plaque ruptures more frequently while these results indicate that it is the more severe stenoses that present higher stress magnitudes. We must first identify what kind of plaques we are dealing with; the more severe stenoses

tend to be also more calcified and have a thicker fibrous cap, and hence are more structurally stable and less prone to rupture. Secondly, the frequency of mild stenoses is far greater than those that are severe and by simple probabilistic terms, we might encounter a large proportion of plaque failures of mild stenosis [89]. Finally, it is possible that the mechanical stresses could lead to a premature rupture of mild stenoses and we could seldom find cases of a high percentage of stenosis with a thin fibrous cap that has survived to rupture, however, there are reports that indicate that ruptured mild plaques sometimes heal through the growth of new tissue on top of the rupture and thus the plaque can grow in size [90]. Large plaques could then be the outcome of a series of consecutive ruptures and repairs through the growth of new tissue in the same specific area. Such plaques would have a high content of collagenous tissue and therefore be structurally stable.

An important lesson from the results of this chapter is that we should look into stress range values or stress distribution behaviours, rather than analyzing single nodes that may exceed a threshold value that may initiate rupture. It is relatively easy to have a discontinuity in the geometrical model that would create an unrealistically high stress concentration, especially when dealing with small details of plaque components modeled after geometries extracted from an imaging technology. We must avoid having sharp edges or discontinuities as much as possible and look for logical stress concentration patterns that make sense. By doing this, we can reduce the source of errors or discrepancies when trying to determine the causes of plaque rupture.

A limitation of this work was that we did not analyze cases of geometrical models were the fibrous cap was thinner than 200 microns. Pathologists like Virmani [27] have reported that the typical thickness at which fibrous caps fail is around 60 microns. In

order to model such thin caps in our geometrical model, we would have had to reduce the size of the elements to at least 30 microns to have good results. This would have resulted in a very large number of elements that would make the analysis lengthy in time and prone to non-convergence as smaller elements can suffer over penetration from the contact elements at the interface between the fibrous cap and the core of the plaque. Another limitation of this model was that we assumed that the fibrous cap shared the exact same mechanical properties of the artery wall. The true mechanical properties of the fibrous cap are still unknown, and they can vary from patient to patient. The fact that the fibrous cap is mostly composed of collagen fibers and smooth muscle cells is the only hint that we have to safely assume that its mechanical properties are similar to the artery wall. It is also important to stress out that these analyses were done considering the core of the plaque as homogenous in nature. This is not the case as it has been observed in numerous histological studies that calcifications and lipid pools tend to exist in a very irregular pattern.

Clinicians can learn from the figures presented in this research that we can mechanically stabilize the plaque either by increasing the fibrous cap thickness, stiffening the core, or reducing the size of the stenosis. Having concluded that mechanical stresses increase with the increasing percentage of area stenosis, it can be inferred that the cases of rupture of non-stenotic plaques must have an important biological cause as there are little or virtually no energy losses in such cases that could translate in the mechanical deformation of the fibrous cap.

#### 3.2 Numerical results plots

In order to better understand the complex phenomenon of the fluid flow passing through each of the models analysed, we present the set of plots of the numerical results of the fluid domain (figure 3.2). It is important to observe that the greatest hemodynamic changes in terms of velocity begin to occur at area stenosis levels of 75% and above. Along this, the pressure gradient forces and pressure drops also become significantly greater at 75% area stenosis and above. It becomes clear then that when there is a high percentage of stenosis (above 75%) all the hemodynamic variable suffer considerable changes and thus affect the mechanical stresses in the same proportion (Figure 2.13). It is very interesting to note from figure 2.13 that there is a low stress region from 19% to 75% area stenosis. This region has a low-rise slope in the peak mechanical stresses in the fibrous cap. This also suggests that hemodynamic variables do not affect significantly the mechanical stresses at these regions.

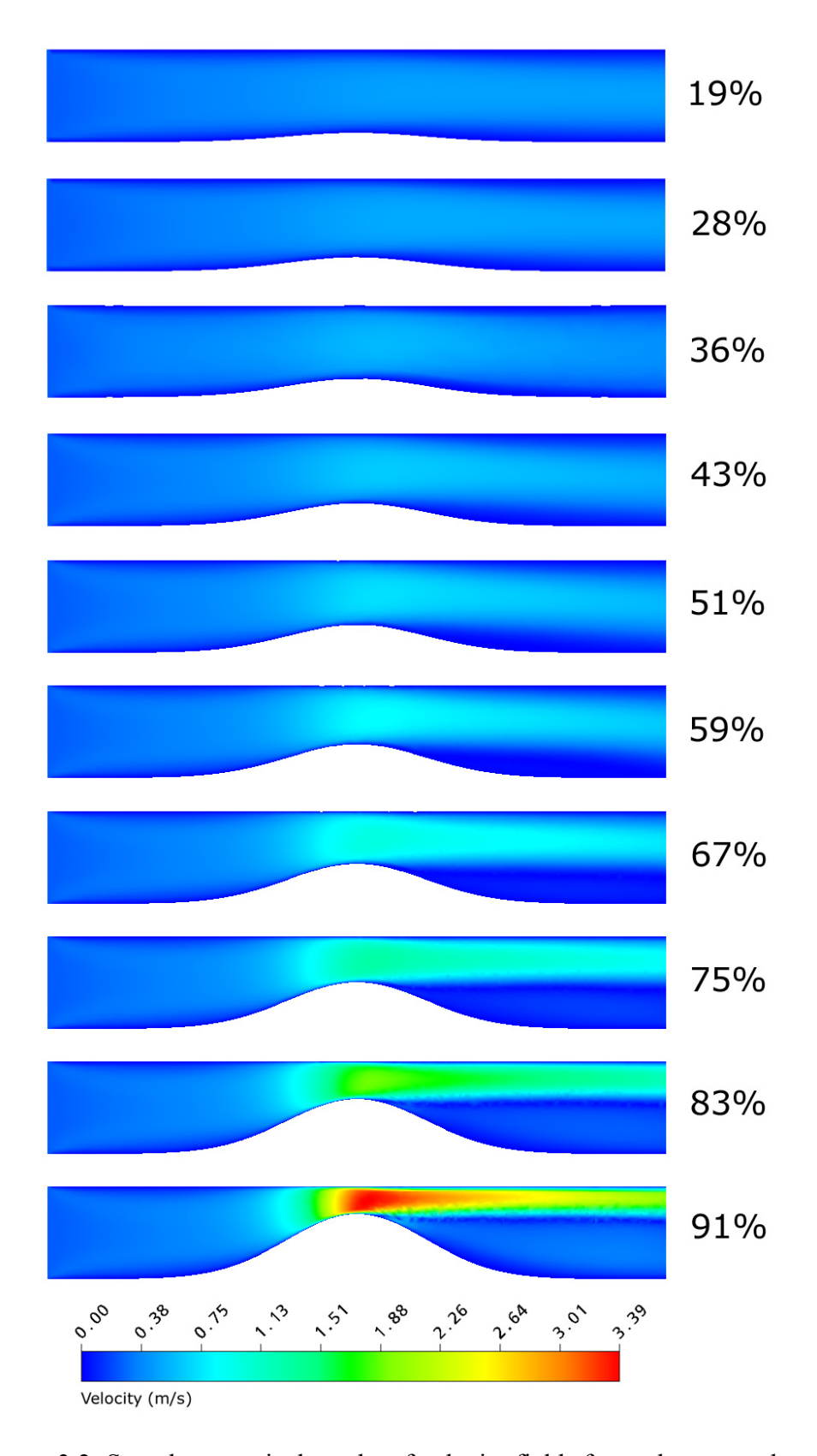


Figure 3.2: Sample numerical results of velocity fields for each case analysed.

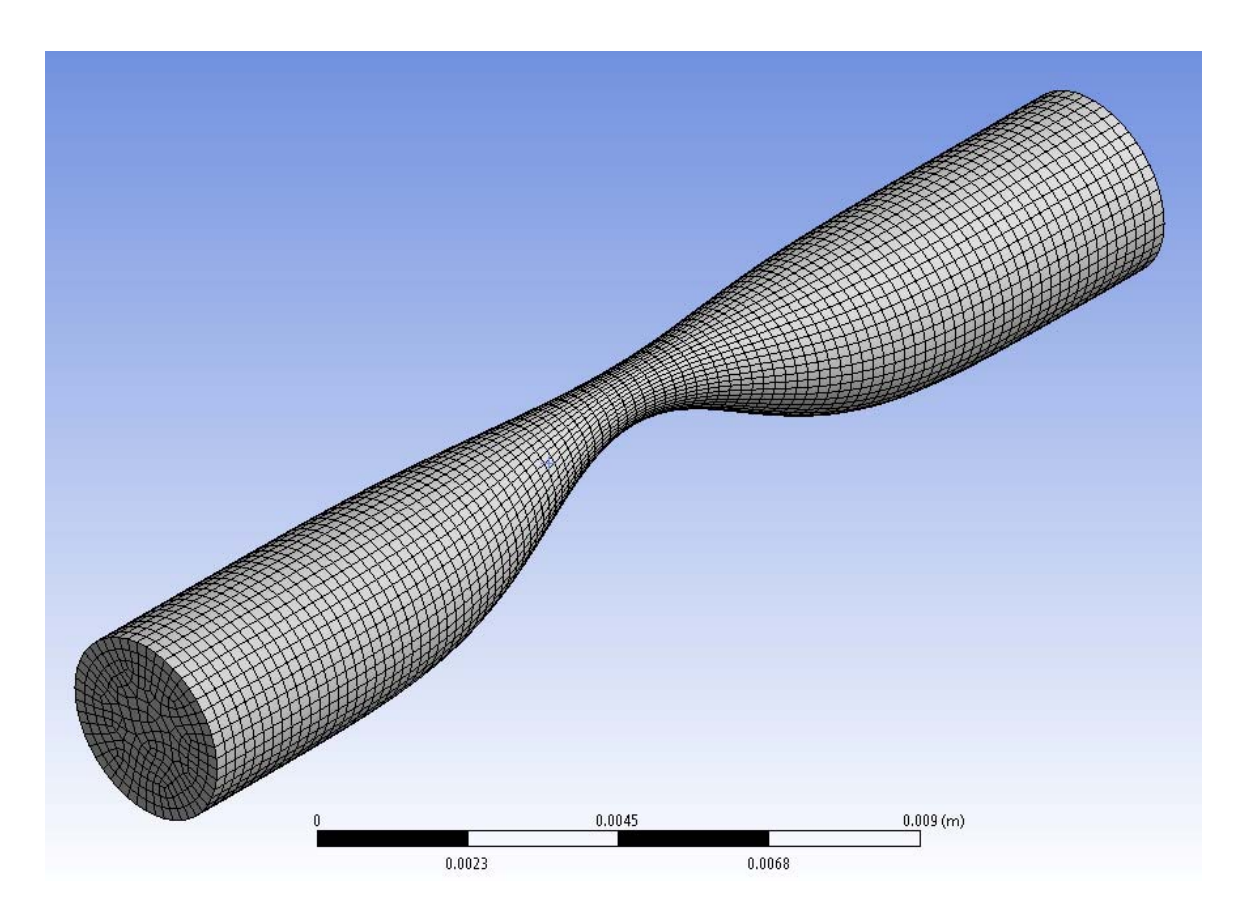


Figure 3.3: Computational Fluid Dynamics (CFD) mesh of the lumen of the 91% area stenosis model.

#### 3.3 Limitations of the analyses

The most important limitation of this set of analyses is that they only represent ideal models of stenoses in the artery. This is a good approach to be able to compare results when doing a sensitivity analysis since the same methodologies of design and physical conditions were applied consistently to all models. However, these are not real-life scenarios and these models can only predict the mechanical stresses under ideal conditions such as perfectly symmetrical plaques defined with a series of perfect circles throughout the entire length of the stenosis and constant and smooth fibrous cap

thickness. If we were to define our models using a different set of rules in terms of shapes, lengths, mechanical properties, different materials (e.g. calcifications and lipid cores co-existing within the plaque), a non-constant thickness of fibrous cap thickness, and non-smooth contours of the plaque shape, then the results could be different and thus exhibit different behaviours. Therefore, it becomes very important to understand that if we want to obtain deterministic results of a particular plaque, we must concentrate our efforts in the accurate reconstruction of patient-specific plaques along with all the various components that form them. Recently, in a study developed by Vengrenyuk et al. [91] they proposed that the existence of cell calcifications near the zone of the fibrous cap can have a great influence in the overall rupture mechanics. It then becomes important to fully characterize all the morphological and mechanical factor of each patient-specific plaque.

In the next chapter, we take a deeper step into the analysis of the phenomenon and study a case of an in-vivo patient-specific reconstructed plaque from intra-vascular ultrasound segmentation images. We study the feasibility of performing realistic reconstructions along with transitory boundary conditions to realistically simulate the physiological blood flow and pressure patterns in the coronary arteries. Moreover, we consider that plaque failure is the result of a chronic progressive injury caused by the transient cyclic stresses due to blood flow pulsatility and that our numerical results could help predict the number of cycles to failure based on a hypothetical S-N fatigue curve.

#### 3.4 Fibrous cap mechanical fatigue concept (FCMF).

An important discussion about the previous chapter is that it aims towards the introduction of the concept of fibrous cap mechanical fatigue. It was demonstrated that

the mechanical and morphological variables involved in these sensitivity analyses played an important role in the mechanical stress concentration in the fibrous cap. However, in order to demonstrate the effect of fatigue failure we must aim to research the time-dependant (transient) analyses under normal coronary flow and pressure patterns. These studies will help to calculate minimum and maximum stress values throughout the cardiac cycle in order to determine the stress amplitude and the mean stress for each node. Such stress values are necessary to calculate a fatigue life of the fibrous cap. In the following chapter we combine the transient analyses using normal coronary flow patterns and the use of patient-specific realistic geometries to further reach more realistic analyses that would prove useful to clinicians.

## Chapter 4 – Article: "Numerical Analyses to Assess the Hemodynamic Effects on the Mechanical Stresses of Patient-Specific Stenotic Coronary Plaques"

#### **Authors:**

Ramses Galaz, Rosaire Mongrain, Valerie Pazos, Richard Leask, Jean Claude Tardif.

#### **Objectives:**

- To study the transient hemodynamic effects on the mechanical stresses in realistic patient-specific coronary plaques.
- To calculate the spatial and transient distribution of the mechanical stresses of each node over one cardiac cycle in order to predict the probable zones of failure and the number of stress cycles before fatigue failure.
- To relate the transient results to the concept of fibrous cap mechanical fatigue (FCMF). Transient analyses are necessary in order to calculate the stress amplitude and mean stress of each node over the cardiac cycle in the numerical analyses.
- To assess the effects of the presence of multiple plaques within the proximal coronary artery.

#### **Hypotheses:**

- The analysis of the transient stresses can help identify the main physical factors involved in plaque failure.
- Plaque failure can occur as the result of a catastrophic failure due to chronic injury progression due to cyclic stresses. Fibrous cap mechanical fatigue (FCMF) is the

result of the combined effects of the cap thickness, relative inclusion stiffness and percentage of stenosis. These variables directly affect the magnitudes of the stress values in time and space and thus affect the stress amplitudes and mean stresses at each location.

• The particular configuration of a multiple plaque scenarios can affect the spatial distribution of the mechanical stresses. FCMF can be influenced by the global structure of the obstructive pathology in particular in the context of multiple stenoses [58, 59]. In this chapter we show that in the case of multiple stenoses (modeled as two adjacent stenoses) that FCMF is higher when the VP is downstream of a stable plaque (SP) as compared to a VP upstream of a SP.

#### 4.1 Abstract

Cardiovascular diseases represent the first cause of death in developed countries. Atherosclerotic plaque rupture in the coronary arteries has been extensively associated with acute myocardial infarctions. The rupture of the fibrous cap may trigger a thrombus formation that could occlude the coronary arteries and impede the flow of blood to the lower parts of the myocardium. In this work, we analyzed the transient hemodynamic effects on the mechanical stresses of the fibrous cap over one cardiac cycle. We reconstructed patient-specific coronary stenotic plaques from in-vivo intravascular ultrasound (IVUS) segments and analyzed them using fluid-structure interaction computational methods. Transient inlet conditions for pressure and flow were used in order to assess the individual and combined effect of these variables on the mechanical stresses. Furthermore, we hypothesized that plaque failure is the result of a chronic progressive injury caused by these cyclic stresses due to blood flow pulsatility and that our numerical results could help predict the number of cycles to failure based on a hypothetical S-N fatigue curve. Our results indicate a high stress concentration at the proximal shoulder region of the plaque when a soft core is present. The highest stresses occurred during peak diastolic flow, suggesting that kinetic forces play a significant role in plaque failure mechanics. Our fatigue analyses indicated that certain nodes located in the proximal shoulder could rapidly fail as a result of cyclic stresses rather than from a nominal stress value. We introduce the concept of fibrous cap mechanical fatigue (FCMF) by relating the transient numerical results to a failure prediction model based on fatigue.

#### 4.2 Introduction

Cardiovascular diseases represent the first cause of death in developed countries [92]. Atherosclerotic plaque rupture and subsequent thrombosis has been strongly correlated by pathological studies to ischemic acute coronary syndromes such as sudden cardiac death, unstable angina and acute myocardial infarction [1, 15, 19]. The disruption of the fibrous cap tissue of the atherosclerotic plaque may trigger a biological response of platelet activation and a subsequent formation of a thrombus, an event that could potentially occlude the coronary artery and impede the flow of blood downstream and possibly result in an acute myocardial infarction. It is estimated that up to 75% of all thrombus formations [16] and 90% of the cases of nonfatal myocardial infarction and sudden cardiac death are associated with the rupture of the coronary atherosclerotic plaque [19]. Studies have shown that such disruption may be initiated by long-term intrinsic changes of the plaque such as progressive lipid accumulation and degradation of the fibrous cap, or by external triggers which can include mechanical stresses due to hemodynamic or physical perturbations [93, 94, 95, 96]. Clinicians have established that ruptured plaques share certain morphological and biological features that make them more vulnerable to rupture such as a large lipid pool, a soft core, a thin fibrous cap and inflammatory cell acivity around the region of rupture [18, 19, 20]. Histopathological studies have shown that people who had died during physical exertion showed that ruptures were usually located at the midcap regions of the plaques, while those who died at rest showed shoulder rupture predominance [74]. Fujii [72] and Hiro [73] observed through longitudinal IVUS imaging that the commonest site of rupture is at the proximal region of the plaque. These findings suggest that different mechanisms act on different

scenarios and that both hemodynamics and mechanical stresses play an important role in the site and mode of failure.

Several authors have contributed to the computational analysis of the rupture phenomena as a consequence of high mechanical stress; their analyses showed a general agreement that the greatest magnitudes of stress occurred near the shoulder region of the plaque in the fibrous cap tissue [21,25, 68, 97, 98, 99]. However, most of these analyses only considered two-dimensional models of cross-sectional or longitudinal slices of the diseased vessels and thus did not provide the true three-dimensional state of the stress tensor. Moreover, without three-dimensionality, the analyses lacked information on how the interaction between the pulsatile hemodynamic waveforms and the morphology of the diseased artery affected the stresses over time. Imoto [100], Tang [88] and Ohayon [101] developed some of the earliest studies on 3D models of the phenomena with different approaches using maximum values of measured pressure at certain points in time of the flow as a baseline for assessing maximum plaque stress.

Our study focused in the assessment of the mechanically induced transient stresses in the fibrous cap tissue due to the hemodynamic changes across the stenosis in a three-dimensional field over one cardiac cycle. This three-dimensional and transient perspective provided information on the spatial and temporal distribution of the principal stresses to assess the possible initiation and paths of fissure propagation. Computational finite element methods and fluid-structure interaction analysis were used to develop a predictive model of the physical interaction between the blood fluid domain and the diseased arterial wall structural domain. The analyses were done using realistic models reconstructed from intravascular ultrasound (IVUS) imaging of in-vivo cases of human diseased coronary arteries. A particular case of a double plaque scenario was chosen for

analysis with realistic boundary and time-dependent conditions taken from measurements of coronary flow and pressure waveforms. Different mechanical properties were assigned to the various components of the model in order to determine a pattern of stress distribution under different circumstances. The local pressure, shear stress, velocity and pressure gradient forces were calculated to assess their overall effect on the arterial wall stresses. Also, using the same methodology of IVUS reconstruction, we reconstructed seven in-vivo cases of ruptured plaques in order to do a reverse engineering approach and compare our analyses with actual cases of ruptures and in order to validate our model. In particular, we show that ruptures tend to occur at the three-dimensional predicted zones of high mechanical stress. Although seven cases is not a statistically sample it provided some insight on how plaque rupture mechanics occurs.

Plaque rupture is a phenomenon that can be approached as either an acute failure of the fibrous cap due to a sudden increase in mechanical stress, or as the culmination of a chronic injury progression due to the cyclic stress or fatigue [35]. We introduce the concept of fibrous cap mechanical fatigue (FCMF) to explain the combined effects of the mechanical factors involved in the failure of tissue within the fibrous cap. The analysis of the realistic and time-dependent conditions of the coronary flow and pressure waveforms acting on the plaque provided more accurate information on the spatial and time distribution of the stresses. Given the appropriate fatigue life curves for the soft tissue, fatigue life could be estimated for each node in the numerical model parting from the calculated mean stress, frequency and the amplitude of the cyclic stresses.

#### 4.3 Methods

### 4.3.1 Morphological reconstruction of diseased vessels through IVUS (intravascular ultrasound)

Patient-specific cases of diseased coronary arteries were reconstructed using IVUS images of cross-sectional views in the longitudinal direction. The spatial resolution of IVUS ranges from 40 to 100 microns, sufficient to image the fibrous caps that usually rupture according to Virmani [27]. All IVUS segment images were created using motorized pullbacks of the ultrasound transducer commencing from the distal side of the stenosis. Only those segments distanced 1 mm apart were kept in order to simplify the 3D geometry reconstruction process even though the IVUS pullback was able to interrogate images at higher resolution intervals.

For each IVUS segment, the lumen boundaries were traced at the innermost echogenic layer: the internal elastic membrane (IEM), which is located in the intimal layer. Since there is no acoustic interface between the true adventitia and the perivascular tissue [64], it becomes difficult to assess the true size of the adventitia. Therefore, it was assumed that its outermost layer was located at a mean offset distance of  $100\mu$ m [65] from the external elastic membrane (EEM) which is located at the medial-adventitial interface.

The coronary arteries are of the muscular type and are normally composed of three layers: intima, media and adventitia. Since intravascular ultrasound (IVUS) cannot clearly distinguish the boundary between the intima and the media or the outermost surface of the adventitia, the artery walls were reconstructed in 3D as a single homogeneous body

comprising all three layers from the innermost surface of the lumen up to the outermost layer of the adventitia. In the presence of an atheromatous core, the fibrous cap tissue would be part of the same single body and thus share the same mechanical properties in the numerical models for the stress analyses.

The contour lines were hand traced and smoothed with spline curves using commercial software (Rhinoceros v3.0, Palo Alto, CA) in order to avoid jagged edges or singularities in the geometry that would result in artifactual stress concentrations when performing the fluid-structure interaction computational analyses as a result of unrealistic sharp corners. None of the reconstructions considered the three-dimensional spatial path of the catheter and therefore the geometries were reconstructed only in a straight formation

We illustrate the approach with the worst simulated case of a double plaque configuration (Figure 4.1). The first plaque presents a 75% eccentric stenosis with an approximate length of 7 mm and the second and more distal plaque presents a 46% eccentric stenosis with an approximate length of 4 mm located on the opposite side of the proximal plaque.

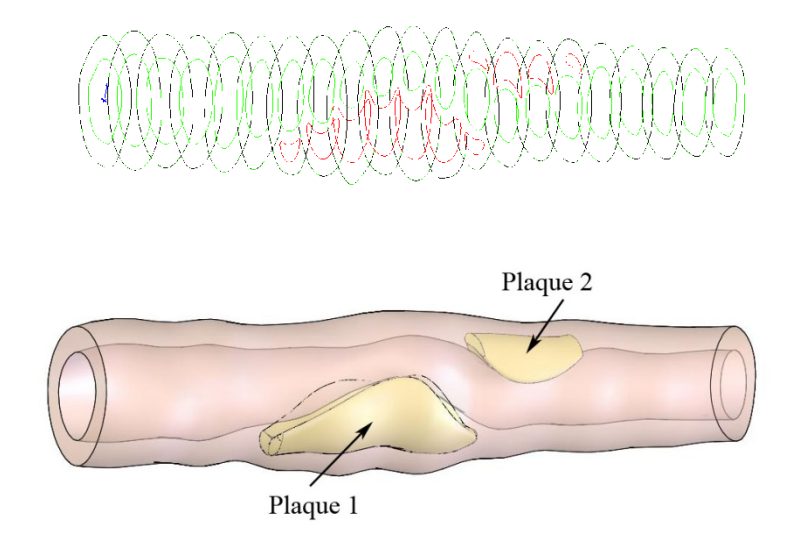


Figure 4.1: Traces of each IVUS segment and the respective 3D reconstruction

Using the same methodology of IVUS segmentation, we also reconstructed seven cases of in-vivo ruptured plaques as they would prove helpful in a reverse engineering approach to correlate the morphology and location of the rupture of the plaques.

#### 4.3.2 Fluid structure interaction methods

The reconstructed model was analyzed with fluid structure interaction computational methods using a commercial software package (ANSYS 10 and CFX 10, ANSYS Inc, Canonsburg, PA). The fluid domain was analyzed assuming a Newtonian fluid model as it has been shown to be a good approximation due to the large content of water-based plasma in the blood [84]. The boundary condition at the inlet was defined as an opening with the typical transient aortic blood pressure ranging from 80 to 120 millimeters of mercury following a typical pressure waveform described by Berne for a left anterior descending (LAD) coronary artery [42]. The outlet boundary condition was defined as an opening following the phasic coronary blood flow waveform for the left

coronary artery also described by Berne (Figure 4.2); the blood flow values ranged from 0 to 100 ml/min. The total time for the transient analyses for each cardiac cycle was 0.78 seconds which corresponds to a normal cardiac rhythm of 77 beats per minute. All analyses were subdivided into 50 equal timesteps, each of 0.0156 seconds. It is of interest to calculate the mechanical stresses during the most critical points in time regardless of the number of timesteps in which we have divided our model. The highest diastolic flow occurs at t = 0.249 seconds at exactly timestep #16. Since our model does not consider viscoelastic effects in the material, there is no retardation in the tensioning or relaxation of the material stresses and thus we can consider individual points in time for peak stresses.

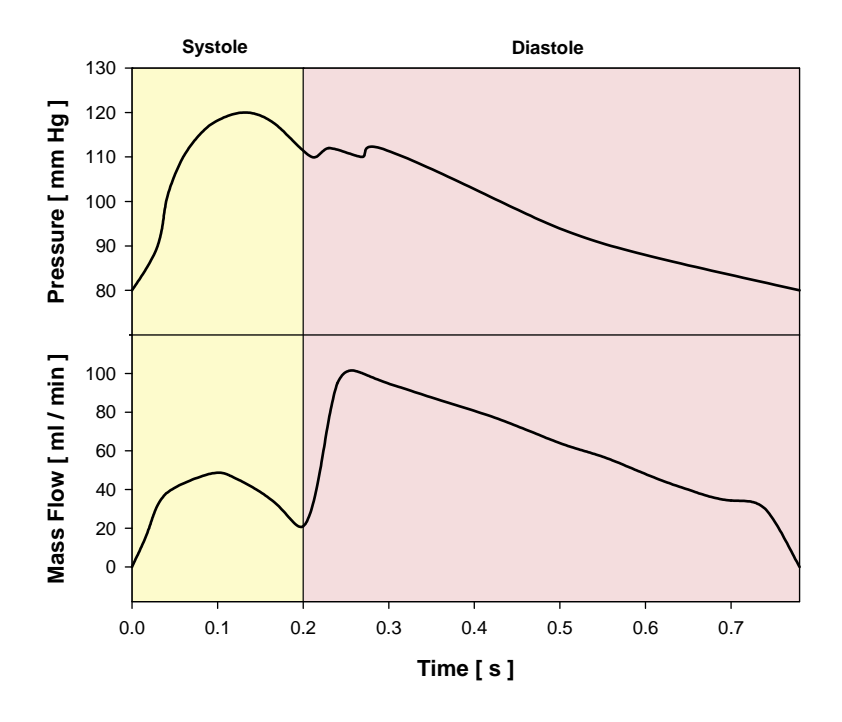


Figure 4.2: Aortic pressure and phasic coronary flow waveform (LAD) [42]

For the particular case that was analyzed, the structural domain was composed of three separate bodies, being the main body the arterial wall structure along with the fibrous cap tissue; the other two bodies represented the proximal and distal plaques (Figure 4.1). The artery models were constrained at the distal and proximal edges so no longitudinal displacement could occur but only allowed for radial displacement.

It is widely known that arteries exhibit hyperelastic behaviours in stress-strain curves. However, since large deformation mechanics were not present in this analysis, the material properties for the arterial wall and fibrous cap were considered to be incompressible and with linear elastic material properties with a Young's modulus of 800 KPa. This value was calculated in previous studies using the Lamé equations for a thick wall cylinder under pressure. The cores of the plaques were defined as single isotropic bodies of linear elastic and nearly incompressible material properties (Poisson's ratio = 0.499).

A value  $\gamma$  was defined to be the ratio between the plaque's core and the artery wall Young's modulii.

$$\gamma = \frac{E_c}{E_a} \tag{4.1}$$

Two sets of analyses were done in order to compare the effect of different plaque mechanical properties on the stress magnitudes: the first using a very soft material for both plaques ( $\gamma_1$ ,  $\gamma_2$ << 1), and the second using a very soft material for the proximal plaque ( $\gamma_1$ <<1) a very hard material for the distal plaque ( $\gamma_2$ >>1) simulating a rigid calcified core.

The mechanical stress levels were calculated using the multifield coupled solver of the ANSYS-CFX software package. Two sets of analyses were performed in order to compare the resulting stress levels of using a fully coupled versus a one-way coupled fluid-structure interaction (FSI) analyses. Fully coupled FSI analyses required significantly more computational time than the one-way FSI method as the former solves iteratively for both the structural and fluid domain deformations by communicating the pressure results through the FSI interface, being the lumen surface of the artery. The one-way method only applies the fluid domain pressure results onto the structural domain but does not consider the deformation of the fluid domain. It is important to mention that the only variable of communication at the FSI interface in both methods is pressure as a global result of the other typical variables such as wall shear stress, pressure gradient and fluid velocity.

This study only analyzed the local mechanical stresses present in the fibrous cap as proposed by Tang [88] since our study focused on determining the cap's failure. Only those nodes that comprised the fibrous cap solid body and those that were in close proximity to it were taken into account (Figure 4.3). By doing this, we discarded high values of stress outside the region of interest and thus increase the sensitivity to stress levels within the fibrous cap tissue.

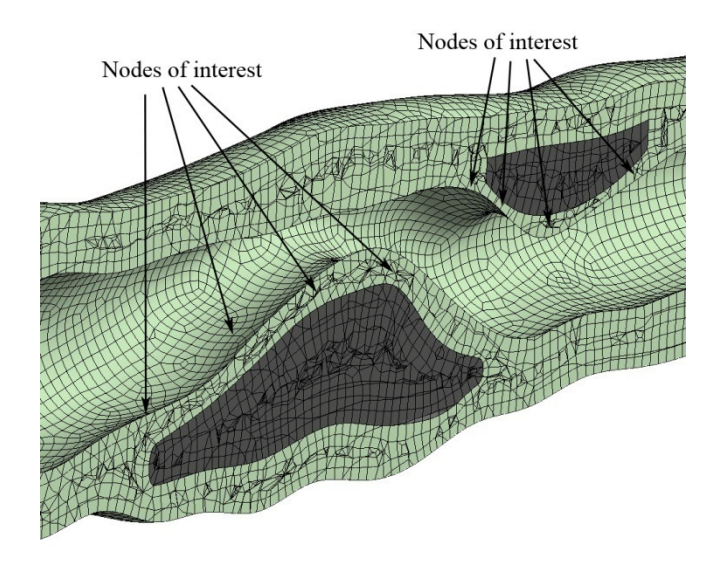


Figure 4.3: Longitudinal section view of the model mesh and the nodes of interest for fatigue analysis

#### 4.3.3 Fatigue analysis

Plaque rupture is a phenomenon that can be approached as either an acute failure of the fibrous cap due to a sudden increase in mechanical stress, or as a fatigue process described as the catastrophic failure of a chronic injury progression due to cyclic stresses [35]. Blood flow pulsatility induces a periodic pattern of tissue stretching and relaxation that translates into localized high mechanical stress concentration zones typically influenced by material irregularities, discontinuities and physical conditions. The presence of the atherosclerotic plaque can exacerbate the mechanical stress levels and thus increase the amplitude of the cyclic stresses that may reduce the number of cycles to failure.

Many authors have analyzed plaque rupture using computational methods and have suggested a threshold value for mechanical stress failure [20, 25, 69, 97]. These approaches implied that rupture is induced by stresses that exceed the ultimate tensile strength of the tissue, and if any node or element in the analysis did not surpass this value, then rupture would not occur. In a fatigue approach, variables such as the stress cycles, the stress amplitude and the mean stress are considered as the critical factors for material failure. Our approach considered fatigue as the main factor driving plaque failure. For our fatigue analysis approach, we assumed that no biologically active remodeling processed were present due to the complex nature of tissue remodeling. This phenomenon would influence the nature of mechanical fatigue failure as damaged tissue may be subjected to inflammatory processes.

Plaques usually rupture at relatively low stress levels under normal physiological conditions when compared against the high pressure levels that percutaneous transluminal coronary angioplasty (PTCA) exerts to fracture the atherosclerotic plaque [102, 103]. Ruptures are usually catastrophic and without warning, crack initiation and propagation usually occur at a slow pace, but when the crack reaches a given critical length, the rate of crack growth increases rapidly and a low critical stress is needed to precipitate the rupture [104]; a small trigger such as an acute increase of blood pressure or heart rate can complete the loop of catastrophically failing plaques that were close to being ruptured. Fatigue life is determined by the number of stress cycles, the stress amplitude and the mean stress [104]; several studies have established a correlation of cardiovascular events with accelerated heart rates that increase the number of cycles [105, 106], blood pressure levels that increase the amplitude of the stresses [107] and morphologically vulnerable plaques that can increase the mean stress levels [25, 88, 96, 101].

For our analyses we used a failure criterion similar to the one proposed by Goodman [37] that considers the mean stress and the amplitude of the cyclic stresses of each node in order to determine its likelihood of failure given an endurance stress limit and ultimate tensile strength values (Equation 4.2).

$$\frac{\sigma_{\text{mean}}}{\sigma_{\text{endurance}}} + \frac{\sigma_{\text{amp}}}{\sigma_{\text{uts}}} = 1 \tag{4.2}$$

Where  $\sigma_{\text{mean}}$  is the mean stress for any particular node calculated as the sum of the Von Mises stress [108] values through the entire cardiac cycle and divided by the number of timesteps t (Equation 4.3).

$$\sigma_{\text{mean, i}} = \frac{\sum_{t=1}^{p} \sigma_{i,t}}{t}$$
(4.3)

The stress amplitude denominated  $\sigma_{amp}$  is calculated as the absolute difference between the lowest and highest stress value of each node through the entire cardiac cycle (Equation 4.4).

$$\sigma_{\text{amp, i}} = \sigma_{\text{i,t max}} - \sigma_{\text{i,t min}} \tag{4.4}$$

The value  $\sigma_{endurance}$  represents the experimentally determined threshold value at which no failure occurs after an infinite or predefined number of cycles. The value of  $\sigma_{uts}$  represents the ultimate tensile strength of the material and it is also obtained experimentally.

We also borrow from ductile metal failure and assume that the exponential behavior of the stress vs. number of cycles to failure curves (S-N curves) is similar (Figure 4.4); there is no available data that has reproduced experimentally the S-N curve of human coronary artery tissue and more specifically of the fibrous cap tissue.

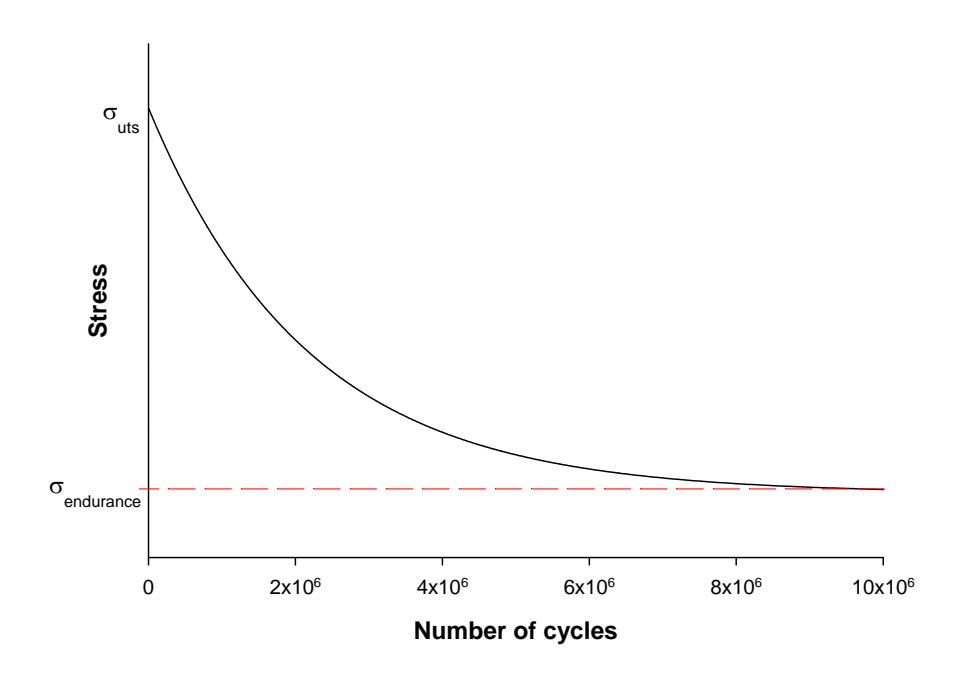


Figure 4.4: Typical exponential behavior of a stress vs number of cycles (S-N) curve

The equation that describes the curve from Figure 4.4 is of the following form:

$$\sigma_f = (\sigma_{uts} - \sigma_{endurance})e^{-\alpha n} + \sigma_{endurance}$$
(4.5)

Where  $\sigma_f$  is the reference stress value for rupture;  $\sigma_{\rm uts}$ ,  $\sigma_{\rm endurance}$  and  $\alpha$  need to be determined experimentally. The Goodman criterion was originally proposed as a design criterion that would prevent fatigue failure by a combination of a low mean stress with a small stress amplitude that would be equivalent to reach an infinite number of cycles, hence the equality of 1. We adapted the Goodman equation with this  $\sigma_f$  reference value in order to have a criterion that could include the S-N curve equation with the values obtained from experimental data (equation 4.6).

$$\frac{\sigma_{\text{mean}}}{\sigma_{\text{endurance}}} + \frac{\sigma_{\text{amp}}}{\sigma_{\text{uts}}} = \frac{\left(\sigma_{\text{uts}} - \sigma_{\text{endurance}}\right)e^{-\alpha n} + \sigma_{\text{endurance}}}{\sigma_{\text{endurance}}}$$
(4.6)

And thus the number of cycles to failure for each node  $n_i$  can be calculated as:

$$n_{i} = -\frac{\ln\left[\left(\frac{\sigma_{i\text{mean}}}{\sigma_{\text{endurance}}} + \frac{\sigma_{i\text{amp}}}{\sigma_{\text{uts}}}\right)\sigma_{\text{endurance}} - \sigma_{\text{endurance}}\right) / (\sigma_{\text{uts}} - \sigma_{\text{endurance}})\right]}{\alpha}$$
(4.7)

From this point, we calculated the number of cycles to fatigue failure for each node using hypothetical values of  $\sigma_{\text{uts}}$ ,  $\sigma_{\text{endurance}}$  and  $\alpha$ . Histograms of the ranges of values of number of cycles were constructed to analyze quantitatively the number of nodes that would fail more rapidly and thus assess the plaque's vulnerability to rupture due to mechanical stress.

#### 4.4 Results

#### 4.4.1 Fluid domain results

Two modalities were used to calculate the hemodynamic and mechanical variables when using the fluid structure interaction methods: one-way coupled and fully coupled. The former analyzed the fluid domain only without feedback from the deformed structural domain, producing quick computational results. The latter iterated and communicated the results from both fluid and structural domains for each timestep, resulting in more accurate but significantly longer computational times: around 110 times the required time than the one-way coupled method using the particular model chosen.

The numerical results yielded a drop in pressure across the length of the stenosis for both FSI modalities (Figure 4.5). Under the fully coupled method, a pressure difference of 11.2% was calculated during peak diastolic flow rate of 100 ml/min, such difference was mostly driven by the geometrical constriction of the stenosis and the increased flow. Conversely, at the beginning of systole when the flow rate was negligible, the pressure difference was only around 2%. On the other hand, when working under the one-way coupled method, the pressure difference was 15.7% during peak diastolic flow but again only 2% at the beginning of systole (Figure 4.5). This indicates that the one-way method tends to slightly overestimate the flow values as a result of an undistorted and therefore more constricted fluid domain. These results are similar to those determined experimentally by Mates for the same degree of stenosis [86].

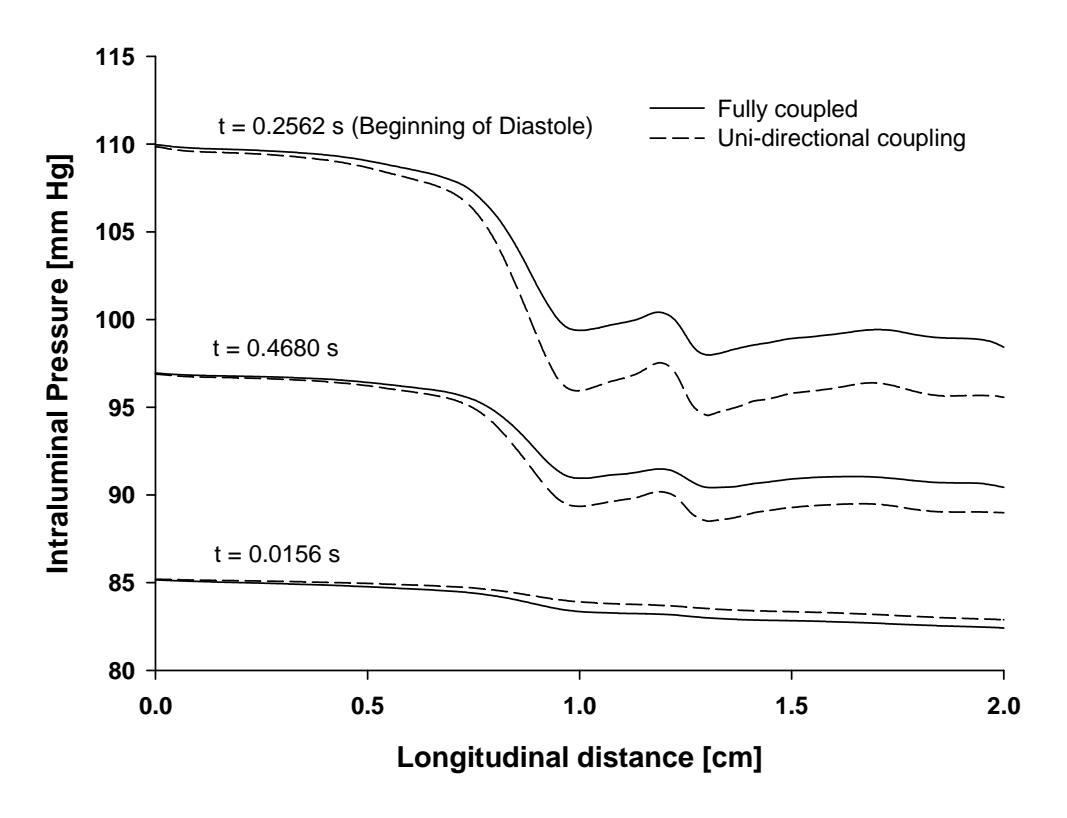


Figure 4.5: Central streamline pressure drop across the model at various point in time

In a previous study, it was demonstrated that at higher percentages of stenosis and constant flow rate the pressure drop was significantly greater. However, geometrical constrictions alone are not the only driving factor behind the pressure drop effect but also by viscous effects, as demonstrated in the equations developed by Back [82]. These equations established a linear relationship of the change of pressure with respect to the flow for the viscous terms and a quadratic relationship for the geometrical terms.

Under the one-way coupled method, the central streamline velocity increased from an average of 34 cm/s at the inlet boundary to 195 cm/s at the peak of the largest stenosis during peak diastolic flow. The fully coupled method produced results that estimated the velocities at lower values than those of the one-way method: velocities of 29 cm/s at the

entrance and 170 cm/s at the peak of the largest stenosis. The one-way method overestimates the velocity as a result of a rigid and therefore more constricted fluid domain (Figure 4.6).

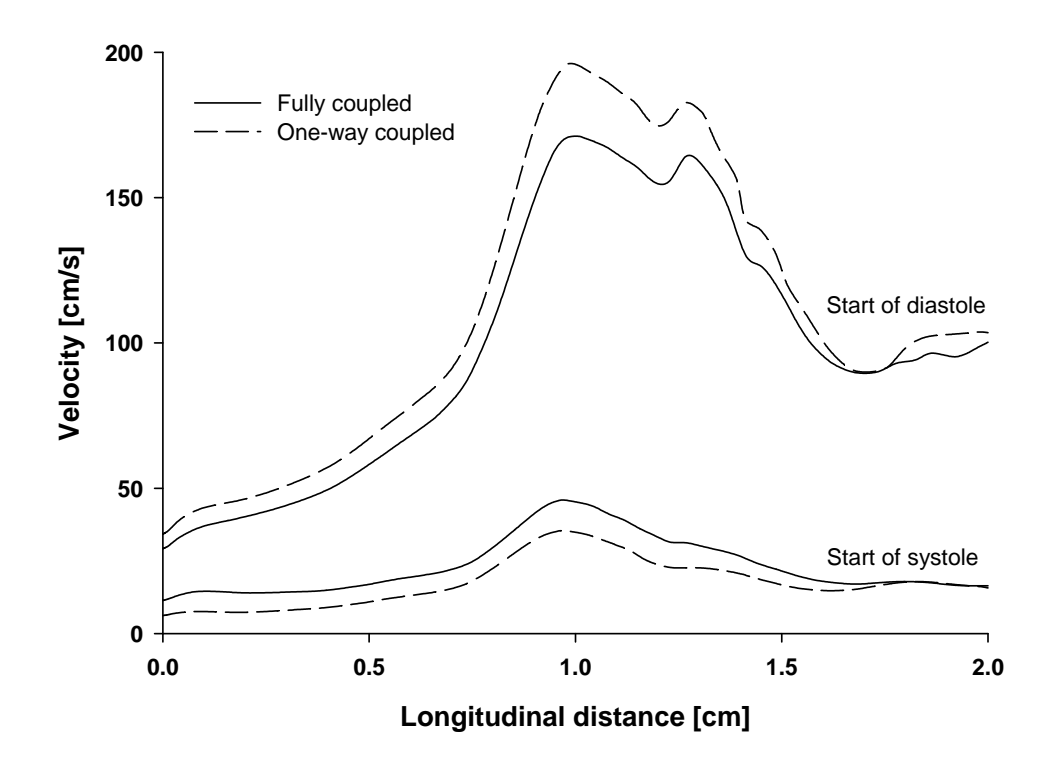


Figure 4.6: Central streamline velocity increase across the length of the model

Physically speaking, both potential and kinetic energy enter the system in the form of pressure and flow respectively. The presence of an obstruction such as the stenosis magnifies the loss of energy, which can escape the system in the form of mechanical deformation of the weakest components of the structural domain or as heat that is carried away by advection. The results obtained from the hemodynamic flow analysis exhibit a pressure drop distal to the stenoses, an increase in the flow velocity, high shear stress near the proximal peak of the stenoses, but more importantly a pattern of pressure gradient forces acting normally to the proximal side of the peak of the stenoses (Figure 4.7). These

pressure gradient forces represent the means of physical communication between the fluid and structural domains at the lumen surface interface in the FSI analyses.

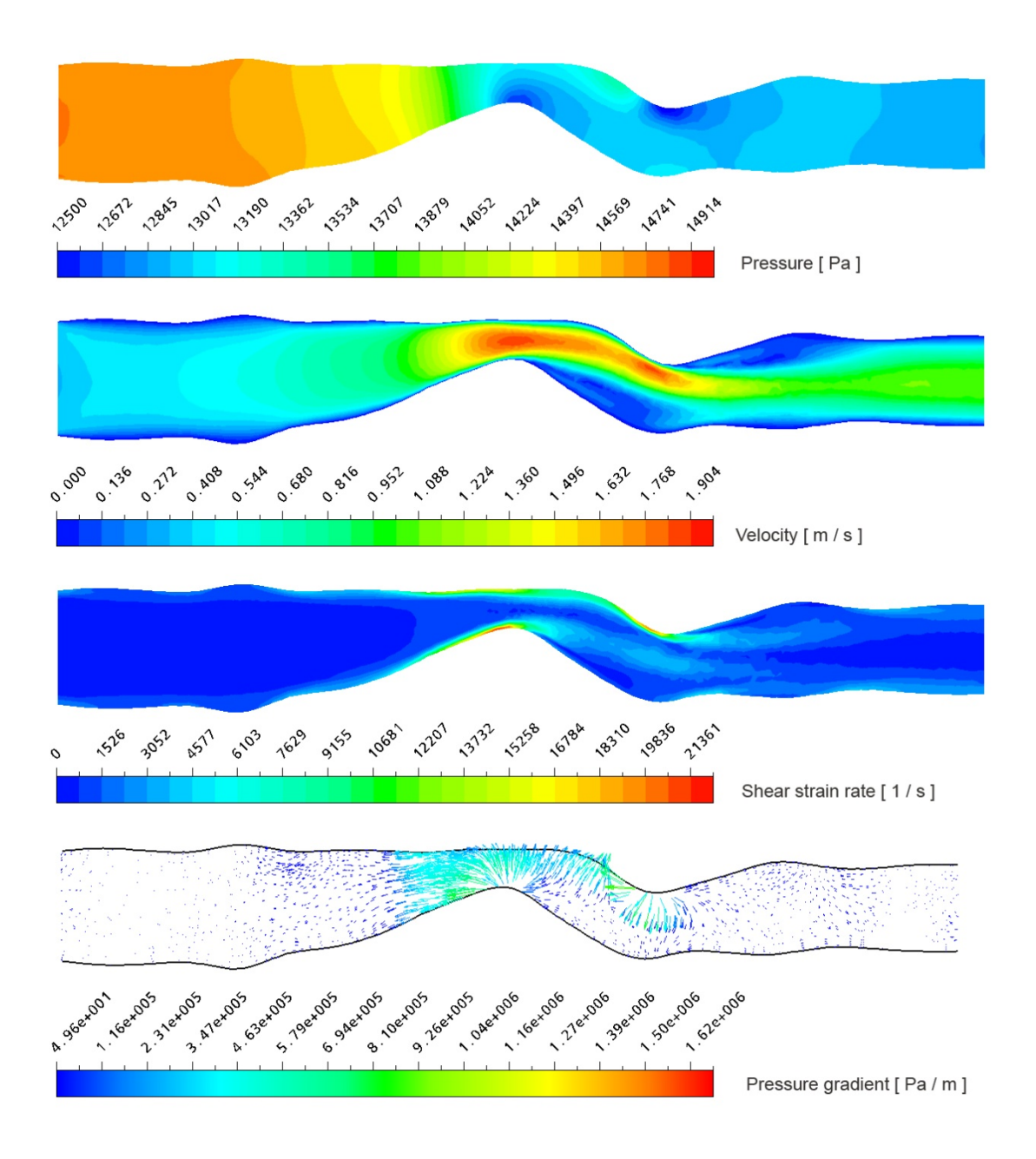


Figure 4.7: Slices of relevant hemodynamic variables from the 3-D numerical results.

#### 4.4.2 Structural domain results

The analysis of the interaction between the fluid and structural domains of this realistic case produced results compatible with similar previous studies using ideal geometries of stenosed arteries: the location of the fibrous cap stress concentration occurred always at the proximal side of the stenosis mainly driven as the result of the pressure gradient forces acting on the surface of the lumen and the plaque. Also, the magnitude of the stress depended on the thickness of the fibrous cap, the percentage of stenosed area and the stiffness of the internal core.

We used the same sets of IVUS reconstructed cases for the structural domain; the first configuration used a soft proximal ( $\gamma_1$ <<1) and soft distal ( $\gamma_2$ <<1) plaque scenario; the second analysis used the same geometrical model but with a soft proximal ( $\gamma_1$ <<1) and hard distal ( $\gamma_2$ >>1) plaque configuration. The results for the soft-soft showed a greater stress concentration in upstream and shoulder side of the distal and smaller plaque with a maximum value of 92 KPa during the peak diastolic flow at which the greatest pressure drop occurs. Conversely, in the soft-hard configuration, the greatest stress concentration occurred in the upstream and shoulder side of the proximal plaque with a maximum value of 87 KPa; very low stresses resulted at the zone of the distal plaque (Figure 4.8). This strongly suggests that not only the stiffness of the cores and the particular morphology of each plaque influence the stresses but also the configuration in multiple plaques scenarios. It also becomes clear that the fibrous cap will exhibit great deformation and high stresses if there is a weak structural support underneath it or it will be mechanically stable if it has a strong support such as a hard calcified core.

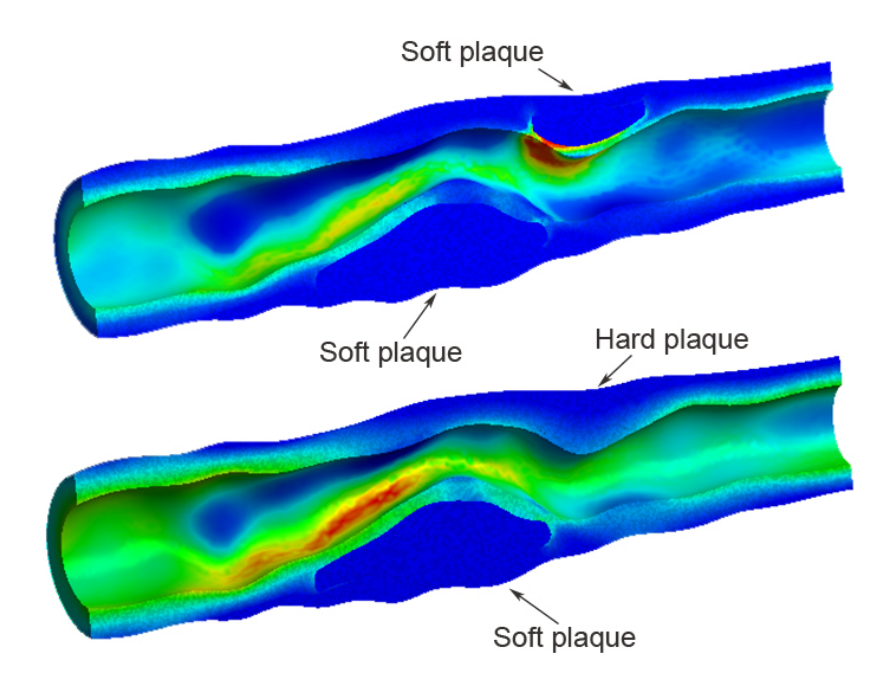


Figure 4.8: Equivalent stress map plot of the structural domain for two different arrangements of material properties using the same geometry

It was of interest to analyze the transient behavior of the maximum stress during the entire cardiac cycle given. Figure 4.9 depicts the maximum stress behavior along with the boundary conditions of pressure and mass flow for the soft-soft plaque configuration case. The one-way coupled method described a curve very similar to the pressure waveform inlet conditions. The fully coupled method resulted in a curve that combined the effects of both the pressure and coronary flow waveforms, particularly the effect of the peak flow occurring at the beginning of diastole, which resulted in the maximum measured stress. The results showed that flow and pressure are important factors in determining the overall magnitude of the stress. At higher flow rates, the pressure drop and kinetic energy losses were greater and thus transformed into a higher mechanical

energy that strained the weakest components of the plaque, more specifically the thin fibrous caps with soft cores.

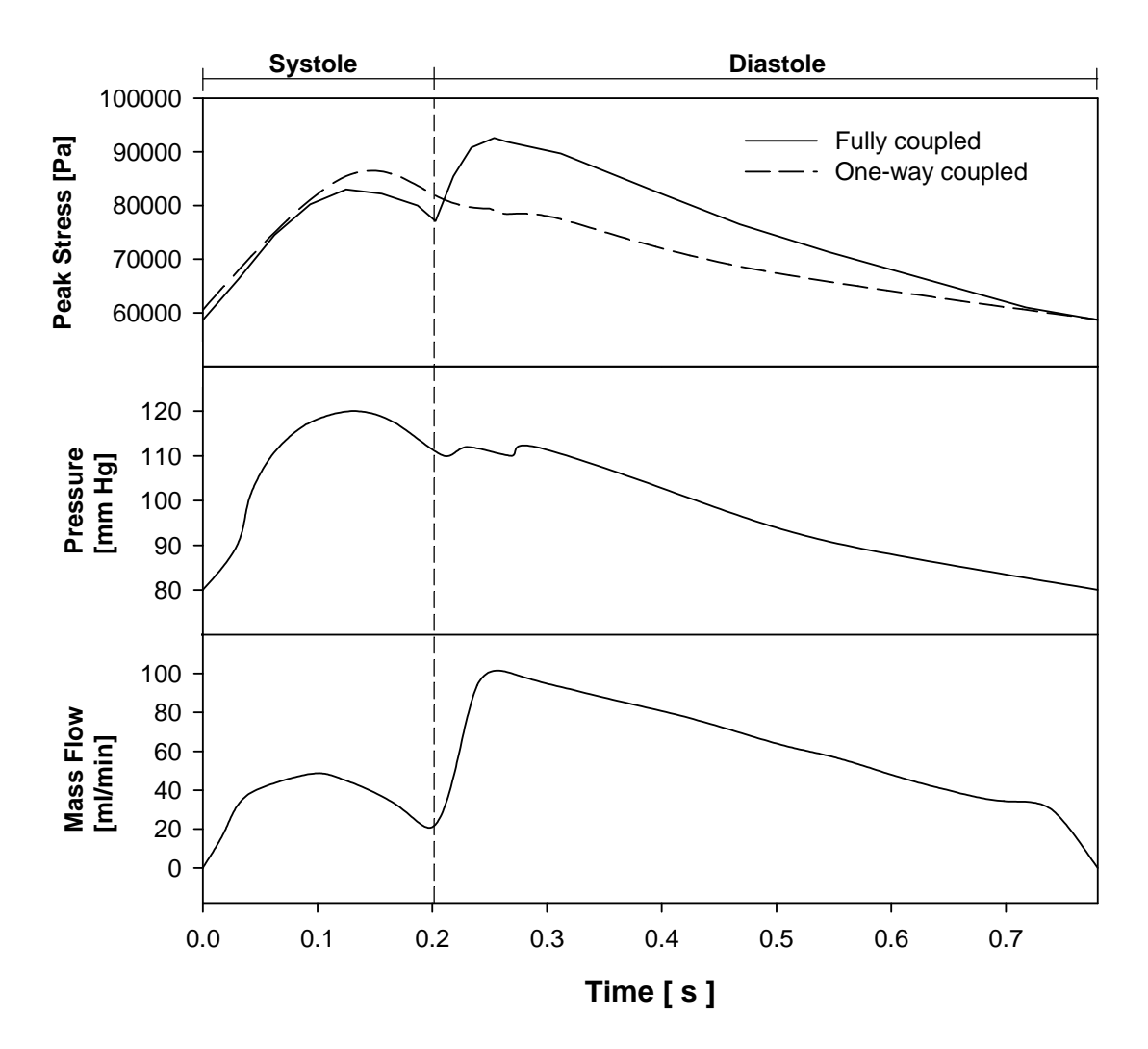


Figure 4.9: Maximum stress patterns and the inlet boundary condition of the soft-soft plaque configuration model analyzed under the one-way and fully coupled methods.

## 4.4.3 Fatigue analysis results

Our approach considered fatigue as the main factor driving plaque failure rather than a maximum monotonic stress value. One study by Gilpin [36] tried to recreate the S-N curve of healthy porcine coronary arteries by extrapolating the curve using a few experimental values of low cycle count results. Since there are no established S-N curves for the human coronary artery tissue even less the fibrous cap tissue, we assigned values in the same order of magnitude as the study by Gilpin [36]. The values assigned were  $\sigma_{\rm uts}$ = 400 KPa,  $\sigma_{\rm endurance}$  = 100 KPa and  $\alpha$  = 4.506e-7 in order to exemplify the feasibility of calculating the mechanical vulnerability due to fatigue; with those values, a fraction of the nodes would fall above the endurance limit and certainly fail due to fatigue. Figure 4.10 depicts a histogram of the stress levels of each node at particular points in time during the cardiac cycle. These values resulted from the soft-soft configuration and using a shifted pressure waveform of 150-110 mmHg and they indicate that only a small number of nodes exceed the endurance limit. These would eventually fail after a determined number of cycles, while the rest of the nodes below the endurance limit value would never reach failure. The stress amplitude was calculated for each node as the absolute difference between the highest stress value during peak diastolic flow and the lowest stress value occurring at the beginning of systole. On average, the stress amplitude was equal to 20 KPa. Figure 4.11 shows the stress range histogram comparing two different inlet pressure waveforms: 150-110 mmHg vs. 120-80 mmHg. The first analysis (150-110 mmHg) indicated that at higher inlet pressure ranges, the number of nodes above the endurance limit increased and thus would reduce the number of cycles to failure only for a certain group of nodes. The second analysis (120-80 mmHg) only yielded that two nodes were above the endurance limit and the number of cycles to failure tended to be a very large number.

The concept of fibrous cap mechanical fatigue (FCMF) assumes that the overall combination of fibrous cap thickness, relative inclusion stiffness, percentage of stenosis, plaque morphology, hemodynamic conditions and cyclic stretching due to pulsatility could all influence the failure mechanism of the fibrous cap. The mechanical stresses within the plaque are influenced by each of these factors by different means and proportions. However, an important result (as depicted in figure 4.11) is that any variable that can affect the amplitude or the mean stress in the cardiac cycle will influence the fatigue life of the fibrous cap. We hypothesize that the concept of fibrous cap mechanical fatigue (FMCF) is more applicable under real life scenarios as opposed to a nominal stress value that would eventually cause rupture.

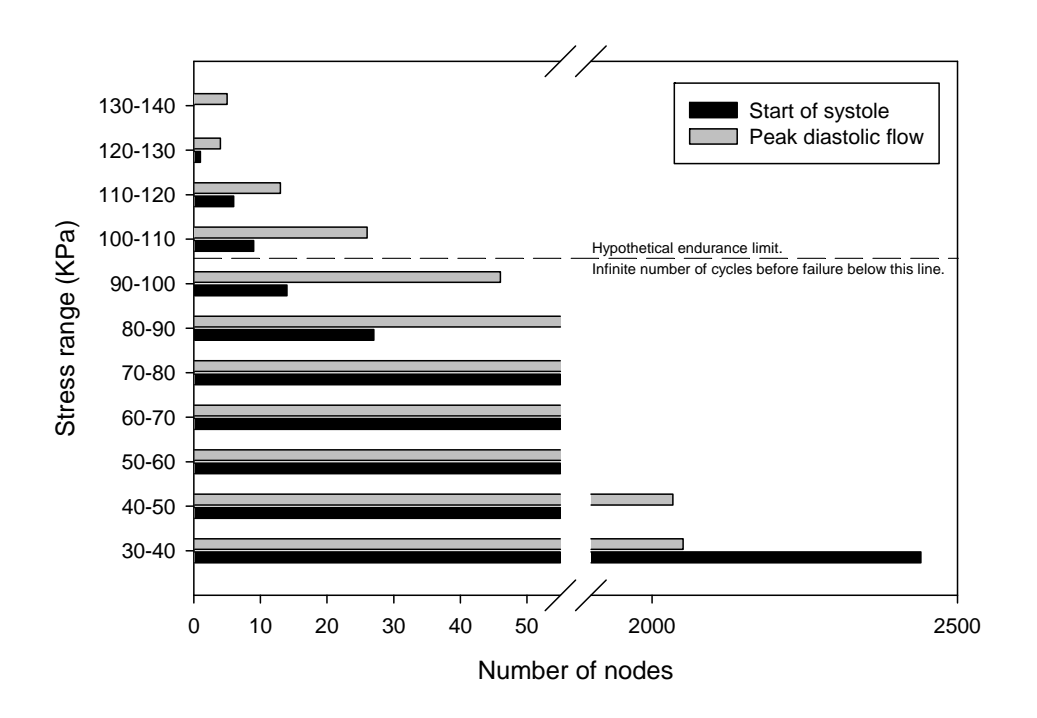


Figure 4.10: Histogram of the number of nodes according to their stress range value.

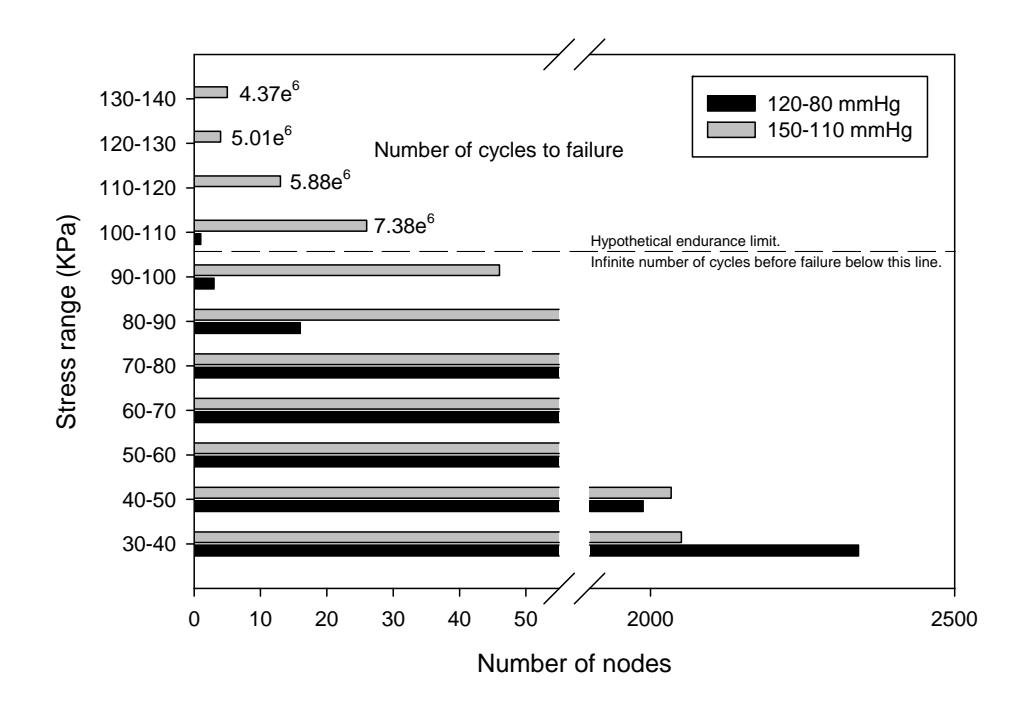


Figure 4.11: Histogram of the number of nodes for the stress range values as a comparison of high (150-110 mmHg) vs. low (120-110 mmHg) pressure ranges at inlet.

#### 4.5 Conclusions

The numerical results showed that the highest stress concentrations occurred in the proximal shoulder zone of the plaque. An explanation of this event is that pressure gradient forces act directly on the proximal side of the plaque. The presence of a stenosis induces flow kinetic energy losses in the form of a pressure drop due to the geometrical constrain and viscous effects. Some of this lost energy translates into a mechanical deformation of the more compliant or weakest structural components of the plaque. A more compliant plaque core would allow for greater displacement than a rigid calcified core. As the plaque is displaced, the shoulder areas where the fibrous cap tissue connects with the artery wall suffer the greatest strains and thus mechanical stresses; as a result, these locations may be more prone to rupture.

The particular morphology of the double plaque scenario that was analyzed provided some insight that the presence of multiple plaques can greatly influence the hemodynamic pattern and thus the mechanical stress distribution within both plaques. Future analyses shall be performed considering all the surrounding morphological factors.

Another interesting finding is that hemodynamic flow induces the greatest mechanical stresses rather than intracoronary pressure alone. However, the resulting stress is influenced by both the flow and pressure inlet conditions. Peak stress in the fibrous cap was calculated during the highest blood flow levels in diastole. Conversely, at low flow levels during the beginning of systole, the mechanical stresses were the lowest and they followed the intracoronary blood pressure pattern.

The comparison between the unidirectional coupled method vs. the fully coupled method of fluid-structure interaction yielded that the former tends to overestimate the

pressure drop difference as it does not account for arterial wall compliance and the flow velocity increases in a rigid artery. Although the unidirectional coupled method provides much faster results in terms of computational time, we should try to use the fully coupled method instead in future analyses as it can provide results that approximate the true physics of the environment.

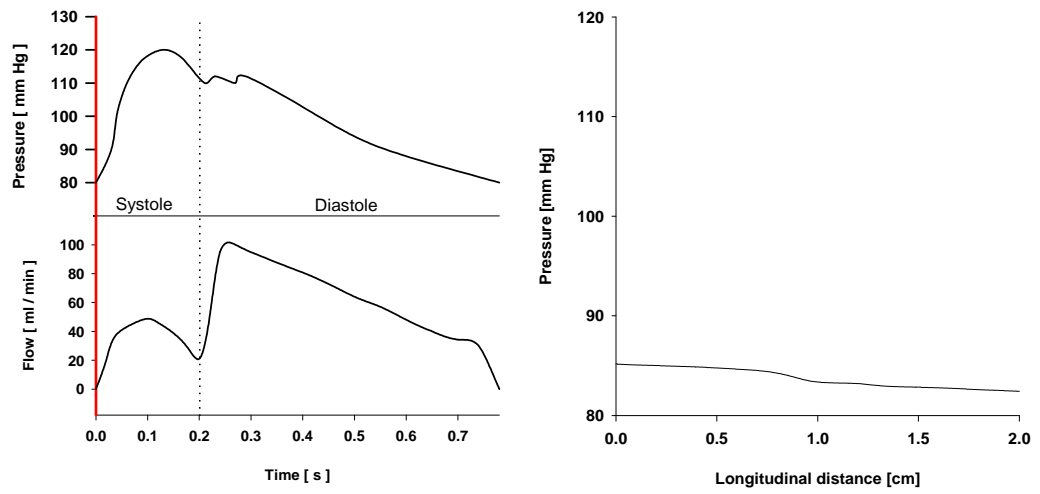
We also showed that in the case of multiple stenoses (modeled as two adjacent stenoses) that fibrous cap mechanical fatigue (FCMF) is higher than when the vulnerable plaque (VP) is downstream of a stable plaque (SP) as compared to a VP upstream of a SP. Vulnerable plaques are also known to be more prone to rupture under physical exercise (1, 2).

Finally, the fatigue analyses showed that under a hypothetical S-N curve, we could determine that certain nodes that could have a more premature failure as a result of the cyclic stresses. The concept of fibrous cap mechanical fatigue (FCMF) was introduced as a mean to explain why some plaques may fail prematurely even though they may not exhibit high nominal mechanical stress values but rather a combination of cyclic stresses whose mean and amplitude might influence the fatigue life of the tissue. Future research needs to address the characterisation of the S-N curve for fibrous cap tissue if we want to accurately predict a fatigue life based on experimental results.

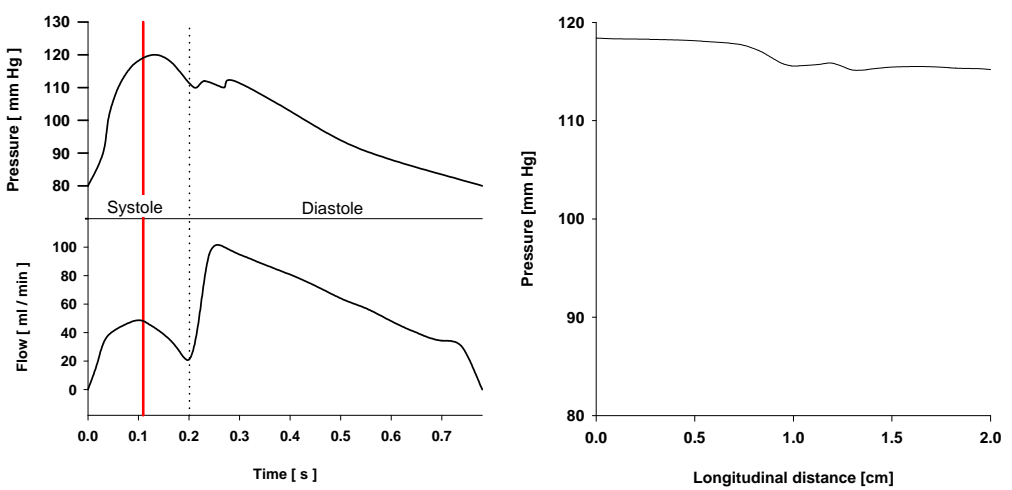
# Chapter 5 – Discussion on article: "Numerical Analyses to Assess the Hemodynamic Effects on the Mechanical Stresses of Patient-Specific Stenotic Coronary Plaques"

## 5.1 Transient analyses

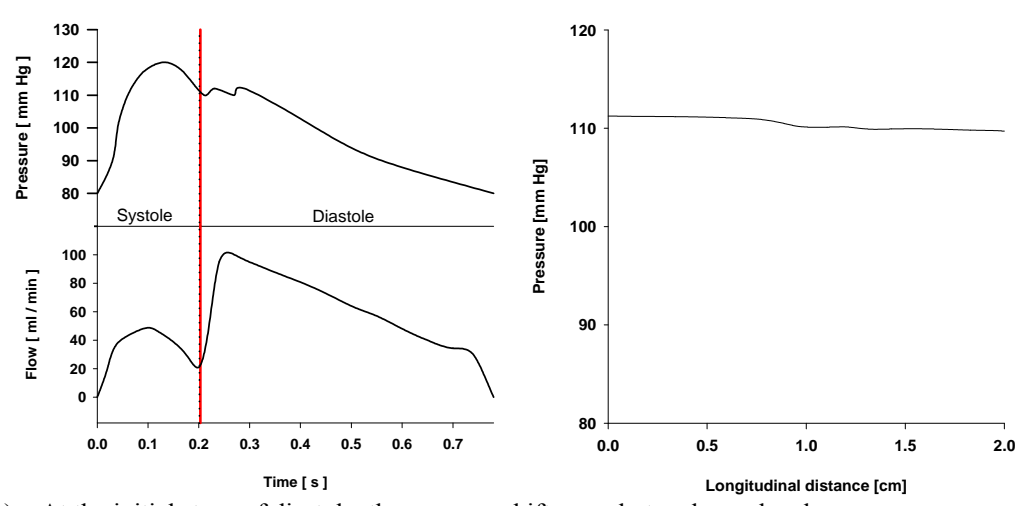
The results described in this article clearly agree to our previous study (chapter 2) by showing a proximal side shoulder stress concentration. The transitory analyses revealed that the greatest pressure drop occurs when maximum flow in the coronaries is present, that is, at the beginning of diastole (Figure 5.1), which also corresponds to the greatest stress magnitude in the proximal shoulder region, this can be interpreted as the fluid energy losses being transformed into the mechanical deformation of the weakest structural component of the plaque. After all, the pressure drop equations developed by Back [82] are based on blood flow Q. The resulting maximum stress is driven by a combination of potential energy in the form of pressure and kinetic energy in the form of flow. The reconstruction of the in-vivo patient-specific coronary plaques from IVUS images represented a challenge if we were to automate such process: currently all the individual image tracing is done by hand, and the surfacing that connects all IVUS traces is still done manually to correct any surfacing errors that might arise and to avoid jagged edges that would induce stress concentrations. During this stage, we also reconstructed seven cases of ruptured plaques to provide some three-dimensional insight to where plaque ruptures occur. The numerical analyses were much more complex at this stage, not only because we were using a more realistic geometry and complex shapes, but because the number of elements increased significantly as some thin areas required more detailed analysis. Also, it is not uncommon to end up with non-convergence from the high number of elements count and the complex geometries involved.



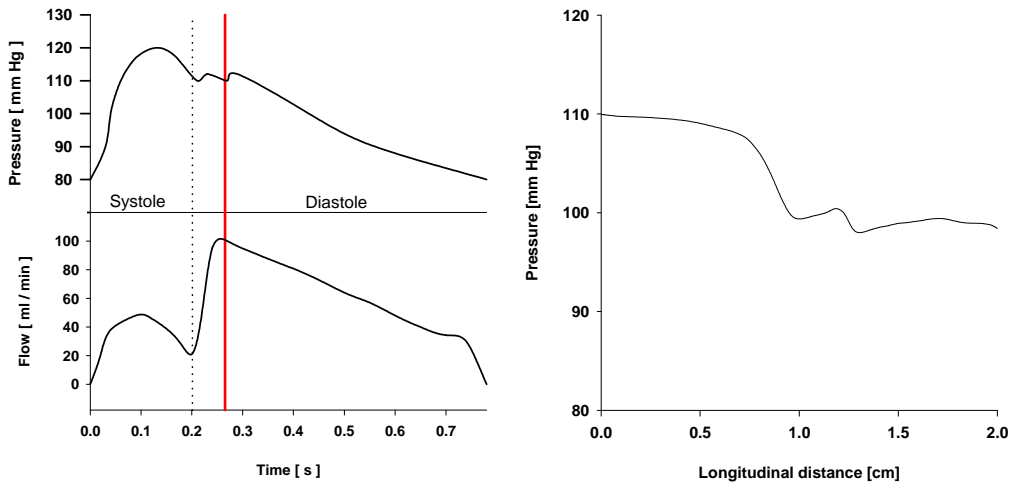
a) At the beginning of systole, there are no significant changes in pressure throughout the stenosis.



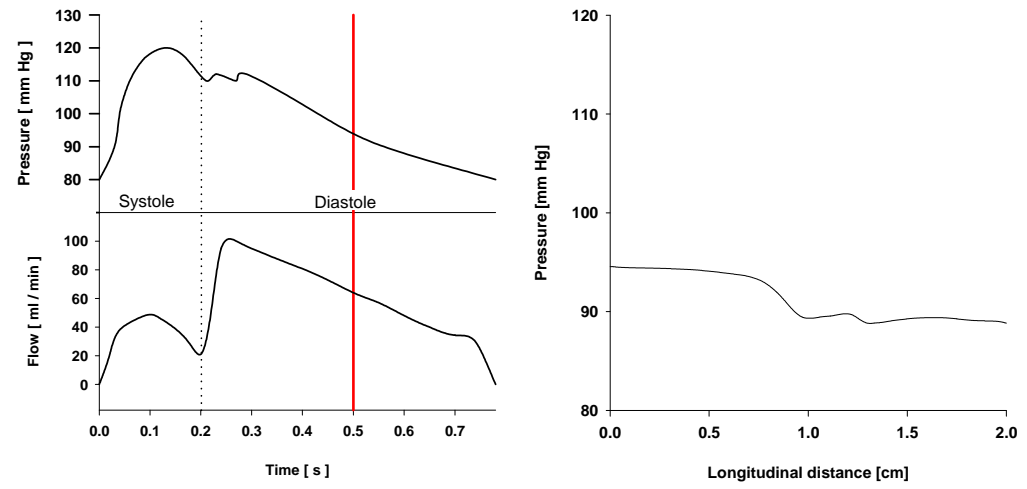
b) During peak pressure in systole, the pressure shifts throughout the entire stenosis.



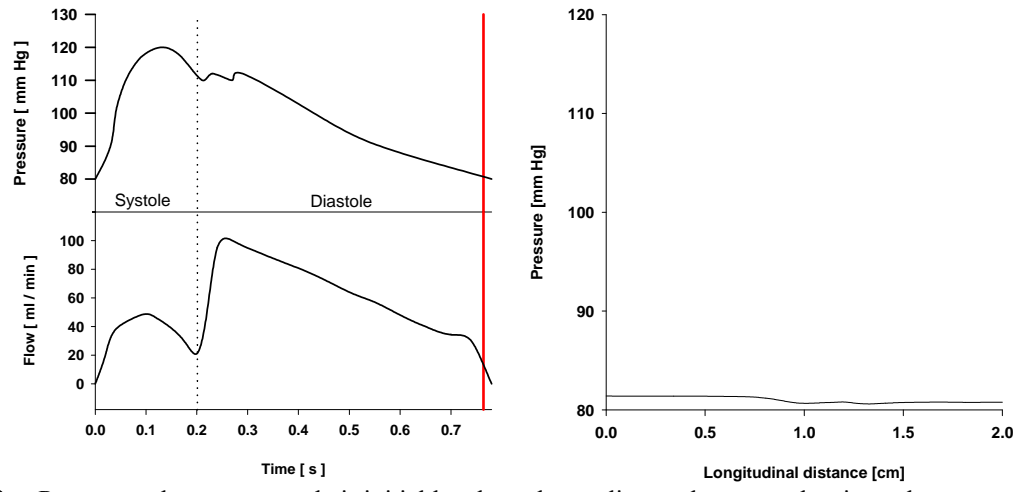
c) At the initial stage of diastole, the pressure shifts evenly to a lower level.



d) A sudden rise in the coronary flow causes a significant pressure drop (or energy loss) across the stenosis. This point in time is when the highest mechanical stresses occur.



e) As pressure and flow are reduced, so are the magnitudes and differences in pressure.



f) Pressure values return to their initial levels as the cardiac cycle approaches its end.

Figure 5.1: Pressure drop values across the length of the stenosis at different timesteps

## 5.2 Transient analyses using unidirectional and fully coupled FSI methods

The transient nature of the analyses and the fluid-structure interaction methods increased significantly the computational time to converge to 27 hours compared to the 15 minutes required by the static analyses. In this article we presented two methods to perform fluid structure interaction analyses. The unidirectional or "one-way" coupled method solves the model by first solving for the fluid domain results and applying the surface pressure results onto the structural domain, but it does not provide feedback about the deformation of the latter. At the next timestep, it again uses the fluid domain results to be re-applied on an intact structural model. Even though this method does not represent the exact physics of the problem, it produced much faster results for the particular model analyzed in this article (about 50 minutes for the entire analysis) than the fully coupled method (27 hours). The fully coupled method solves for the fluid domain first and applies the results to the structural domain, the deformation values of the latter are used to modify the new fluid domain and it iteratively solves both domains by communicating the results between the two until convergence is reached. The greatest calculated difference in pressure between the two methods was 15.7% during maximum flow. In our study we focused on demonstrating the feasibility of performing the numerical studies on realistic geometries under realistic flow for fatigue analyses. It is difficult to make deterministic conclusions about plaque rupture when analyzing a single patient-specific geometry. However, we were able to learn that the same pattern of proximal shoulder stress concentration exists and that the maximum stresses and pressure drops occur during the peak diastolic flow. In future analyses, it would be useful to verify the results using intravascular pressure sensors along with intravascular ultrasound reconstructions.

# 5.3 Reconstructions of ruptured plaques using IVUS

Our study showed that the highest stress concentration of the fibrous cap occurs at the upstream side in the shoulder region of the plaque. In a reverse engineering approach, we reconstructed seven cases of ruptured plaques using in-vivo IVUS to determine the average location of the fissure. All cases analyzed presented upstream sides rupture with an underneath empty cavity. Figure 5.2 presents four of the seven cases in which the rupture was more evident.

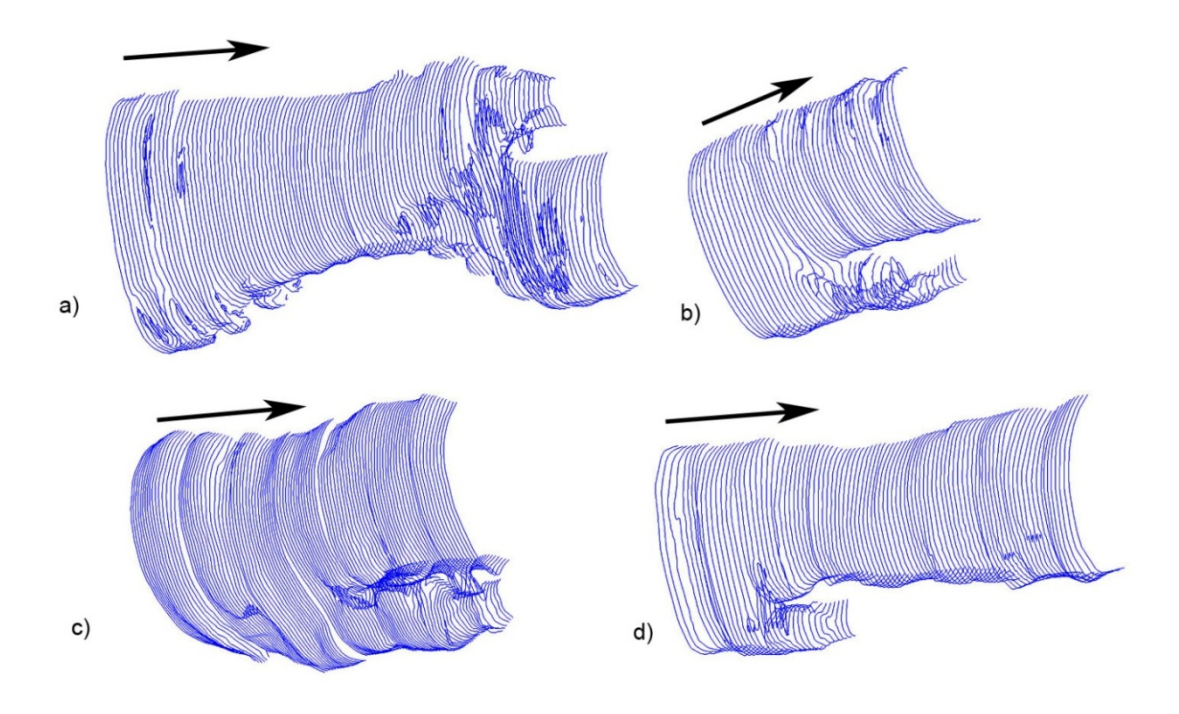


Figure 5.2: IVUS Reconstructed geometries of ruptured plaques arrows indicate blood flow direction. a) Double plaque scenario with rupture present at the proximal side of the distal stenosis. b, c, d present the typical underneath empty cavity at the proximal sides of the plaques.

Even though seven cases of ruptured plaques are not statistically significant to make a conclusion, they provide a trend and some insight to the real three-dimensional environment of plaque rupture. We can learn from those cases that they indeed have a proximal shoulder rupture. This is in agreement with those findings of plaque rupture using longitudinal IVUS imaging reported by Hiro [73]. While more cases of ruptured plaques are necessary to make a strong statement on proximal shoulder rupture. It is somewhat difficult to obtain those cases as they come from in-vivo imaging.

## 5.4 Linear elastic vs. hyperelastic materials

It is widely known that arteries in general exhibit hyperelastic material behavior, in particular large elastic arteries such as the aorta. Muscular arteries such as the coronaries still tend to show such hyperelastic behavior to a lesser degree. However, the degree of mechanical strains to which the coronaries are subjected to during normal physiological conditions is relatively small and thus the stress-strain relationship can be approximated as linear. An article by Van Andel [109] published experimental data in which the beginning of the hyperelastic stiffening region of human coronary arteries oscillated between 0.15 and 0.20 strain values. Our maximum calculated stress during peak diastolic flow was calculated at approximately 92 KPa, which corresponds to a strain value of 0.115 when using a Young's modulus of 800 KPa. The elastic region in which coronary arteries act under normal physiological conditions is indeed below the stiffening region. Therefore, it is justified to approximate the material properties using a linear elastic model (Young's modulus). However, for future analyses that consider the

anisotropic properties of the material, hyperelastic materials need to be used as the strain energy density function constants consider such properties in the material behavior.

## 5.5 Fatigue analyses

We proposed in this study to treat the phenomenon of plaque failure as the outcome of a progressive chronic injury caused by the cyclic stretching of the fibrous cap. For this, we incorporated a simple fatigue criterion developed for ductile metals by Goodman and modified it to our needs to predict the number of cycles before failure rather than predicting a single threshold value were no rupture would occur.

Gilpin [36] developed in her work a series of stress vs. number of cycles (S-N) curves of porcine coronary arteries ex-vivo using a mechanical tensile tester. In her work, she foresaw that it would be very lengthy to characterize the material samples to a very large number of cycles and the specimen availability for this was very limited. Instead, she proposed to develop a series of short-life cyclic tests under high mechanical stress to rupture the tissue at a very early stage and extrapolate the experimental results to an exponential S-N curve similar to the fatigue behavior seen in ductile metals. Although this approach can potentially be sensitive to errors, it avoids time consuming experiments and allows to construct the S-N curve with a very limited number of specimens. For future analyses, it would be very useful to characterize human coronary tissue with methods that closely resemble in-vivo conditions. More specifically, it would be more useful to characterize the fibrous cap tissue as it is likely to have different mechanical properties as the rest of the artery wall due to its high content of collagen. However, the

size and the number of available specimens would prove this to be a very challenging task.

The available information can serve as a basis to introduce the concept of fibrous cap mechanical fatigue (FCMF). As mentioned before, plaque failure can be the outcome of a progressive chronic injury caused by the cyclic stretching of the fibrous cap rather than a monotonic stress value. Plaques with similar morphological and mechanical features can exhibit different different behaviours when they are exposed to different hemodynamic conditions. Therefore, we cannot suggest a single stress threshold value that would trigger the plaque's failure. We must carefully evaluate each case with its own particular morphology, mechanical properties and hemodynamic conditions in time in order to achieve accurate results that would be clinically relevant. The time-dependant results will allow us to calculate the stress amplitude and mean stress over each cardiac cycle, those values are essential to calculate a fatigue life based on a given S-N curve.

## 5.6 Multiple plaque vulnerability

The results presented in chapter 4 clearly suggest that we must establish new criteria when defining what a vulnerable plaque is. The reason is that a single plaque in a coronary artery may have a particular stress concentration pattern. However, in the presence of nearby or adjacent plaques, the hemodynamics of the system change; the kinetic energy that entered such system of plaques now dissipates throughout the multiple plaques; the highest mechanical deformation will firstly occur at the weakest structural components of such system. Therefore, we should define new terms such as multiple

plaque vulnerability (MPV) and single plaque vulnerability (SPV) and evaluate if the system is vulnerable to rupture, instead of individual plaques.

## 5.7 Collagen tissue characterization

In the following pages, we discuss the further possibility of refining our numerical analyses by incorporating the anisotropy of the collagenous structure of the fibrous cap. We approached the problem by using different imaging methods that would depict the particular orientation of the fibers in localized regions of the fibrous cap. Ideally, this spatial anisotropy information could be used in a computer code to define the particular anisotropy of each element in the numerical models and produce an accurate anisotropic tissue model. The outcome of doing this is that we will not only get more accurate results in terms of mechanical stress distribution but also we would learn if these stresses influence the mode of failure by following the crack propagation path and see if it follows the fiber orientations.

# Chapter 6 – Article: "Fibrous cap collagen fiber remodeling increases atherosclerotic plaque vulnerability"

#### **Authors:**

Ramses Galaz, Marika Archambault-Wallenburg, Rosaire Mongrain, Richard Leask, Jean Claude Tardif.

## **Objectives:**

- To characterize the anisotropic map of the collagenous structure of the fibrous cap
  based on computational image analysis. The orientation of the collagenous
  structure will provide insight in determining the degree of anisotropy of the
  fibrous cap and consequently what are the preferred stress orientations of the
  individual fibers.
- To develop a computational tool to perform image analyses to map the local
  orientations of bundles of collagen fibers based on image processing techniques.
  This would serve to assess the degree of anisotropy of each image analyzed and
  spatially map the orientations of each individual fiber in the images.
- To construct the respective histogram of orientation angles of the analyzed region.
- To link the fiber orientations to fracture modes of atherosclerotic plaques. The
  architecture can influence the mode of failure in terms of crack initiation and
  propagation.

### **Hypotheses:**

- The collagen fiber orientations remodel according to the modified mechanical loading induced by the geometrical changes within the fibrous cap in order to better respond to the mechanical loads. This suggests that individual fibers should have different orientations depending on their spatial location within the fibrous cap.
- The fibrous cap has localized arrangements of fiber orientations and thus has different anisotropic properties depending on the location. This can make the fibrous cap prone to certain fracture modes and consequently increase its vulnerability under certain conditions such as exercise.
- The possible role of the ultrastructure in the fibrous cap mechanical fatigue (FCMF). Specifically, we considered the anisotropic effects of the collagen fibers architecture in the caps to influence the mode of failure in terms of crack propagation. We hypothesize that these cracks are likely to be parallel to the fibers as the tissue matrix would exhibit weak mechanical properties along this path.

#### 6.1 Abstract

Atherosclerotic plaque rupture has been associated in 70% of the cases of acute coronary syndromes [16]. The rupture of the plaque's fibrous cap may lead to a sudden thrombus formation and subsequently an acute myocardial infarction. The fibrous cap acts as a protective layer that covers the atherosclerotic plaque and it is mainly composed of collagenous tissue and smooth muscle cells [27] and it prevents the contact of blood with the highly thrombogenic contents inside the core of the plaque. Many computational finite element studies have been performed in order to analyze the failure mechanics of the fibrous cap tissue. However, the failure phenomenon is not yet fully understood. Our work focused on assessing the role of the collagen fiber orientations in the fibrous cap tissue for its propensity to rupture. We developed a computational code to obtain the vector map and histograms of the orientations of the collagen fibers using tracking algorithms and based on histology images from human specimens of atherosclerotic plaques. The results showed that the collagen fibers of the fibrous cap do not follow a unique orientation but are circumferentially oriented at the shoulders of the cap, and they gradually shift to a longitudinal orientation as they progress towards the peak of the plaque. The fiber tracking algorithm provided good results with respect to the histology images and was able to analyze the tissue to any desired level of resolution as long as the provided images showed good contrast between the fibers and the void spaces. The information on the collagen fiber organization could help refine the numerical analyses for predicting the sites and modes of failure and fissure propagation of the fibrous cap based on a more accurate anisotropic model. The numerical models can provide a better insight to determine the probable zones of crack initiation and the fiber orientation maps

can provide possible paths of crack propagation. The anisotropic effects of the collagen fibers architecture in the caps can influence the mode of failure in terms of crack propagation. We hypothesize that these cracks are likely to be parallel to the fibers as the tissue matrix would exhibit weak mechanical properties along this path. More specifically, we hypothesize that the new arrangement of collagen fiber which was established essentially under rest conditions to better sustain the new mechanical loading associated with the morphological change induced by the plaque would be very weak under modified morphologies resulting from exercise or any other physiological reasons for vasodilations.

#### 6.2 Introduction

Cardiovascular diseases represent one of the main causes of death in developed countries. Atherosclerosis is a chronic inflammatory disease that narrows the lumen of the arteries by the gradual growth of a plaque that is composed of fatty deposits, cholesterol crystals, cellular waste products, calcium minerals, and connective tissue. The fibrous cap is a protective layer that covers the atherosclerotic plaque and it is mainly composed of collagenous tissue and smooth muscle cells [27], in particular collagen type I [110, 111, 112]. This fibrous cap prevents the contact of blood with the highly thrombogenic contents inside the core of the plaque. The rupture of the fibrous cap has been extensively associated with acute coronary syndromes such as myocardial infarctions. This study focused on the analysis of the structural anisotropy of the fibrous cap in order to assess its spatial mechanical properties to better understand how plaque ruptures might occur.

Collagen is the main protein of connective tissue in most biological materials and it is present in the form of long fibers [113]. These fibers act as the main structural component of soft tissue and they are biologically designed to act under tension. The structure and functionality of living tissue is constantly modified through changes in mass, geometry and the rearrangement of the microstructure according to its mechanobiological environment [114, 115]. It has been proposed that collagen fibers reorient over time to align themselves with respect to the principal stresses when analyzing collagenous tissue such as aortic heart valves, tendons, and porcine coronary arteries [116, 117, 118]. These changes in the microarchitecture affect the localized mechanical properties of these materials and thus the anisotropy strongly depends on the orientation of the fibrous phase [119, 120].

The fibrous cap in atherosclerotic plaques of coronary arteries is mostly composed of collagen fibers and smooth muscle cells [16, 27]. The presence of a stenotic eccentric plaque in the coronaries alters the hemodynamics [86] and produces a non-uniform pressure distribution along the fibrous cap of the plaque. The magnitude and orientation of the strains within the different regions of the fibrous cap greatly depend on the particular morphology, the stiffness of the core, and the thickness and structural integrity of the fibrous cap. Plaque characteristics vary significantly from case to case, therefore it is expected that the anisotropy of the fibrous cap varies as well in accordance to the localized mechanobiological environment. Other authors have found good correlation between the fibrous phase orientations and the typical tensile stresses of the particular tissue analyzed [121, 122, 123, 124, 125]; other authors such as Gasser et al. [126] have determined the mechanics of layered structures of artery walls based on anisotropic models. Based on this information, we hypothesized that the fibrous cap tissue

should have similar reorganization characteristics. It then becomes important to characterize the full anisotropic map of the collagenous structure of the fibrous cap to couple these fiber orientations with the patient-specific finite element models to produce more accurate estimations of the mechanical stresses. The results from these numerical analyses would provide insight on rupture initiation and fissure propagation.

#### 6.3 Methods

## 6.3.1 Numerical models of flow through stenosed arteries

A set of computational models of stenosed coronary arteries from the study performed in chapter 2 of this thesis were used for the numerical analyses to compute and map the principal stresses orientations. The models were constructed using cylindrical tubes of the typical dimensions of a coronary artery. These dimensions were set to be 3 mm for the internal diameter of the artery, 0.5 mm for the artery wall thickness, 20 mm for the length of the cylinder and 15 mm length for the stenosis. The stenosis geometry was modeled as an eccentric protrusion using Gaussian curves along the longitudinal axis with different heights to account for the different degrees of stenosis. The percentage of stenosed area ranged from 19% to 91% and the thickness of the fibrous cap ranged from 200 to 500 microns.

The material was assumed to be incompressible due to the high water percentage content in the tissue, therefore a Poisson's ratio of v=0.49 was defined. The material's Young modulus for both the artery wall and the fibrous cap together was assumed to be 800 KPa agreeing with other reports of linear elastic modulus values [32, 68]. The models

were analyzed with static fluid-structure interaction methods and subjected to a constant blood flow of 100 ml/min that corresponds to the normal maximum diastolic flow of the LAD coronary branch reported by Berne [42] and a normal intraluminal mean pressure of 100 mmHg. The maximum diastolic flow value was chosen as it was demonstrated in a previous study to be the point in time where the maximum stresses occurred within the plaque's components.

The fluid-structure interaction studies of the coronary flow in the presence of the stenotic plaque found that the principal stress orientations of the nodes within the fibrous cap were arranged non-uniformly. These orientations followed the stress distribution caused by the hemodynamic pressure gradient forces acting on the lumen surface of the plaque and affecting its different structural components. The principal stress orientations were mainly circumferential in the non-stenosed sections of the artery, while those at the peak of the fibrous cap tended to be axially oriented (Figure 6.1). As the percentage of stenosis increased from 19% to 91% the effect of longitudinal principal stresses atop the plaque became more evident.

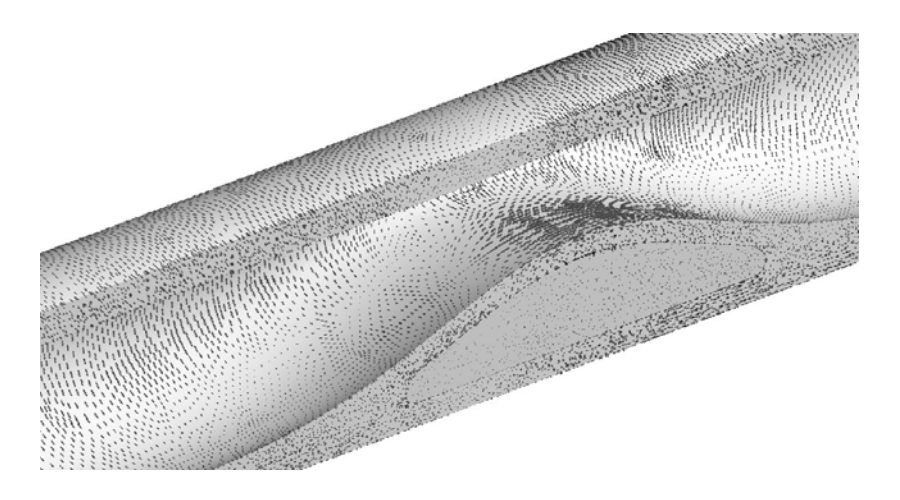


Figure 6.1: Vector plot of the principal stress orientations within the fibrous cap tissue from a fluid-structure interaction numerical model using idealized and realistic geometries

## 6.3.2 Tissue preparation

In order to obtain images of the collagen fiber bundles, we decided to use microscopy images of histological studies. Two coronary plaques were excised from the same human subject and kept in a 10% formalin solution. The first plaque was located in the branching point of the LAD and LCx arteries while the second plaque was located approximately 13 mm further downstream of the LAD. The specimens were prepared for histological studies by embedding them in paraffin and slicing at a layer thickness of 4 microns. The first plaque specimen was sliced in the longitudinal direction from a lateral perspective of the plaque in order to visualize the orientation of collagen in the fibrous cap region from the side (Figure 6.2). The second plaque was sliced also longitudinally but from a top perspective. The slices were prepared using the Masson Trichrome (TRI) staining protocol as it is a well known method for visualizing collagen by differentiating

it from smooth muscle cells [127, 128]. The collagen fibers stain blue, the nuclei stain black and the background (muscle, cytoplasm, etc.) is stained red. The specimens were observed under a microscope at the magnifying factors that would best depict the collagen fiber orientations in the particular region of interest.



Figure 6.2: Longitudinal cut of the diseased branching point of the left coronary artery specimen

## 6.3.3 Image processing software development

The analysis of the fiber orientations was done using the Matlab software environment (Mathworks, Natick, Massachusetts). The images were created by digital photography under a microscope at 10X magnifying factor of the regions of interest. The images were cropped so that the source data was 1024 x 1024 pixels. The images were first binarized and filtered to obtain black and white images with as little noise as possible (Figure 6.3), with the threshold being set by the user with the criterion of producing good contrast between fibers and void spaces. The image was separated into sections and

binarization was performed section by section in order to avoid the loss of data resulting from the uneven illumination of different regions of the image. The Euclidean distance transform of each binary image was then computed using Matlab's integrated bwdist function. This gave us images where the fibers were clearly discernable. The program first proceeded to find starting points of the fibers from which the rest of the length of each fiber would be traced. This was done by identifying the centroids of the regions of local maxima in the Euclidean distance mapping. Once the starting points had been provided, the program searched a box surrounding this starting point for the next point along the fiber. For each starting point (x,y), the program searched the boundary of a box of radius r, where r is the value of the same pixel in the Euclidean distance mapping. The orientations of the new segments constituting potential prolongations of the fiber were compared to the orientations of the previous segments. If the new segments backtracked along the fiber had a difference in the XY plane greater than  $3\pi/8$ , or any other user-set threshold, they were rejected. When multiple potential points were encountered, only one was appended to the fiber's list of coordinates while the rest are stored as so many more starting points. The candidate point which was the most likely to follow in a multiple point scenario was selected on the basis of both the value of the Euclidean distance map and the difference of orientations between this new segment and the previous one; the remaining points of the branch were added to the list of coordinates of starting points, and served as the next central point around which to seek continuations. The program recursively marched from one point to the next until either the end of the fiber or of the image was reached (Figure 6.3).



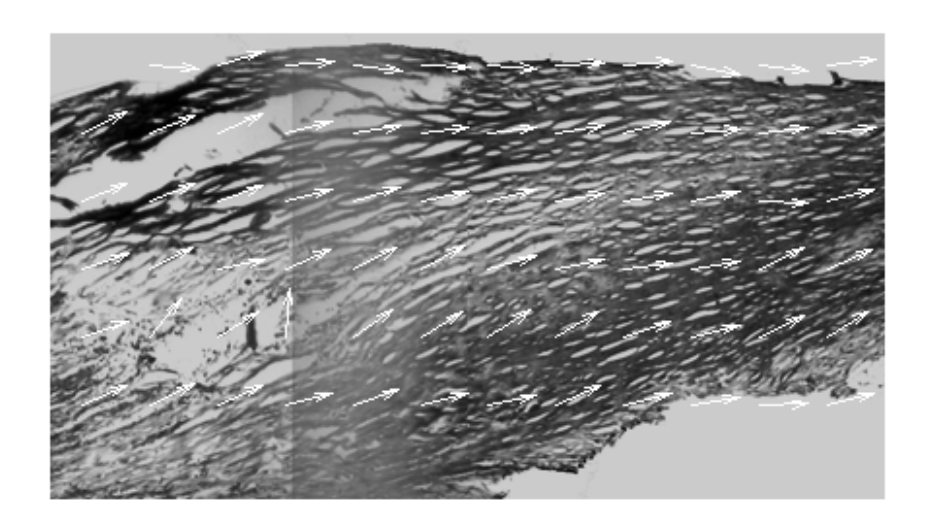


Figure 6.3: (top) Binarised image of the histopathological specimen. (bottom) Fiber orientations as computed by image processing superimposed on a grayscale image of collagen fibers. The image corresponds to a lateral view of a longitudinal section of the fibrous cap at 10X magnification.

At the end of the each fiber tracking process all points were then fitted to a linear regression curve which gave a direction vector for the fiber. The distances from one point

to the next were added in order to find the length of each fiber. It was assumed that longer fibers have a more reliable direction and are more likely to reflect the overall orientation of the collagen fibers within a specific area. Therefore, the mean direction of the fibers in a stack of images was found by computing the eigenvector of the direction cosine matrix, which was calculated from the direction vectors multiplied by the length of the corresponding fibers rather than directly from all the direction vectors. This had the effect of giving the orientation of the longer fibers more weight, and thus avoiding the relevant orientation data being lost in a large number of very small fibers, whose directions are much less accurate than those of the longer ones.

The code was written to be able to perform 3D tracking of fibers when presented with a stack of images of known separation between them. Imaging technologies such as confocal or multi-photon microscopy are able to create stacks of images of the sample at various depth levels. The code was written in order to process two modalities of 3D fiber tracking: slice per slice analysis and full 3D analysis.

The slice per slice method grouped together the collagen branches that were located almost directly one above each other (i.e. fibers on contiguous slices, and the x,y coordinates of their center-of-masses are not apart more than the user-defined value of 15 pixels). Because of the way the images were obtained, it was likely that fibers that were parallel to the imaging plane would be apparent on more than one slice and appear quite clearly on a few successive images. By grouping together the branches that seemed to represent the same fiber, we reduced the artificial multiplication of fibers. These longer lists of points consisting of merged planar branches are then three-dimensional, and the same analysis can be performed on them as on the branches found with the 3D analysis.

The full 3D analysis analyzed the whole stack of images at once and the fiber tracking took place in 3D, with the program scanning the surface of a "cube" instead of a square centered at the starting points. However, since the vertical distance between two pixels on different slices is much more that the horizontal distance between two contiguous pixels on a same slice, an allowance is made for this and a different radius of search is defined in the z direction.

The level of resolution that the code can analyze is only limited by the imaging technology. There are no strict restrictions on the size of the map or resolution level as long as the images provided have good contrast levels. The collagenous map could then be reconstructed at any particular size and level of resolution desired.

Finally, once the fiber orientation information was obtained for each image or set of images, polar histograms of the weighted number of fibers and their respective angles were reconstructed to visualize their global orientations. The xy orientations of the fibers were illustrated on a rose plot. The data plotted is simply the xy projection of the direction fibers for each fiber, with no distinctions of length or size. Since the orientation of the fibers is axial (ie. orientations of 45 degrees or of -135 degrees are equivalent), the rose plot is symmetric.

#### 6.4 Results

## 6.4.1 Tissue preparation and staining

The specimens were fixed in a 10% formalin solution, embedded in paraffin and cut at various thicknesses for histopathological studies. It was found that slices of a thickness of 4 microns provided appropriate image data for our image analysis purposes. We were interested in obtaining images of high contrast between the blue stained collagen fibers and the white void spaces so that they would clearly show the orientations of the bundles of fibers. The Masson Trichrome staining protocol [127, 128] provided not only good contrast images but also a clear identification of the collagenous tissue locations by staining the fibers in blue. Two sets of analyses were done for the different plaques; the plaque that was located near the main branching point of the Left Anterior Descending (LAD) coronary plaque was cut longitudinally to show the fibrous cap tissue from a lateral perspective (Figure 6.4). The second plaque specimen was also cut longitudinally and to show the fibrous cap from the top view (Figure 6.5).

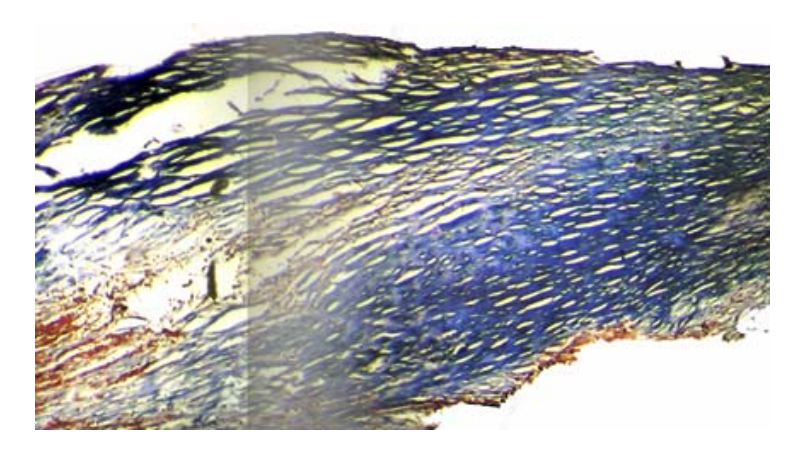


Figure 6.4: Composition of images of collagen fibers (stained blue) in a longitudinal section of the peak of the fibrous cap stained with the Masson Trichrome protocol at 10X magnification factor

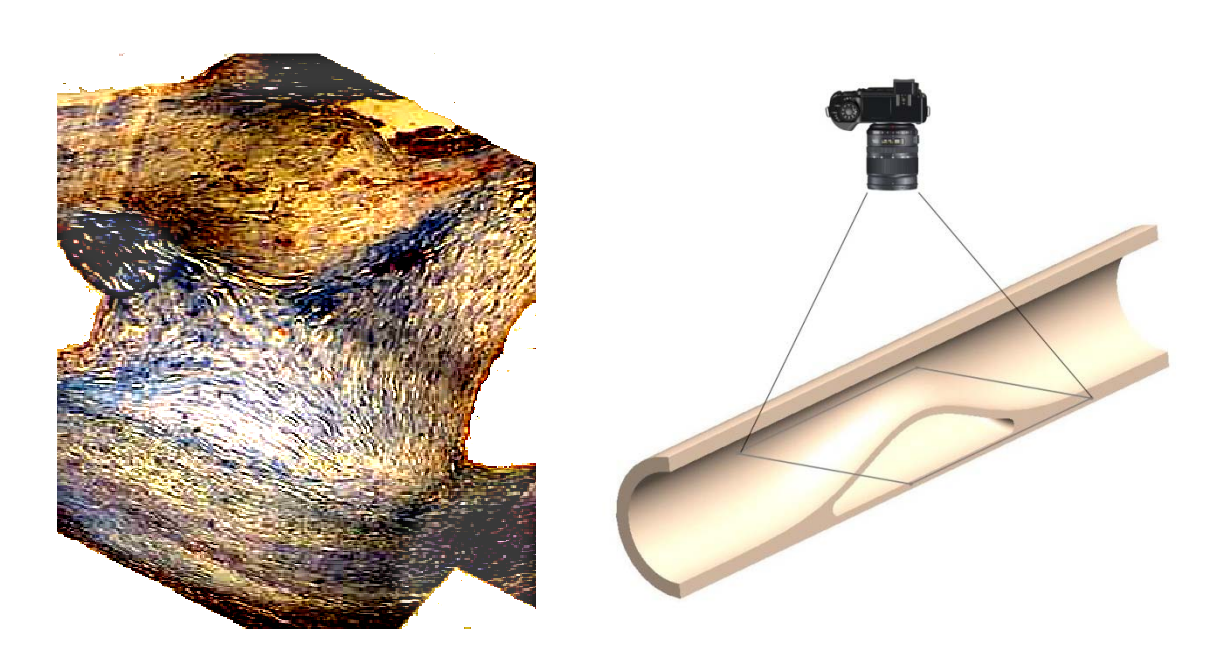


Figure 6.5: Top view of a longitudinal section of the fibrous cap tissue processed with the Masson Trichrome staining protocol

## 6.4.2 Principal stresses orientations according to the numerical models.

In order to demonstrate that there is a reorientation of the principal stresses orientations within the fibrous cap, we used the same numerical models described in chapter 2 of this thesis, we probed the magnitude and orientation of the principal stress located at the closest point (or node) atop the peak of the plaque. From figure 6.1, we can establish that the principal stresses within the fibrous cap are not homogeneous in either magnitude or orientation. Figure 6.6 shows the maximum principal stress calculated at the closest point to the peak of the plaque. Figure 6.7 shows the respective angle of orientation of that particular principal stress with respect to the longitudinal axis or blood flow direction. Figure 6.8 is a schematic drawing of how the angle of the principal stress varies depending on each case of different percentage of area stenosis.

It is interesting to notice that the angle of orientation of the maximum principal stress is 90° when the area stenosis is 0%. This makes perfect sense as all of the principal stresses are oriented circumferentially as this is the case of a perfectly healthy artery. There are no hemodynamic perturbations and thus there is no inflection in the mechanical stresses in the artery wall, which only "feels" the intraluminal pressure. As we progress towards higher percentages of stenosis, we notice in figure 6.7 that the orientation of the principal stress quickly drops to 0° in the range of 19% to 43% and becomes aligned with the blood flow direction afterwards. The magnitude of such principal stress increases gradually in a non-linear fashion as the percentage of area stenosis increases. In simpler terms, it is when the plaque is small or mild that we can observe these gradual changes in the orientations of the principal stresses. In the more severe stenoses (above 43%), we can

only identify an increase in the magnitude in the principal stress and its orientation remains aligned to the blood flow direction.

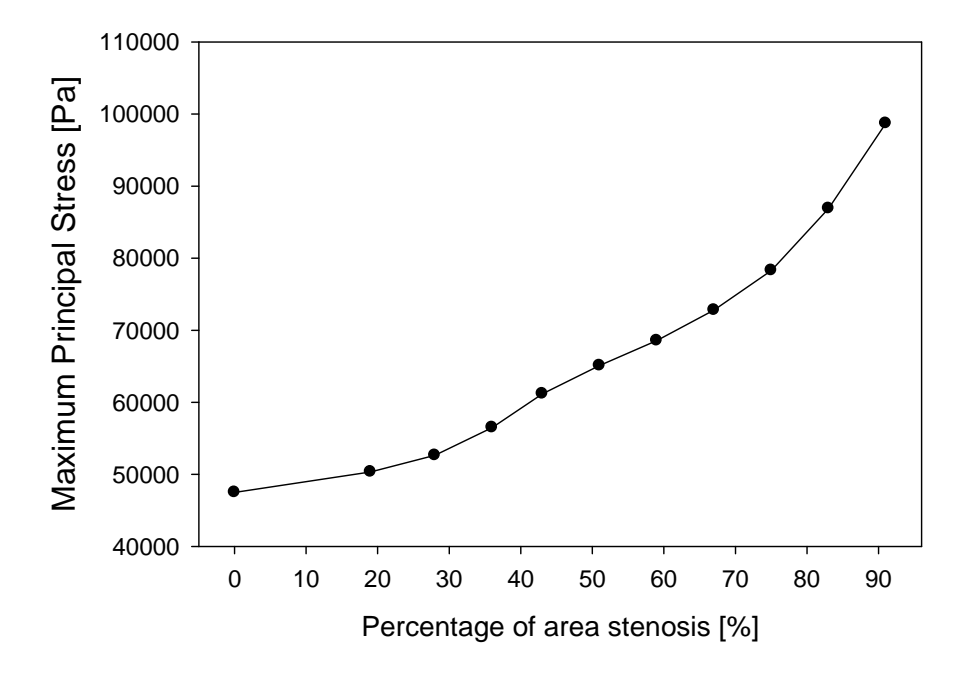


Figure 6.6: Maximum principal stress vs. percentage of area stenosis at the closest point of the peak of the fibrous cap.

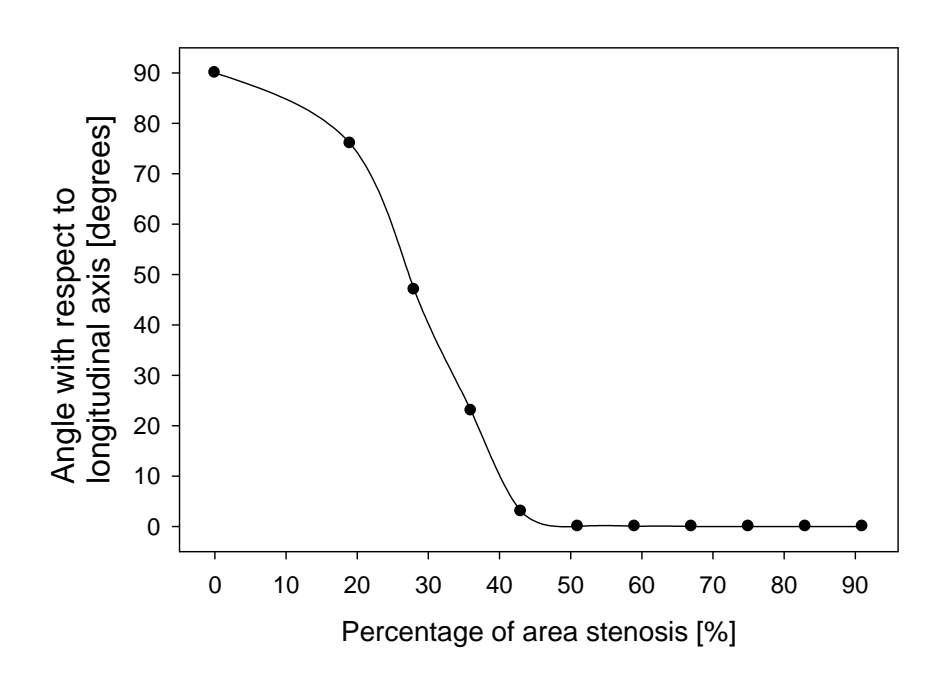


Figure 6.7: Deviation angle of the principal stress point atop the peak of the plaque vs. percentage of area stenosis.

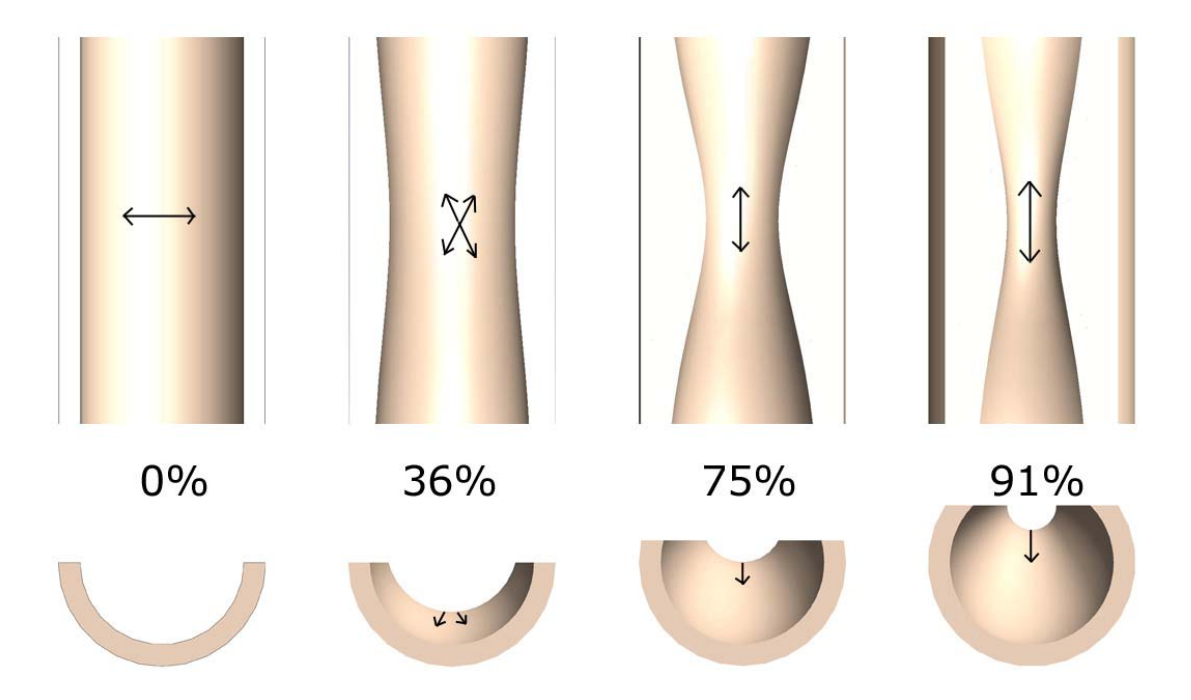


Figure 6.8: Schematic drawing of the orientations of the principal stresses atop the peak of the plaque in different percentages of area stenosis.

# 6.4.3 Fiber tracking

The fiber tracking results are displayed in figures 6.9 to 6.12. As expected, the computer code can track the fibers in any particular region or level of resolution as long as the code is provided with a images with high contrast between the void spaces and the collagen bundles. However, with poor contrast the program can generate results with significant errors. Figures 6.9 and 6.11 are the results of the image dataset presented in Figures 6.4 and 6.5 with the fiber direction arrows superimposed.

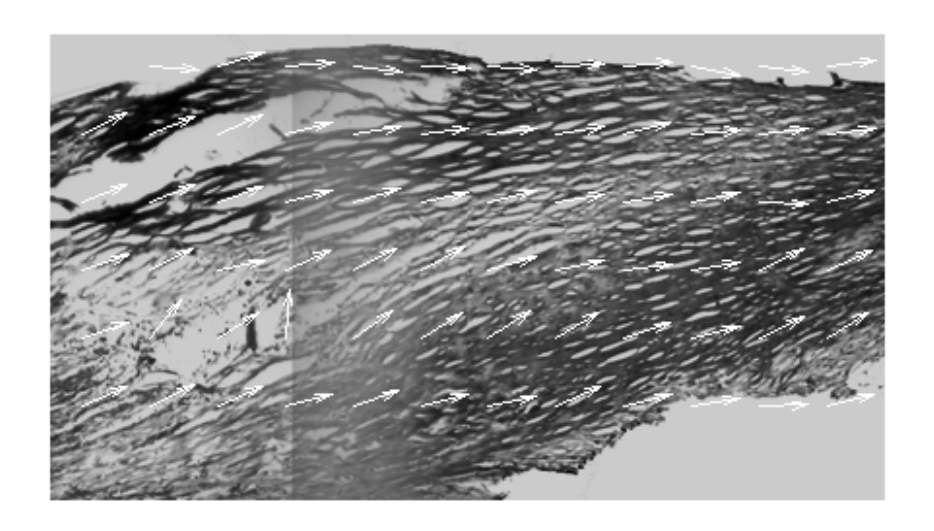


Figure 6.9: Collagen fiber orientation vector plot as a result of computational image analysis of the lateral-longitudinal section of the peak of the fibrous cap

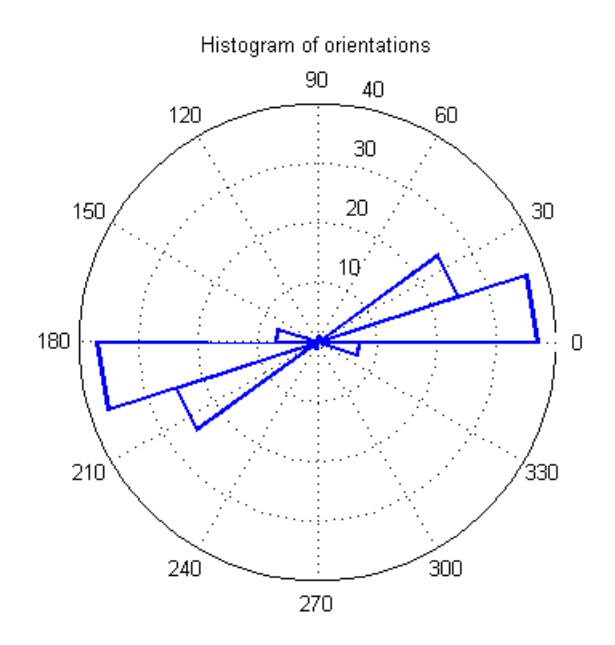


Figure 6.10: Rose plot histogram of the image analysis in Figure 6.9

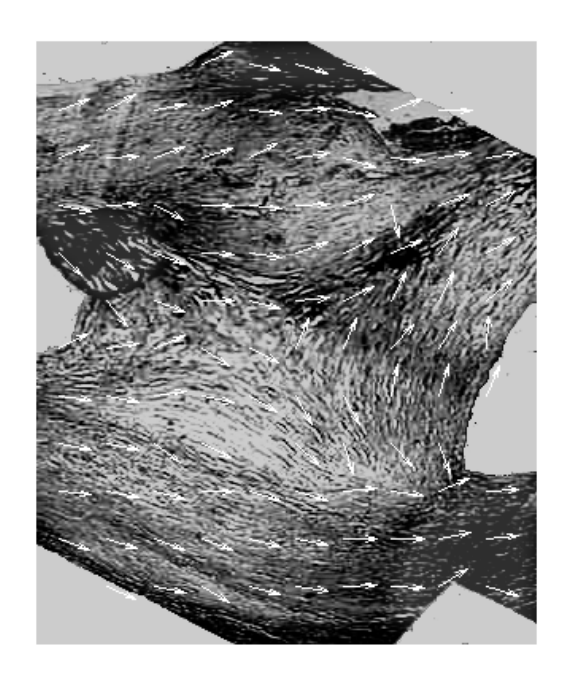


Figure 6.11: Collagen fiber orientation vector map as a result of computational image analysis (Top view of fibrous cap)

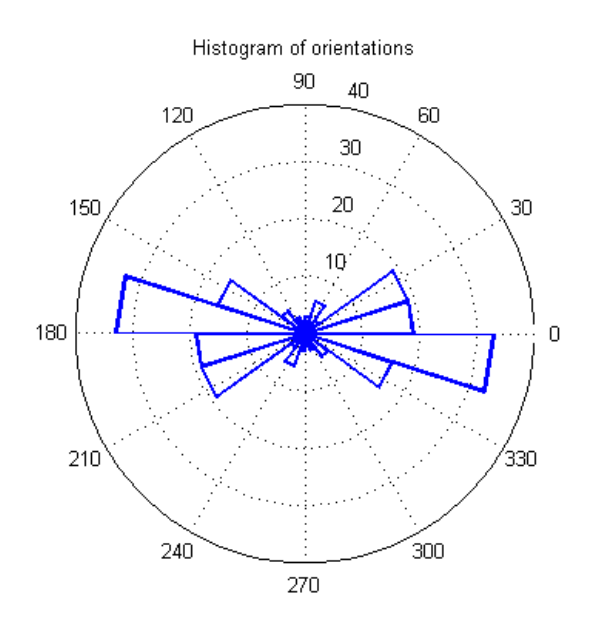


Figure 6.12: Rose plot histogram of the image analysis in Figure 6.11

#### 6.5 Discussion and conclusions

From the image analyses, it becomes clear that the collagenous tissue of the fibrous cap does not have a unique architecture and the fiber orientations vary with respect to the spatial location.

Our hypothesis suggests that the fibers within the fibrous cap are arranged to sustain the mechanical loading which is translated as the corresponding principal stresses. This phenomenon has been demonstrated for other human and non-human biological tissues [114, 115, 116, 117]. Two human specimens of coronary plaque is limited, however, it is coherent with literature results obtained with other tissue. These two specimen results are not absolute proof that fibers follow the principal stresses, however, they obviously demonstrated that anisotropy is an important factor. The information on the collagen fiber organization could help refine the numerical analyses by incorporating the spatial anisotropy into the finite element models for predicting the sites and modes of failure of the fibrous cap. The same methodology can also be used to analyze other pathological conditions such as aneurysms where the understanding of tissue failure mode is as critical.

In this study we used images processed through histopathology in order to obtain high contrast images that would clearly depict the collagen fiber bundles. The Masson trichrome staining protocol provided good contrast images and a clear identification of the collagenous tissue locations by staining them in blue. The appropriate images for processing were those sectioned at 4 micron thicknesses as they clearly showed the void spaces between the fibers. Other imaging techniques such as confocal and multi-photon microscopy can be used to obtain high contrast images of collagen fibers either as

individual planes or as stacks of images for three-dimensional reconstruction. The model however has limits, if there are any large voids that are not necessarily derived from the collagen architecture and that they seem to have a particular orientation, they could be confused with a large fiber that would outweigh the rest and thus show an incorrect histogram.

In this chapter, we show that the anisotropy of the collagen fibers is strongly dependent on the stress in the fibrous cap. In fact, the collagen fibers align with the principle stresses orientations to sustain the new loading conditions. As a result, for certain plaque morphologies the collagen fibers will establish certain anisotropies (characterized with a transversely anisotropic model with certain values of angular orientations of the fibers). This new arrangement is mainly established under rest conditions. However, at exercise the plaque is deformed due to an increase of blood pressure and flow rate which create new loading conditions for which the deformed fibers arrangement with respect to rest condition which render the composite fibrous cap weak to these transient loading conditions. This effect would directly affect the fatigue life of the fibrous cap as it can induce certain stress conditions that may not be oriented in the usual patterns and thus the endurance limit under these "unusual" stress conditions may decrease and make the fibrous cap fail prematurely.

Future work would involve patient-specific plaque virtual modeling, stress it under a virtual hemodynamic environment, and calculate the mechanical stresses and their orientations.

# Chapter 7 – Discussion on article: "Fibrous cap collagen fiber remodeling increases atherosclerotic plaque vulnerability"

# 7.1 Collagen fiber visualization through histopathological studies

Histopathological studies proved to be a useful method when analyzing single view images of particular sections of the specimens. We used this method for the purposes of demonstrating that our computer code worked in the proper manner. It is a current technique in most hospitals. However, we encountered certain limitation:

- The microtome exerts some degree of damage to the fibers when cutting them even though they are embedded in paraffin.
- Once the tissue is embedded in paraffin we lose to a certain degree the accuracy of the orientation with respect to the longitudinal axis of the artery, therefore, when performing the cuts in the microtome, there is some imprecision concerning the exact longitudinal alignment.
- Histopathology could become a cumbersome task for mapping the entire coronary plaque, for example we would have to do 4 microns cuts to the whole extension of the plaque, which could be in the range of 5-10 mm.
- The staining process and the organization of all the slices make the task slow and expensive.
- It depends on the skill of the histopathology technician to correctly position the slice onto the microscope slide without damaging the specimen.

It would be very useful to the purposes of this research to have a non-destructive technology that could provide us with the collagen fiber mapping orientation in a threedimensional field. In such a way we could recreate the plaque geometry in detail and learn about the localized arrangement of fibers at the same time we know the geometry. We could easily then input the particular anisotropy of an element in the numerical analyses using the same technique.

# 7.2 Plaque analysis through MicroCT scans

The micro-computed tomography data simply did not have the required spatial resolution. The tomographic images did not produce enough contrast of the void spaces between the collagen fibers.

An interesting observation was done when analyzing a heavily calcified plaque, while the exterior of the plaque seemed hard and tough from the exterior, the interior had little or no calcification when seen from a cross-sectional MicroCT view (Figures 7.1, 7.2), and this suggests that the calcification process might take place around the edges of the core where most inflammatory activity occurs. Mechanically speaking, this could mean that potentially fully calcified cores might be weaker as only the exterior shell of the core is hard, while the center of the core is still filled with lipids. Further research needs to be done in this particular area.

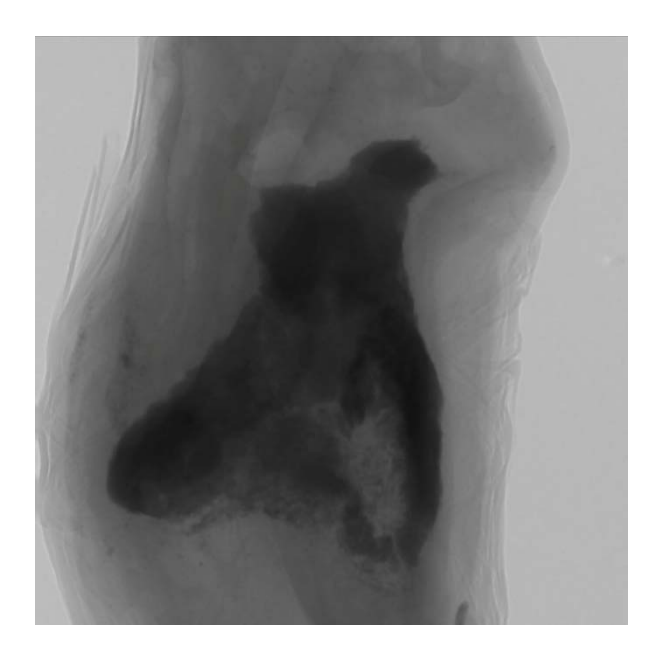


Figure 7.1: MicroCT longitudinal image of a calcified atherosclerotic plaque

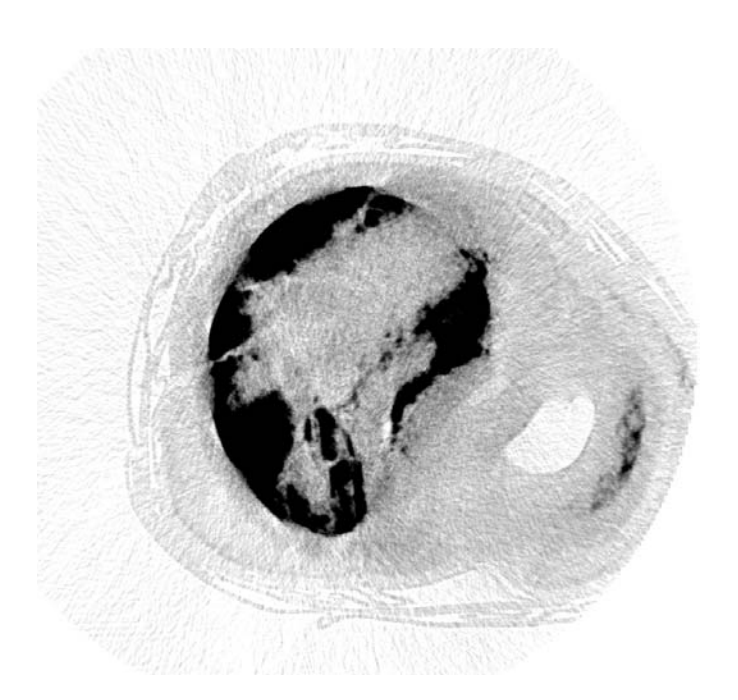


Figure 7.2: MicroCT image of a cross-section of the same specimen above. Notice the calcified areas around the edges of the plaque's core.

# 7.3 Other methods

Other technologies that could assess the collagenous structure include Confocal Microscopy, which can image collagen fibers when stained with picrosirius red. Confocal Microscopy can image up to a certain depth, therefore it still is a semi-destructive methodology as we still need to perform slicing of the specimen, although thicker slices are allowed. This technology was not tested due to tissue unavailability at the time.

Collagen fiber visualization through an experimental setup of a Second Harmonic Multiphoton Microscope was an option [129], however, since the setup was experimental in nature it was limited in the depth of visualization and it lacked a visual reference on the particular location of the microscope's field of view.

# 7.4 Future improvements

While the two-dimensional results have proven to be effective and accordingly to the images analyzed, two-dimensionality still limits us to have "slices" of the specimen and not assess the intrinsic three-dimensional nature of the fiber arrangements. Future enhancements to the computer code are to be able to map in a 3D path each fiber using stacks of images and to use this information in a spatial matrix where we could incorporate fiber orientations results into the anisotropic properties of the material in a finite element analysis. The most probable outcome of incorporating anisotropy in the numerical analyses is that the resulting principal stress fields (which by hypothesis are followed by the collagen fiber) could be lower than the values predicted using isotropic

materials as the tissue would be stiffer in the direction of the fibers. This means that the stress magnitudes could be overestimated in isotropic materials. Using the true anisotropy of the tissue we could obtain more accurate results and a better understanding of how tissue failure initiates and propagates.

# 7.5 Fibrous cap mechanical fatigue relation to collagen fiber orientation

In chapter 6, we thoroughly discussed the relationship between collagen fiber orientations with the principal stress patterns. Several authors have reported this relationship and we have also demonstrated that the fibrous cap's collagen fiber orientations are arranged differently depending on their spatial location; these orientations were most probably induced by the artery wall remodeling due to the continuous repetitive pattern of cyclic stretching. However, in the case of a sudden jump of cardiac output, the local intraluminal pressure and flow may rise and thus induce hemodynamic changes that are not "usual" to a particular plaque's fibrous cap. The principal stress magnitudes and orientations may suddenly have different conditions that would precipitate a premature failure due to the mechanical fatigue of the collagenous structure of the fibrous cap.

# **Final conclusions**

Our analyses on ideal geometries with static flow have demonstrated that the highest stress concentrations always occurred in the proximal side of the plaque under perfectly symmetrical geometries. This suggests that hemodynamics does play a role in the preferred zones of stress concentrations. The numerical results also demonstrated that these stress concentrations are mostly located in the "shoulder" region where the fibrous cap joins the artery wall. This implies that the fibrous cap is being "pushed" away by the hemodynamic forces and the zone of reactive stress is located at the shoulder as such zone is less "displaceable" than the rest of the fibrous cap. Furthermore, the level of displacement of the fibrous cap is directly related to the degree of stiffness of the core. In this scenario, the plaque's core acts as the structural foundation of the fibrous cap. If the core is very soft, it will allow for a great displacement of the fibrous cap as it is pushed by the hemodynamic forces. On the contrary, if it is hard (or calcified), the structural stability will not allow great displacements of the cap and thus it would experience mechanical strains of lesser magnitude. The fibrous cap thickness also plays an important role in the plaque's structural stability. From the results, it is evident that thinner fibrous caps translate directly into higher stress magnitudes that could potentially rupture the plaque. The analysis from the first article clearly indicates that a combination of critical factors, such as a thin fibrous cap, a mild to large percentage of stenosis and a soft lipid core increases the chances of the fibrous cap failure.

A very interesting finding was that for the most critical cases of thin fibrous cap and soft inclusion at various levels of stenosis, the peak stress behavior showed a "plateau" region (Figure 2.13) for stenoses between 43% and 75%. This region may explain why

mild stenoses are equally vulnerable to rupture than severe stenoses given the fact that they are subjected to mechanical stresses similar to those of severe stenoses. The results derived in chapter 2 suggest what are the morphological and mechanical conditions to induce rupture under ideal conditions. However, the time-dependent flow requires to introduce the concept of fibrous cap mechanical fatigue (FCMF) as it is essential to calculate the stress amplitude and mean stress of each node in the numerical analysis in order to assess the global effects of these variables for the fatigue life.

The second article provides more information about the particular physics that take place during the transient flow over one cardiac cycle. The analyses with time-dependent inlet conditions on coronary flow and pressure resulted in a significant pressure drop across the proximal and distal sides of the stenosis when the blood flow was highest, coinciding with the highest stress magnitudes in the proximal shoulder region of the fibrous cap in the same timestep. Results also suggest that the greatest energy losses occur whenever it translates into the mechanical deformation of the weakest structural components of the plaque. Whenever the flow was at its lowest (such as at the beginning of systole), the maximum magnitude of stress followed a similar pattern as the intracoronary pressure inlet conditions. The treatment of plaque failure as a fatigue problem provided some insight that some particular zones in the model could prematurely fail as a consequence of a progressive injury due to the pulsatile cyclic stresses rather than a nominal stress threshold value. More research needs to be done in this area and it is ultimately necessary to construct an S-N curve for fatigue failure of arterial wall or fibrous cap.

The third article also provided evidence that indeed the fibrous cap's collagen fibers have preferred orientations depending on the particular spatial location and associated

mechanical loading conditions. Our results suggest that they follow the principal stress orientations as the artery fibers rearrange their orientation to be aligned with the principal stresses. An hypothesis we put forward is that once the tissue has remodeled into a "stable" fiber pattern under rest conditions, a sudden increase in flow and pressure can alter the normal stress pattern and thus solicitate the composite structure of the fibrous cap in its weakest orientation and trigger a premature failure of the tissue due to fibrous cap mechanical fatigue (FCMF). The histology pictures and their respective computer image analyses provided direct evidence that we must account for the fibrous cap's true anisotropy in order to further refine the numerical models in order to better understand the initiation of plaque fissuring and crack propagation. Our computer code for mapping the fibrous cap's anisotropy provided good results in terms of tracking the fibers from the images, however, further refinements to the code need to be done in order to incorporate the 3D spatial data and the anisotropy information into the model for finite element analyses.

Finally, we provided in this thesis some possible explanation for the paradoxical rupture of mild vunerable plaques. Indeed, we show that plaques of around 40% stenosis are subjected to stresses equivalent to those of about 75% stenosis in the "plateau" region observed in the results. In addition, we have also showed that the orientation of collagen fibers for such mild plaques was near the weakest possible orientation that would result in rupture. Also, we showed that the vulnerability to rupture of a multiple plaque scenario may be different than that of single plaques with similar morphologies and material properties. The spatial location of the multiple plaques as well as their material properties affect the hemodynamics and thus the overall distribution of the mechanical stress.

# **Appendix Section**

This section contains the following:

- Ethical approval from the hospital involved in the tissue research
- Ethical approvals from McGill University
- Author's Curriculum Vitae

# Ethical approvals from McGill University for tissue research



Faculty of Medicine 3655 Promenade Sir William Osler Montreal, QC H3G 1Y6 Faculté de médecine 3655, Promenade Sir William Osler Montréal, QC, H3G 1Y6

Fax/Télécopieur: (514) 398-3595

August 14, 2007

Dr. Richard Leask
Department of Chemical Engineering
M. H. Wong Building
3610 University Street
Montreal Quebec H3A 2B2

RE: IRB Study Number A06-M62-04B entitled "Geometric and Biomechanical Data for Modeling the Left Ventricular Outflow Tract and Proximal Coronary Arteries"

Dear Dr. Leask,

We are writing in response to your request for continuing review for the study A06-M62-04B entitled "Geometric and Biomechanical Data for Modeling the Left Ventricular Outflow Tract and Proximal Coronary Arteries"

The progress report was reviewed and expedited re-approval for this study was provided by the IRB Chair on August 16, 2007. The renewed ethics certificate (enclosed) is valid until June 30, 2008. The record of this renewal will be reported to the full Board at the next schedule meeting of the Institutional Review Board on August 27, 2007

We ask that you take note of the investigator's responsibility to assure that the current protocol and consent document are deposited on an annual basis with the Research Ethics Board of each hospital where patient enrolment or data collection is conducted.

Should any modification or unanticipated development occur prior to the next review, please advise the IRB promptly.

Yours sincerely,

Serge Gauthier, MD

Chair

Institutional Review Board

cc: A06-M62-04B

#### DATE OF I.R.B. McGill Faculty of Medicine APPROVAL · San Good Sand Institutional Review Board AUG 1 \$ 2007 - Continuing Review Form Faculty of Medicine McGill University Department/Institution: Chem Eng/McGi Principal Investigator: Richard L. Leask IRB Review Number A06-M62-04B Study Number (if any): Review Interval: 3 Title of Research Proposal: Geometric and Biomechanical Data for Modeling the Left Ventricular Outflow Tract and Proximal Coronary Arteries INTERIM REPORT (PLEASE CHECK OR SPECIFY) Current Status of Study : Active Study | On Hold Closed to Enrolment Interim Analysis X Final Analysis Study Not Activated \*\*\* \*\*If the study has not become active at McGill, please enclose correspondence to explain or provide explanation: McGill hospital(s) where study is being conducted and has received acceptance of local Research Ethics Board(s) (if applicable): Douglas: ☐ JGH: ☐ MUHC/MCH (Mtl Children's): ☐MUHC/MCI (Mtl Chest Ins).: ☐ MUHC/MGH: ☒ MUHC/MNH-MNI: MUHC/RVH: Shriners Hospital SMH: Other: MONTREAL HEART INSTITUTE McGill hospital(s) where study is being conducted and has NOT received acceptance of local Research Ethics Board(s) (if applicable): In the case of a clinical trial, has the lead sponsor registered the study in the WHO Clinical Trials Registry http://isrctn.com/ No ☐ or the NIH Clinical Trials Registry http://www.clinical.trials.gov? Yes ☐ No ☐ If study sponsorship or financial support has changed, please provide correspondence to explain; enclosed: Total number of subjects to be enrolled in the study: 15 Number of subjects to be enrolled at McGill sites: 5 Number of subjects enrolled by McGill PI to date: 10 Number of subjects enrolled by McGill PI since the last review: 0 Have any of these subjects withdrawn from the study, and if yes, how many? Yes Has the study been revised since the last review? Yes ☐ No ☒ Has the consent form been revised since the last review? Yes ☐ No ☒ Have the study and consent form revisions been submitted and approved by the IRB? Yes 🔲 No 🖂 Are there any new data since the last review that could influence a subject's willingness to provide continuing consent?:

Have all Serious Adverse Experiences (SAEs) and Safety Reports relevant to the study been reported to the IRB?: Yes ☐ No ☒

Date:

Have there been any Serious Adverse Experiences (SAEs)?: Yes ☐ No ☒

SIGNATURES:

Principal Investigator:

IRB Chair:

# Ethical approval from the hospital involved in the tissue research



HOSPITAL GENERAL DEL ESTADO "DR. ERNESTO RAMOS BOURS" JEFATURA DE LA DIVISIÓN DE ENSEÑANZA, INVESTIGACIÓN Y CAPACITACIÓN

05 de Julio del 2007

ING. RAMSÉS GALAZ MÉNDEZ DR. ROSAIRE MONGRAIN DR. JEAN CLAUDE TARDIF P R E S E N T E.-

#### Estimado Señores:

Por medio del presente le informamos que él C. Doctor Minor Raúl Cordero Bautista participará como Investigador y coordinador del proyecto Titulado:

"Análisis de la ruptura y mapeo de la anisotropía estructural del tejido fibroso de la placa ateroesclerótica coronaria."

Dicho proyecto de Investigación concluirá el 31 de diciembre del 2007. Se realizo la presentación de dicho protocolo ante los integrantes del Comité de Investigación y Bioética de este hospital, estando presente su Servidor. Posterior a la presentación del proyecto se acepto concluyéndose que es un estudio relevante y de utilidad para mejorar la calidad científica y asistencial de nuestra institución, por lo que no hay inconveniente para su realización.

Agradeciendo de antemano su apoyo, quedo a sus apreciables órdenes

ATENTAMENTE

DR. JOAQUÍN SÁNCHEZ GONZÁLEZ

Jefe de la División de Enseñanza, Investigación y Capacitación

C.c.p. Dr. C. Rafael De la Ree Abril.- Director General. Edificio

C.c.p. Dr. Leoncio Vindiola Córdova.- Director Médico. Edificio

C.c.p. Comité de Investigación

C.c.p. Interesado.

JSG/gbu\*

Blvd., Luis Encinas s/n Col. Centro C.P. 83000 Hermosillo, Sonora Tel.: 01662-259-25-34 y 259-25-90 Fax: 259-25-95



# Translation of the ethical approval letter given by the Mexican Hospital where all tissue research was performed

STATE GENERAL HOSPITAL
"DR. ERNESTO RAMOS BOURS"
TEACHING, RESEARCH AND TRAINING DIVISION HEADQUARTERS

July 5, 2007 Ing. Ramsés Galaz Mendez Dr. Rosaire Mongrain Dr. Jean Claude Tardif Present

Dear Sirs,

We would like to inform you that Dr. Minor Raúl Cordero Bautista will participate as a researcher and coordinator of the project titled:

# "Rupture analysis and mapping of the structural anisotropy of the fibrous tissue of the atherosclerotic coronary plaque"

Such research project wll conclude on December 31<sup>st</sup> 2007.

A formal presentation of the research protocol was presented to the Research and Bioethics Committee of this hospital, being myself present. After the presentation, such project was accepted as it was concluded that it is a relevant study and of great usefulness to improve the scientific quality of our institution, therefore, there is no inconvenience for it to be done.

We thank your support beforehand,

Truly yours,

(signed)

Dr. Joaquín Sanchez González Chief of the Teaching, Research and Training Division

- cc. Dr. Rafael De la Ree Abril General Director
- cc. Dr. Leocio Vindiola Córdova Medical Director
- cc. Research Committee
- cc. Interested person

JSG/gbu

# Author's curriculum vitae

Ramsés Galaz Mendez

Permanent address: Blvd. Justo Sierra 60, Col. Pitic, Hermosillo, Sonora, 83150, México

Date of birth: November 26, 1976

e-mail address: ramses.galaz@gmail.com

# **EXPERIENCE**

- **Adjunct Professor**, Instituto Tecnológico y de Estudios Superiores de Monterrey. Monterrey Campus. Department of Biomedical Sciences. August 2008 present.
- Director, TAUVEX S.A. de C.V. A company that designs, manufactures and distributes class I and II medical devices to the Latin American market. September 2004 – present.
- Graduate Student Research Assistant, Cardiovascular Engineering Laboratory, McGill University and Montreal Heart Institute, September 2002 – March 2008, Montreal, Canada.
- Manufacturing Engineer and Production Supervisor, Cooper Industries, Bussmann Division, August 1999 August 2000, Chicago, Illinois. Supervised 60 team workers and floor supervisor to produce electric line items worth \$23M USD in annual sales. Performed Lean Manufacturing, Kaizen, ERP Systems projects within the plant. Outsourced an entire production line to a plant in Cd. Juarez, México.
- **Manufacturing Engineering Consultant**, Center for Integrated Manufacturing Systems, ITESM, September 1996 May 1999. Monterrey, México.

# **EDUCATION**

- Doctor of Philosophy candidate Biomedical Engineering. McGill University, Montréal, Québec, Canada. Research field in computational modeling of atherosclerotic plaque rupture. Expected dissertation date: October 2008.
- Master of Engineering Mechanical Engineering. McGill University, Montréal, Québec, Canada. June 2004.
- Bachelor of Science in Mechanical Engineering and Management. Instituto Tecnológico y de Estudios Superiores de Monterrey. México. May 1999.
- Minor in Artificial Intelligent Systems. Center for Artificial Intelligence. Instituto Tecnológico y de Estudios Superiores de Monterrey. México. May 1999.
- Certified Manufacturing Technologist. Society of Manufacturing Engineers. Detroit, Michigan. September 1998.

# **AFFILIATIONS**

- President of the Mexican Chapter of the Society of Manufacturing Engineers (SME) 1998

   1999.
- Member of the American Society of Mechanical Engineers since 1996.

#### **CONFERENCES**

- Galaz R., Mongrain R., Ranga A., El-Khoury N., Tardif J.C., Structural analysis of a coronary stent interacting with an hyperelastic arterial wall, Endocoronary Biomechanics and Restenosis Symposium, Paris, France, 2003.
- Galaz R., Mongrain R., Ranga A., Brunette J., Bertrand O.F., Tardif J.C., FEA Structural Analysis of a Coronary Stent Interacting with an Hyperelastic Wall, Proceedings of the 1 International New Cardiovascular Congress, Québec City, Sept 10-11, Abstract P-11, p 68, 2004.
- Galaz R., Mongrain R., Ranga A., Brunette J., Bertrand O.F., Tardif J.-C., FEA Structural Analysis of a Coronary Stent Interacting with a Hyperelastic Arterial Wall, Les Dixseptièmes Entretiens du Centre Jacques Cartier, Nano-biointerfaces pour les dispositifs intelligents, Oct 7-8, Montréal, 2004.
- Galaz R., Pazos V., Mongrain, R., Leask R., Tardif, J.C., A numerical model of the rupture mechanics of the fibrous cap in atherosclerotic plaques, PACAM IX - Ninth Pan American Congress of Applied Mechanics, Mérida, Yucatán, México, January 2-6, 2006.
- Galaz R., Mongrain R., Pazos V., Leask R., Tardif J.C., Modelling of Hemodynamic Stress Effects on Rupture Mechanics and Fibrous Cap Collagen Architecture of Atherosclerotic Plaques, Book of the Proceedings of The IASTED Conference on Modelling and Simulation, Montreal, 2006 Editor(s): R. Wamkeue 630 pages, ISBN: 0-88986-592-2.
- Galaz R., Mongrain R., Pazos V., Leask R., Tardif J.C., Modelling the stress condition dependant anisotropy and rupture mechanics of atherosclerotic plaques, Proceedings of the 2006 ASME Summer Bioengineering Conference, Amelia Island, Florida, 2006.
- **Galaz R.**, Mongrain R., Pazos V., Leask R., Tardif J.C., Fluid-structure interaction computational modeling of realistically reconstructed atherosclerotic plaques to assess their vulnerability to rupture based on collagen fiber architecture # 6721, Proceedings of the 5th World Congress of Biomechanics. Munich, Germany, 2006.
- **Galaz R.**, *Mongrain R.*, *Pazos V.*, *Leask R.*, *Tardif J.-C.*, Fluid-structure interaction computational modelling of realistically reconstructed atherosclerotic plaques to assess their vulnerability to rupture based on collagen fibre architecture, Journal of Biomechanics Vol. 39, 2006 Supplement 1 [abstract].
- Galaz R., Mongrain R., Pazos V., Leask R., Tardif J.C., Transient Fluid Structure Interaction Computational Analyses to Assess Patient Specific Atherosclerotic Plaque Vulnerability, CompMed SSH Symposium on Computer Simulation in Medicine 2007, Montreal, Quebec, Canada, 2007.

- **Galaz R.**, *Mongrain R.*, *Pazos V.*, *Leask R.*, *Tardif J.C.*, Computational sensitivity analyses to assess atherosclerotic plaque vulnerability, 21<sup>st</sup> Canadian Congress on Applied Mechanics, Toronto, Ontario, Canada, 2007.
- Galaz R., Mongrain R., Pazos V., Leask R., Tardif J.C., Computational analysis to assess atherosclerotic plaque vulnerability due to hemodynamic effects, Proceedings of the 2007 ASME Summer Bioengineering Conference, Keystone, Colorado, 2007.
- Galaz R., Mongrain R., Leask R., Tardif J.C., Patient-specific coronary plaque vulnerability analyses based on 3D computer models of the mechanical interaction between hemodynamics and plaque constituents., Accepted abstract at the Canadian Cardiovascular Congress 2007, Quebec City, Canada, 2007.
- Mongrain R., Galaz R., Ranga A., El-Khouri N., Bertrand O.F., Tardif J.C., Structural Analysis of a Coronary Stent Interacting with the Vascular Wall during Angioplasty. Archives of Physiology and Biochemistry, 111, Supp. p. 8, 2003.
- Mongrain R., Galaz R., Bertrand O., Deep wall injury due to atherosclerotic plaque reconfiguration during angioplasty and in-stent restenosis, 5 World Congress of Biomechanics, Munich, Germany, 2006.
- Mongrain R., Galaz R., Bulman-Fleming N., Ruzzeh B., Bertrand O.F., Tardif J.-C., Multidisciplinary Design Optimization of Stents, Proceedings of the ASME Summer Bioengineering Conference ISBN 0-9742492-1-1, Vail, Colorado, June 22 - 26, 2005.
- Mongrain R., Galaz R., Ranga A., El-Khoury N., Bertrand O.F., Tardif J.C., Structural
  analysis of a coronary stent interacting with the vascular wall during angioplasty, XXVIII
  Congres de la Societé de Biomecanique, Poitiers, France, 2003.
- Pazos V., Mongrain R., Galaz R., Leask R. Tardif J.C., Development of an atherosclerotic phantom with a lipid inclusion, Proceedings of the 5th World Congress of Biomechanics, Munich, Germany. 2006.

#### JOURNAL PUBLICATIONS

- Galaz R., Mongrain R., Leask R., Tardif J.C., Fluid structure interaction numerical studies on the assessment of mechanical stress of the coronary atherosclerotic plaque. [submitted to the Journal of Medical Engineering & Physics, July 2008]
- Brunette J., Mongrain R., Laurier J., Galaz R., Tardif J.C., 3D flow study in a mildly stenotic coronary artery phantom using a whole volume PIV method, Journal of Medical Engineering & Physics, (Article in press DOI:10.1016/j.medengphy.2008.02.012), April 2008.
- Ranga A., Mongrain R., Galaz R., Biadillah Y., Cartier R., Large displacement 3D structural analysis of an aortic valve model with nonlinear material properties. Journal of Medical Engineering & Technology, 28(3):95-103, 2004.

# **BOOK CHAPTERS**

Mongrain R., Leask R., **Galaz R.**, Ranga A., Brunette J., J.C. Tardif, O.F. Bertrand, Image Based Biomechanics of Coronary Plaque, Plaque Imaging: Clinical analysis and its applications using MR, CT, Ultrasound and Microscopic., eds J. Suri, C. Yuan, D. Wilson, S. Laxminarayan, IOS Press, Amsterdam, 2005.

**Galaz R.**, *Mongrain R.*, *Pazos V.*, *Leask R.*, *Tardif J.-C.*, Fluid-structure interaction computational modelling of realistically reconstructed atherosclerotic plaques to assess their vulnerability to rupture based on collagen fibre architecture. Publisher: MEDIMOND, Bologna, Italy. (Book contribution of the Proceedings of the 5th World Congress of Biomechanics)

#### **PATENTS**

 Bifurcated stent with a side branch protrusion. Mongrain R., Galaz R., Bertrand O., Submitted to the Office of Technology Transfer of McGill University, July 2007, Montreal, Canada.

#### **INVITED LECTURES**

- Biomecánica, Congreso Internacional de Ingeniería Mecánica, ITESM, Monterrey, México. October 2003.
- Onceavo Día del Ingeniero Mecánico, Biomecánica, ITESM, Monterrey, México. April 2004.
- Optimización del diseño de prótesis endovasculares, III Congreso Internacional de Ingeniería Biomédica, ITESM, Monterrey, Mexico. April 2007.
- Interacción Fluido Estructura y Biomecánica de Tejidos, III Congreso Internacional de Ingeniería Biomédica, ITESM, Monterrey, Mexico, April 2007.

#### **RESEARCH INTERESTS**

Cardiovascular haemodynamics in pathological conditions, Atherosclerosis, Plaque rupture, Tissue mechanics, Biomechanics, Medical device design for endovascular, orthopaedic, respiratory and gastrointestinal applications.

# **SKILLS**

CAD/CAM/CAE, Product Design, Large Deformation Mechanics, Finite Element Analysis, Medical Product Design, Manufacturing processes.

# **LANGUAGES**

Spanish 100% English 100% French 50%

# References

- 1. Fuster V. Human lesion studies. Ann N Y Acad Sci 1997; 811:207-224; discussion 224-225.
- Wissler RW, Strong JP. Risk factors and progression of atherosclerosis in youth.
   PDAY Research Group. Pathological Determinants of Atherosclerosis in Youth.
   Am J Pathol 1998; 153:1023-1033.
- 3. Steinberg D. Lipoproteins and the pathogenesis of atherosclerosis. Circulation 1987; 76:508-514.
- 4. Steinberg D. Low density lipoprotein oxidation and its pathobiological significance. J Biol Chem 1997; 272:20963-20966.
- Quinn MT, Parthasarathy S, Fong LG, Steinberg D. Oxidatively modified low density lipoproteins: a potential role in recruitment and retention of monocyte/macrophages during atherogenesis. Proc Natl Acad Sci USA 1987; 84:2995-2998.
- 6. Parthasarathy S, Quinn MT, Steinberg D. Is oxidized low density lipoprotein involved in the recruitment and retention of monocyte/macrophages in the artery wall during the initiation of atherosclerosis? Basic Life Sci 1998; 49:375-380.
- 7. Hennig B, Chow CK. Lipid peroxidation and endothelial cell injury: implications in atherosclerosis. Free Radic Biol Med 1988; 4:99-106.
- 8. Ross R, Glomset J, Harker L. Response to injury and atherogenesis. Am J Pathol 1977; 86:675-684.
- 9. Kockx MM, Knaapen MW. Pathological changes in the coronary arteries in the acute coronary syndromes. Heart 2006; 92:1557-1558.

- Berman JW, Kazimi M, Ma H. Cardiovascular plaque rupture: Chapter 1, Development of atherosclerotic plaque. Marcel Dekker Publishers Inc. 2002; 1-50. ISBN 082470276-X.
- 11. Small DM. Progression and regression of atherosclerotic lesions. Insights from lipid physical biochemistry. Arterioscl 1988; 32:283-285.
- 12. Guyton JR, Klemp KF. The lipid-rich core region of human atherosclerotic fibrous plaques. Prevalence of small lipid droplets and vesicles by electron microscopy. Am J Pathol 1989; 134:705-717.
- 13. Geng YJ, Libby P. Evidence for apoptosis in advanced human atheroma. Am J Pathol 1995; 147:251-266.
- 14. Ball RY, Stowers EC, Burton JH, Cary NRB, Skepper JN, Mitchinson MJ. Evidence that the death of macrophage foam cells contributes to the lipid core of atheroma. Atherosclerosis 1995; 114:45-54.
- 15. Gonzalez ER, Kannewurf BS. Atherosclerosis: a unifying disorder with diverse manifestations. Am J Health Syst Pharm 1998; 55:S4-7.
- 16. Libby P, Theroux P. Pathophysiology of coronary artery disease. Circulation 2005; 111:3481-3488.
- 17. Rohde LE, Lee RT. Cardiovascular plaque rupture: Chapter 6, Role of mechanical stress in plaque rupture: mechanical and biological interactions. Marcel Dekker Publishers Inc. 2002; 147-166. ISBN 082470276-X.
- 18. Falk E. Morphologic features of unstable atherothrombotic plaques underlying acute coronary syndromes. Am J Cardiol 1989; 63:114E-120E.
- 19. Davies MJ. Anatomic features in victims of sudden coronary death. Coronary artery pathology. Circulation 1992; 85:I19-24.

- 20. Richardson PD, Davies MJ, Born GV. Influence of plaque configuration and stress distribution of coronary atherosclerotic plaques. Lancet 1989; 2:941-944.
- 21. Lee RT, Kamm RD. The unstable atheroma. Arterioscler Thromb Vasc Biol 1997; 17:1859-1867.
- 22. Lundberg B. Chemical composition and physical state of lipid deposits in atherosclerosis. Atherosclerosis 1985; 56:93-110.
- 23. Gertz SD, Roberts WC. Hemodynamic shear force in rupture of coronary arterial atherosclerotic plaques. Am J Cardiol 1990; 66:1368-1372.
- 24. Davies MJ, Richardson PD, Woolf N, Katz DR, Mann J. Risk of thrombosis in human atherosclerotic plaques: role of extracellular lipid, macrophage, and smooth muscle cell content. Br Heart J 1993; 69:377-381.
- 25. Loree HM, Kamm RD, Stringfellow RG, Lee RT. Effects of fibrous cap thickness on peak circumferential stress in model atherosclerotic vessels. Circ Res 1992; 71:850-858.
- 26. Randomised trial of cholesterol lowering in 4444 patients with coronary heart disease: the Scandinavian Simvastatin Survival Study (4S). Lancet 1994; 344:1383-1389.
- 27. Virmani R, Burke AP, Farb A, Kolodgie FD. Cardiovascular plaque rupture: Chapter 2, Clinical and Pathological Correlates. Marcel Dekker Publishers Inc. 2002; 51-61. ISBN 082470276-X.
- 28. Birgelen C, Klinkhart W, Mintz G, Wieneke H, Baumgart D, Haude M, Bartel T, Sacl S, Ge, J, Erbel R. Size of emptied plaque cavity following spontaneous rupture is related to coronary dimensions, not to the degree of lumen narrowing. A study with intravascular ultrasound in vivo. Heart 2000; 84(5):483-488.

- 29. Pasterkamp C, Falk E. Atherosclerotic plaque rupture: an overview. J Clin Bas Cardiol 2000; 3:81-86.
- 30. Glagov S, Weisenberg E, Zarins CK, Stankunavicius R, Kolettis G. Compensatory enlargement of human atherosclerotic arteries. N Engl J Med 1987; 316:1371-1375.
- 31. Loree HM, Kamm RD, Stringfellow RG, Lee RT. Effects of fibrous cap thickness on peak circumferential stress in model atherosclerotic vessels. Circ Res 1992; 71:850-858.
- 32. Lee RT, Schoen FJ, Loree HM, Lark MW, Libby P. Circumferential stress and matrix metalloproteinase 1 in human coronary atherosclerosis: implications for plaque rupture. Arterioscler Thromb Vasc Biol 1996; 16:1070-1073.
- 33. Kumar RK, Balakrishnan KR. Influence of lumen shape and vessel geometry on plaque stresses: possible role in the increased vulnerability of a remodeled vessel and the "shoulder" of a plaque. Heart 2005; 91:1459-1465.
- 34. Ohayon J, Teppaz P, Riouffol G, Finet G. In vivo prediction of human coronary plaque rupture location using intravascular ultrasound and finite element method. Cor Art Dis 2001; 12:655-663.
- 35. Versluis A, Bank AJ, Douglas WH. Fatigue and plaque rupture in myocardial infarction. J Biomech 2006; 39:339-347.
- 36. Gilpin CM. Cyclic loading of porcine coronary arteries. Master's thesis: Georgia Institute of Technology. May 2005.
- 37. Shigley JE, Mischke CR, Gordon-Budynas R. Mechanical Engineering Design.

  McGraw Hill. 2003. ISBN 0012520361, 9780072520361.

- 38. Zeng D, Ding Z, Friedman MH, Ethier CR. Effects of cardiac motion on right coronary artery hemodynamics. Ann Biomed Eng 2003; 31(4):420-429.
- 39. Ramaswamy SD, Vigmostad SC, Wahle A, Lai YG, Olszewski ME, Braddy KC, Brennan TMH, Rossen JD, Sonka M, Chandran KB. Fluid dynamic analysis in a human left anterior descending coronary artery with arterial motion. Ann Biomed Eng 32: 1628–1641, 2004.
- 40. Kolandavel MK, Fruend ET, Ringgaard S, Walker PG. The effects of time varying curvature on species transport in coronary arteries. Ann Biomed Eng 34(12):1820-1832.
- 41. Doriot PA. Estimation of the supplementary axial wall stress generated at peak flow by an arterial stenosis. Phys Med Biol 2003; 48: 127–138.
- 42. Berne RM, Levy M. Cardiovascular Physiology, p. 201. 1967. Mosby. St. Louis, MO.
- 43. Ionescu I, Guilkey JE, Berzins M, Kirby RM, Weiss JA. Simulation of soft tissue failure using the material point method. J Biomech Eng 2006; 128(6); 917-924.
- 44. Zoumi A, Lu X, Kassab GS, Tromberg BJ. Imaging coronary artery microstructure using second-harmonic and two-photon fluorescence microscopy. Biophys J 2004; 87:2778-2786.
- 45. Purslow PP, Wess TJ, Hukins DWL. Collagen orientation and molecular spacing during creep and stress relaxation in soft connective tissues. J Exp Biol 1998; 201:135-142.
- 46. Sellaro TL, Hildebrand D, Qijim L, Vyavahare N, Scott M, Sacks MS. Effects of collagen fiber orientation on the response of biologically derived soft tissue biomaterials to cyclic loading. J Biomed Mat Res 2007; 80(1):194-205.

- 47. Becker AE, Van der Wal AC. Cardiovascular plaque rupture: Chapter 3, The role of inflammation in plaque rupture. Marcel Dekker Publishers Inc. 2002; 63-78. ISBN 082470276-X.
- 48. Munro JM, Cotran RS. The pathogenesis of atherosclerosis: atherogenesis and inflammation. Lab Invest 1988; 58:249-261.
- 49. Ross R. The pathogenesis of atherosclerosis: a perspective for the 1990s. Nature 1993; 362:801-809.
- 50. Van der Wal AC, Becker AE, Van der Loos CM, Das PK. Site of intimal rupture or erosion of thrombosed coronary atherosclerotic plaques is characterized by an inflammatory process irrespective of the dominant plaque morphology. Circulation 1994; 89:36-44.
- 51. Van der Wal AC, Becker AE. Atherosclerotic plaque rupture pathologic basis of plaque stability and instability. Cardiovasc Res 1999; 41:334-444.
- 52. Libby P. Molecular bases of the acute coronary syndromes. Circulation 1995; 91:2844-2850.
- 53. Nikkari ST, O'Brien KD, Fergusin M, et al. Interstitial collagenase (MMP-1) expression in human carotid atherosclerosis. Circulation 1995; 92:1393-1398.
- 54. Woessner JF. The family of matrix metalloproteinases. Ann N Y Acad Sci 1994; 732:11-21.
- 55. Galis ZS, Sukhova GK, Lark MW, Libby P. Increased expression of matrix metalloproteinases and matrix degrading activity in vulnerable regions of human atherosclerotic plaques. J Clin Invest 1994; 94:2493-2503.
- 56. Ye S, Humphries S, Henney A. Matrix metalloproteinases: implication in vascular matrix remodeling during atherogenesis. Clin Sci (Colch) 1998; 94:103-110.

- 57. Finet G, Ohayon J, Rioufol G, Lefloch S, Tracqui P, Dubreuil O, Tabib A. Morphological and biomechanical aspects of vulnerable coronary plaque. Arch Mal Coeur Vaiss. 2007; 100(6-7):546-553.
- 58. Tigen K, Mutlu B, Cevik C, Karavelioglu Y, Basaran Y. Multiple plaque ruptura and intracoronary thrombosis: two successful therapeutic strategies in the same patient. Cardiovasc Revasc Med. 2008; 9(2):95-97.
- 59. Tanaka A, Shimada K, Namba M, Sakamoto T, Nakamura Y, Nishida Y, Yoshikawa J, Akasaka T. Relationship between longitudinal morphology of ruptured plaques and TIMI flow grade in acute coronary syndrome: a three-dimensional intravascular ultrasound imaging study. Eur Heart J. 2008; 29(1):38-44.
- 60. Panse N, Brett S, Panse P, Kareti K, Rewis D, Gilmore P, Zenni MM, Wilke N, Bass T, Costa MA. Multiple plaque morphologies in a single coronary artery: insights from volumetric intravascular ultrasound. Catheter Cardiovasc Interv. 2004; 61(3):376-380.
- 61. Kalaga RV, Malik A, Thompson PD. Exercise related spontaneous coronary artery dissection: case report and literature review. Med Sci Sports Exerc. 2007; 39(8):1218-1220.
- 62. Fertels, SH, Heller DR, Maniet A, Zalewski A. Acute myocardial infarction due to exercise-induced plaque rupture. Clin Cardiol. 1998; 21(10):767-768.
- 63. Hong YJ, Mintz GS, Kim SW, Okabe T, Bui AB, Pichard AD, Satler LF, Waksman R, Weissman NJ. Impact of plaque rupture and elevated C-reactive protein on clinical outcome in patients with acute myocardial infarction: an intravascular ultrasound study. J Invasive Cardiol. 2008; 20(9):428-435.

- 64. Mintz GS, Nissen SE, et al. American College of Cardiology clinical expert consensus document on standards for acquisition, measurement and reporting of intravascular ultrasound studies (IVUS). J Am Coll Cardiol 2001; 5:1478-1492.
- 65. Rioufol G, Elbaz M, Dubreuil O, Tabib A, Finet G. Adventitia measurement in coronary artery: an in vivo intravascular ultrasound study. Heart 2006; 92:985-986.
- 66. Kolodgie FD, Virmani R, Burke AP, Farb A, Weber DK, Kutys R, Finn AV, Gold HK. Pathologic assessment of the vulnerable human coronary plaque. *Heart* 2004; 90:1385-1391.
- 67. Burke AP, Farb A, Malcolm GT, Liang Y-H, Smialek J, Virmani R. Coronary risk factors and plaque morphology in patients with coronary disease dying suddenly. N Engl J Med 1997; 336:1276-1282.
- 68. Finet G, Ohayon J, Rioufol G. Biomechanical interaction between cap thickness, lipid core composition and blood pressure in vulnerable coronary plaque: impact on stability or instability. Coronary Artery Dis 2004; 15(1):13-20.
- 69. Williamson SD, Lam Y, Younis HF, Patel S, Kaazempur-Mofrad MR, Kamm RD.

  On the sensitivity of wall stresses in diseased arteries to variable material properties. J Biomech Eng 2003; 125(1):147-155.
- 70. Lovett JK, Rothwell PM. Site of carotid plaque ulceration in relation to direction of blood flow: an angiographic and pathological study. Cerebrovasc Dis 2003; 16: 369–375.
- 71. Li ZY, Howarth SP, Tang T, Gillard JH. How critical is fibrous cap thickness to carotid plaque stability?: a flow-plaque interaction model. Stroke 2006; 37:1195-1199.

- 72. Fujii K et al. Intravascular ultrasound assessment of ulcerated ruptured plaques: a comparison of culprit and nonculprit lesions of patients with acute coronary syndromes and lesions in patients without acute coronary syndromes. Circulation 2003; 108: 2473–2478.
- 73. Hiro T, Fujii T, Yoshitake S, Kawabata T, Yasumoto K, Matsuzaki M. Longitudinal visualization of spontaneous coronary plaque rupture by 3D intravascular ultrasound. *Circulation*. 2000; 101(1):e114.
- 74. Burke AP et al. Plaque rupture and sudden death related to exertion in men with coronary artery disease. J Am Med Assoc 1999; 281:921–926.
- 75. Falk E et al. Coronary plaque disruption. Circulation 1995; 92: 657–671.
- 76. Mattsson EJ et al. Increased blood flow induces regression of intimal hyperplasia.

  Arterioscler Thromb Vasc Biol 1997; 17: 2245–2249.
- 77. Timoshenko S, Strength of Materials, Part II, Advanced Theory and Problems, 3rd edition. Van Nostrand Co. Inc., New York, 1956, p. 205.
- 78. Wang JC, Normand ST, Mauri L, Kuntz RE. Coronary artery spatial distribution of acute myocardial infarction occlusions. *Circulation* 2004; 110:278-284.
- 79. Weissman NJ, Palacios IF, Weyman AE. Dynamic expansion of the coronary arteries: Implications for intravascular ultrasound measurements. Am Heart J 1995; 130(1):46-51.
- 80. Fung YC, Biomechanics: Mechanical Properties of Living Tissues, Springer, Berlin, 1993.
- 81. J van Andel C, Pistecky PV, Borst C. Mechanical properties of porcine and human arteries: implications for coronary anastomotic connectors. *Ann Thorac Surg* 2003; 76:58-64.

- 82. Back MR, White RA, Kwack EY, Back LH. Hemodynamic consequences of stenosis remodeling during coronary angioplasty. Angiology 1997; 48: 99–109.
- 83. Young DF, Tsai FY. Flow characteristics in models of arterial stenoses. I. Steady flow. J Biomech 1973; 6: 395–410.
- 84. Johnston BM, Johnston PR, Corney S, Kilpatrick D. Non-Newtonian blood flow in human right coronary arteries: Transient simulations. J Biomech 2006; 39:1116–1128.
- 85. Baumgart D, Haude M, Goerge G, Ge J, Vetter S, Dagres N, Heusch G, Erbel R. Improved assessment of coronary stenosis severity using the relative flow velocity reserve. Circulation 1998; 98:40-46.
- 86. Mates RE, Gupta RL, Bell AC, Klocke FJ. Fluid dynamics of coronary artery stenosis. Circ Res 1978; 42:152-162.
- 87. Krzanowski M, Bodzon W, Dudek D, Heba G, Rzeszutko, Nizankowski R, Dubiel J, Szczeklik A. Transthoracic, harmonic mode, contrast enhanced color Doppler echocardiography in detection of restenosis after percutaneous coronary interventions. Prospective evaluation verified by coronary angiography. Eur J Echocardiogr 2004; 5(1):51-64.
- 88. Tang D, Yang C, Zheng J, Woodard PK, Saffitz JE, Petruccelli JD, Sicard GA, Yuan C. Local maximal stress hypothesis and computational plaque vulnerability index for atherosclerotic plaque assessment. Ann Biomed Eng 2005; 33(12): 1789-1801.
- 89. Maier W, Meier B. Cardiovascular plaque rupture: Chapter 21, plaque sealing.

  Marcel Dekker Publishers Inc. 2002; 429-445. ISBN 082470276-X.

- 90. Rioufol G, Gilard M, Finet G, Ginon I, Boschat J, André-Fouët X. Evolution of spontaneous atherosclerotic plaque rupture with medical therapy: long-term follow-up with intravascular ultrasound. Circulation 2004; 110:2875-2880.
- 91. Vengrenyuk Y, Cardoso L, Weinbaum S. Micro-CT based analysis of a new paradigm for vulnerable plaque rupture: cellular microcalcifications in fibrous caps. Mol Cell Biomech. 2008; 5(1):37-47.
- 92. Reddy KS, Yusuf S. Emerging epidemic of cardiovascular disease in developing countries. Circulation 1998; 97:596-601.
- 93. Gronholdt ML, Dalager-Pederson S, Falk E. Coronary atherosclerosis: determinants of plaque rupture. Eur Heart J 1998; 19(suppl C):C24-C29.
- 94. Mittleman MA, Maclure M, Tofler GH, Sherwood JB, Goldberg RJ, Muller JE.

  Triggering of acute myocardial infarction by heavy physical exertion. N Engl J

  Med 1993; 329:1677-1683.
- 95. Tofler GH, Stone PH, Maclure M, Edelman E, Davis VG, Robertson T, Antman EM, Muller JE. Analysis of possible triggers of acute myocardial infarction (The MILIS study). Am J Cardiol 1990; 66:22-27.
- 96. Willich SN, Arntz HR. Triggers of sudden cardiac death. Triggering of acute coronary syndromes. Dodrecht, Boston, London: Kluwer Academic Publishers, 1996; 267-283.
- 97. Lee RT, Loree HM, Cheng GC, Lieberman EH, Jaramillo N, Schoen FJ. Computational structural analysis based on intravascular ultrasound imaging before in vitro angioplasty: prediction of plaque fracture locations. J Am Coll Cardiol 1994; 21:777-782.

- 98. Cheng GC, Loree HM, Kamm RD, Fishbein MC, Lee RT. Distribution of circumferential stress in ruptured and stable atherosclerotic lesions. A structural analysis with histopathological correlation. Circulation 1993; 87(4):1179-1187.
- 99. Li ZY, Howart SPS, Tang T, Gillard JH. How critical is fibrous cap thickness to carotid plaque stability?: a flow-plaque interaction model. Stroke 2006; 37:1195-1199.
- 100. Imoto K, Hiro T, Fujii T, Murashige A, Fukumoto Y, Hashimoto G, Okamura T, Yamada J, Mori K, Matsuzaki M. Longitudinal structural determinants of atherosclerotic plaque vulnerability: a computational analysis of stress distribution using vessel models and three-dimensional intravascular ultrasound imaging. J Am Coll Cardiol 2005; 46(8):1507-1515.
- 101. Ohayon J, Finet G, Treyve F, Rioufol G, Dubreuil O. A three-dimensional finite element analysis of stress distribution in a coronary atherosclerotic plaque: in-vivo prediction of plaque rupture location. Biomechanics applied to computer assisted surgery. Research Signpost, 2005: 225-241. ISBN 8130800314.
- 102. Rekhter MD, Hicks GW, Brammer DW, Work CW, Kim JS, Gordon D, Keiser JA, Ryan MJ. Animal model that mimics atherosclerotic plaque rupture. Circ Res 1998; 83:705-713.
- 103. Chenu P, Zakhia R, Marchandise B, Jamart J, Michel X, Schroeder E. Resistance of the atherosclerotic plaque during coronary angioplasty: a multivariate analysis of clinical and angiographic variables. Cath Card Diag 1993; 29:203-209.
- 104. Bank A, Versluis A, Dodge SM, Douglas WH. Atherosclerotic plaque rupture: a fatigue process?. Med Hyp 2000; 55(6)480-484.

- 105. Haskell WL. Cardiovascular risk complications during exercise training of cardiac patients. Circulation 1978; 57:920-924.
- 106. Kannel WB. Blood pressure as a cardiovascular risk factor: prevention and treatment. J Am Med Assoc 1996; 275:1571-1576.
- 107. Madhavan S, Ooi WL, Cohen H, Alderman MH. Relation of pulse pressure and blood pressure reduction to the incidence of myocardial infarction. Hypertension 1994; 23:395-401.
- 108. Von Mises R. Mechanik der lastischen foränderung von kristallen. Zeitschrift fuer Angewandte Mathematik und Mechanik 1928; 8:11-185.
- 109. Van Andel CJ, Pistecky PV, Borst C. Mechanical properties of porcine and human arteries: implications for coronary anastomotic connectors. Ann Thorac Surg 2003; 76:58-64.
- 110. Rekhter MD, Zhang K, Narayanan AS, Phan S, Schork MA, Gordon D.
  Type I collagen gene expression in human atheroscleroris. Localization to specific plaque regions. Am J Pathol 1993; 143:1634-1648.
- 111. Waksman R, Serruys PW. Handbook of the vulnerable plaque. Informa Health Care 2004. p 38. ISBN 18418443237.
- 112. Sethuraman S, Amirian JH, Litovsky SH, Smalling RW, Emelianov SY. Ex vivo characterization of atherosclerosis using intravascular photoacoustic imaging. Optics express 2007; 15(25): 16657-16666.
- Di LulloDagger GA, Sweeney SM, Korkko J, Ala-Kokko L, San Antonio JD. Mapping the ligand-binding sites and disease associated mutations on the most abundant protein in the human, type I collagen. J Biol Chem 2002; 277(6):4223-4231.

- Hariton I, deBotton G, Gasser TC, Holzapfel GA. Stress-driven collagen fiber remodeling in arterial walls. J Biomech Model Mechanobiol 2006; 6(3):163-175.
- 115. Kunzelman KS, Cochran RP, Chuong C, Ring WS, Verrier ED, Eberhart RD. Finite element analysis of the mitral valve. J Heart Valve Dis 1993; 2(3):326-340.
- 116. Driessen NJB, Boerboom RA, Huyghe JM, Bouten CVC, Baaijens FPT. Computational analyses of mechanically induced collagen fiber remodeling in the aortic heart valve. J Biomech Eng 2003; 125(4):549-557.
- 117. Kuhl E, Garikipati K, Arruda EM, Grosh K. Remodeling of biological tissue: mechanically induced reorientation of a traversely isotropic chain network.

  J Mech Phys Solids 2005; 25(7):1552-1573.
- 118. Grenier G, Remy-Zolghadri M, Larouche D, Gauvin R, Baker K, Bergeron F, Dupuis D, Langelier E, Rancourt D, Auger FA, Germain L. Tissue reorganization in response to mechanical load increases functionality. Tissue Eng 2005; 11(1-2):90-100.
- 119. Bigi A, Ripamonti A, Cojazzi G, Pizzuto G, Roveri N, Koch MH. Structural analysis of turkey tendon collagen upon removal of the inorganic phase. Int J Biol Macromol 1991; 13(2):110-4.
- 120. Wu J, Herzog W. Elastic anisotropy of articular cartilage is associated with the microstructures of collagen fibers and chondrocytes. J Biomech 2002; 35(7):931-942.

- 121. Noorlandr ML, Melis P, Jonker A, Van Noorden CJF. A quantitative method to determine the orientation of collagen fibers in the dermis. J Histochem Cytochem 2002; 50:1469-1474.
- 122. Israelowitz M, Rizvi SWH, Kramer J, Von Schroeder HP. Computational modeling of type I collagen fibers to determine the extacellular matrix structure of connective tissues. Prot Eng Des Sel 2005; 18(7):329-335.
- 123. Kunzelman KS, Cochran RP. Stress / strain characteristics of porcine mitral valve tissue: parallel versus perpendicular collagen orientation. J Card Surg 1992; 7(1):71-78.
- 124. Arts T, Costa KD, Covell JW, McCulloch AD. Relating myocardial laminar architecture to shear strain and muscle fiber orientation. Am J Physiol Heart Circ Physiol 2001; 280:H2222-H2229.
- 125. Little JS, Khalsa PS. Material properties of the human lumbar facet joint capsule. J Biomech Eng 2005; 127(1):15-24.
- 126. Gasser TC, Ogden RW, Holzapfel GA. Hyperelastic modeling of arterial layers with distributed collagen fibre orientations. J R Soc Interface. 2006; 3(6):15-35.
- 127. Sheehan DC, Hrapchack BB. Theory and Practice of Histotechnology. 2<sup>nd</sup> Ed. 1980, Battelle Press, 189-190.
- 128. Bancroft J, Stevens A. Theory and practice of histological techniques, 2<sup>nd</sup> ed. 1982. Churchill-Livingston, NY. 131-135.
- 129. Cox G, Kable E. Cell imaging techniques: second-harmonic imaging of collagen. Humana Press. 2006; 15-35. ISBN 9781588291578.